THE ROLE OF TUMOR NECROSIS FACTOR – ALPHA IN THE ADULT LEYDIG CELL APOPTOSIS UPON ETHANE DIMETHANE SULFONATE (EDS) ADMINISTRATION

A DISSERTATION

SUBMITTED IN PARTIAL FULFILLMENT OF THE REQUIREMENTS

FOR THE DEGREE OF DOCTOR OF PHILOSOPHY

IN THE GRADUATE SCHOOL OF THE

TEXAS WOMAN'S UNIVERSITY

DEPARTMENT OF BIOLOGY

COLLEGE OF ARTS AND SCIENCES

BY

BARKHA SINGHAL, B.Sc., M.Sc.

DENTON, TEXAS

AUGUST, 2015

TEXAS WOMAN'S UNIVERSITY
DENTON, TEXAS

06/24/2015

To the Dean of the Graduate School:

I am submitting herewith a dissertation by Barkha Singhal entitled " The Role of Tumor Necrosis Factor – Alpha in the Adult Leydig Cell Apoptosis upon Ethane Dimethane Sulfonate (EDS) Administration." I have examined this dissertation for form and content and recommend that it be accepted in partial fulfillment of the requirements for the degree of Doctor of Philosophy with a major in Molecular Biology.

Nathaniel Mills
Dr. Nathaniel Mills, Major Professor

We have read this dissertation and recommend its acceptance:

Department Chair

Accepted:

Dean of the Graduate School

DEDICATION

I dedicate my dissertation work to my grandparents Mrs. Kiran Singhal and Dr. Gyan Chand Singhal, my parents Mrs. Chandra Singhal and Mr. Prakash Chand Singhal, and to my husband Mr. Ajay Sanganeria. Thank you for your unconditional love and support.

ACKNOWLEDGMENTS

I had immense support during planning, research and dissertation writing from a vast number of people. Foremost, I am thankful to my mentor, Dr. Nathaniel Mills, for allowing me to work in his lab and for providing me an opportunity to earn the highest and the most powerful degree in molecular biology. Dr. Mills served as a primary advisor on my doctoral committee and guided me as a mentor. I am extremely thankful to Dr. Nathaniel Mills for being my advisor, my mentor and a father like figure while I was away from my family. Dr. Mills has taught me research skills, professional skills and the skills of self-motivation and self-initiation. Due to these skills I am surely a very independent person from what I was at the beginning of my doctoral degree. As well, I am extremely thankful to Dr. Lynda Uphouse who has been my backbone when it came to running statistics and writing this document. Dr. Uphouse has helped me improve my writing skills and excel. In addition, she has also been my primary mentor when it came to discussing both personal and professional concerns.

My other committee members were Dr. Laura Hanson, Dr. DiAnna Hynds and Dr. Nancy DiMarco. Dr. Hanson guided me on the results from ELISA assay and has been very helpful when it came to answering the questions related to immunology. Dr. Hynds is one of the sweetest people I came across, with always a smile on her face and ready to sort out student problems. Dr. Hynds has been a great support as I learned a lot from her regarding cell signaling and cell cross-talking. Dr. DiMarco has been very

helpful during the entire time of my degree. She instantly builds great student - professor relationships, that are extremely important for a long - term support system. I am also thankful to Dr. Huanbiao Mo, as he served as an external professor on my committee before Dr. DiMarco. I cannot thank my doctoral committee members enough for their support and motivation. I am also thankful to Dr. Sarah McIntire - the chair of biology department. She has always tried to make my life and other's life easier by listening to our problems and instantly taking action. Dr. McIntire has always provided me an opportunity to work as a teaching assistant in the Department of Biology during my entire enrollment at the University. After Dr. McIntire, when it comes to providing me the job opportunities on campus, the first person I can think of is Mrs. Reta "Smiddy" Foreman. Smiddy has been one of my strongest pillars, a great boss/friend and a great motivator. I will love to have my future employers be just like Smiddy.

I am also thankful to the other graduate faculty members in the Department of Biology, technicians, staff, lab colleagues, students I taught, friends and family for being immensely supportive and for alleviating my problems. You all have made a huge impact in my life and have helped me grow as an individual. Last, but not the least, I want to thank Texas Woman's University (TWU) for admitting me as a Ph.D. student and hiring me as a teaching assistant. I am a product of TWU and will make my university proud. Thank You!

ABSTRACT

BARKHA SINGHAL

THE ROLE OF TUMOR NECROSIS FACTOR – ALPHA IN THE ADULT LEYDIG CELL APOPTOSIS UPON ETHANE DIMETHANE SULFONATE (EDS) ADMINISTRATION

AUGUST 2015

In mammals, the primary function of testis is to synthesize testosterone that helps maintain spermatogenesis and secondary sexual characteristics in males. Immunomodulatory agents such as busulfan, used in bone marrow transplants and chemotherapeutic drugs, destroy cancer cells, but also have long-term cytotoxic effects on stem cells and differentiating spermatogonia in human testes. The action of busulfan is not understood well in testes; therefore, to further understand the action of such alkylating drugs, we used ethane dimethane sulfonate (EDS), an analogue of busulfan that has two carbons less in its backbone. EDS primarily depletes Leydig cells in the rat testes, which synthesize testosterone, and the loss of testosterone later alters spermatogenesis.

Rats were injected with a single dose of 75 mg/kg EDS and its effects were investigated at 6, 15 and 24 hr after EDS. By 24 hr we found a 75-96% reduction in the mRNA transcript of the Leydig cell markers – StAR, INSL3, LHR and HSD-3β. For the first time, all these markers were detected together in the same study to give comparable results. Hematoxylin and eosin staining showed observable cell loss in the interstitium of testes. Using TUNEL assays, we found a 3- and 5-fold increase in

interstitial cell apoptosis at 15 and 24 hr, respectively. Both the Leydig cell mRNAs and the TUNEL assays showed increased cell loss with increased time of treatment. An increased CD163/CD68 mRNA ratio at 15 hr suggested testicular resident macrophage (TRMs) proliferation and/or an influx of monocytes from blood circulation. Upregulation of cytokines, IL-1β and TNF-α, mRNA, and TNF-α protein, suggested that EDS created an inflammatory microenvironment leading to monocyte invasion in the testes. As we detected no changes in the mRNA of TNF-β, Fas and FasL, we assume no direct involvement of Fas in Leydig cell apoptosis. The two TNF-α receptors, TNFR1 (apoptotic and anti-apoptotic) and TNFR2 (anti-apoptotic), were upregulated and downregulated, respectively, at different times. We know that the receptors for both IL-1β and TNF-α, are localized on Leydig cells and we also know that the imbalance in the expression of these two TNFRs determines the fate of the cell to survive or undergo apoptosis. Therefore, our results support a possible role of TNF-α in Leydig cell apoptosis after EDS treatment.

With a single-dose of 50 mg/kg lenalidomide (putative TNF- α inhibitor), we found no upregulation in the mRNA of INSL3 and HSD-3β. IL-1β is also known to inhibit LH/human chorionic gonadotropin (hCG) and/or cAMP stimulated testosterone production. Both IL-1β and TNF-α, are known to reduce the transcription of LHR, StAR and HSD-3β. Therefore, it is possible that TNF-α and IL-1β separately, or in combination, may be playing a role in altering steroidogenesis by downregulating the transcription of LHR, StAR and HSD-3β but is not directly involved in Leydig cell apoptosis.

TABLE OF CONTENTS

Page

LIST OF TABLES

Table Page

LIST OF FIGURES

Figure Page

CHAPTER I

INTRODUCTION

In mammals, the primary role of testis is to synthesize testosterone that helps maintain spermatogenesis (process of sperm formation and maturation) and secondary sexual characteristics in males. Immunomodulatory and alkylating drugs, such as 1,4-butanediol dimethanesulfonate (busulfan; $CH_3OSO_2(CH_2)_4OSO_2CH_3$), is a well-known alkylating neoplastic agent in cancer treatment and is used as conditioning agents prior to bone marrow transplants and also as chemotherapeutic agents in the treatment of leukemia. Along with destroying the cancerous cells, busulfan also has long-term cytotoxic effects on stem cells and differentiating spermatogonia in human testes (Bucci & Meistrich. 1987). Busulfan has acute and chronic side effects on mammalian testes. Thus, to have a clearer understanding of the function of chemotherapeutic agents, it is important to understand the mode of action of these drugs. Better knowledge of the mechanism of action of anti-cancer drugs can also help in designing more targeted drug therapies and drugs with reduced side effects. Our study is focused on understanding the mechanism of action of an alkylating agent, ethane dimethane sulfonate (EDS), in adult rats testes. EDS is an analogue of busulfan and primarily damages Leydig cells in the testes, which synthesize testosterone, and later alters spermatogenesis.

Mammalian testis is an immunologically privileged site as exogenous antigens and graft alloantigens can be tolerated in testis without eliciting an inflammatory

response (Suescun *et al.* 2003). The anatomy of testes makes it possible to inhibit inflammatory responses when attacked by exogenous toxicants because it segregates germ cell autoantigens into two compartments. In mammals, the two testicular compartments: (a) seminiferous tubules and (b) interstitial compartment, are divided by peritubular cells and the basal lamina (Fijak & Meinhardt. 2006, Lagarrigue *et al.* 2011, Nasr *et al.* 2005). Spermatogenesis occurs within the seminiferous tubules and is maintained by testosterone, synthesized by Leydig cells that are located in the adjoining interstitium compartment. Leydig cells are vital for the function of male gonads and fertility. The presence and maintenance of the Leydig cells is important for normal testicular functions, and are the primary source of testosterone. Testosterone supports germ cell formation and the function of related tissues such as prostate and seminal vesicles (Chen *et al.* 1999, Kim *et al.* 2007, Matsui. 2009). Testosterone helps to maintain secondary sexual characteristics, such as muscle mass and bone density (Horstman *et al.* 2012, Windahl *et al.* 2011). Under physiological condition, testosterone protects germ cells from apoptosis but a number of normal developing germ cells die by apoptosis before reaching maturity. If the testes are exposed to irradiation and toxicants, such as EDS, more apoptosis is observed when compared to the normal physiological apoptosis (Henriksén *et al.* 1996, Lee *et al.* 1997, Richburg & Boekelheide. 1996, Virve *et al.* 1999).

Effects of EDS and other chemical toxicants in testes

Many chemical agents used in chemotherapy for cancer treatment, such as busulfan, and environmental chemicals, are hormonal disruptors and destroy testicular

function, causing considerable challenges to male fertility and alter immune function in mammals (Bishop & Wassom. 1986). Busulfan causes prolonged infertility in mammals and may induce genetic mutation or permanent sterilization at non-lethal doses, as observed in mice (Bucci & Meistrich. 1987). Mice with testicular xenografts from monkey also showed increased cytotoxic effects of busulfan on spermatogenesis, and suggested this to be a good model for non-human EDS studies (Jahnukainen *et al.* 2006). Ethane dimethane sulfonate (EDS; chemical formula $CH_3OSO_2(CH_2)_2OSO_2CH_3$), a sulfonic diester, causes loss of testosterone, which indirectly disrupts spermatogenic epithelium in rats resulting in testicular weight decline (Bartlett *et al.* 1986, Kerr *et al.* 1985). In addition, the ventral prostate, seminal vesicles and epididymis regress due to the lack of circulating levels of testosterone (Matsui. 2009). In rat testis, EDS primarily injures the adult Leydig cells resulting in reduced local testosterone levels, and the continued low levels of testosterone lead to degenerative processes in the germinal epithelium (Molenaar *et al.* 1985, Nandi *et al.* 1999, Woolveridge *et al.* 1999). Reduced levels of testosterone may also lead to male hypogonadism (Yang. 2015).

Cytotoxic and steroidogenic inhibitory effects of EDS show an intriguing species and age specificity (Payne & Hardy. 2007, Rommerts *et al.* 1988). In adult rat testes, EDS causes a reversible inhibition of mature Leydig cell steroidogenesis as stem cells repopulate to form new Leydig cells (Matsui. 2009). Rats receiving a single intraperitoneal injection of EDS (85 mg/kg) showed reduced serum testosterone levels that correlated with the reduced intratesticular testosterone levels post-EDS treatment

(Bartlett *et al.* 1986, Nandi *et al.* 1999, Zirkin *et al.* 1989). The first morphological and apoptotic change that appears in Leydig cells under the influence of EDS are the signs of irreversible condensation of nuclear chromatin (pyknosis) (Payne & Hardy. 2007). Later stages show nuclear fragmentation, chromosomal DNA fragmentation, membrane blebbing and cell shrinkage (Elmore. 2007, Payne & Hardy. 2007).

For testicular treatment, in some cases, testosterone replacement maintains the germinal epithelium in the testis that would otherwise be lost after EDS treatment (Kerr *et al.* 1985, Molenaar *et al.* 1985). In another testicular treatment model, mouse embryonic stem cells (mESCs) could be differentiated into Leydig cells by the overexpression of certain transcription factors, such as steroidogenic factor (SF-1) (Yang. 2015). These differentiated Leydig cells from mice may develop normally into adult Leydig cells (ALCs) when transplanted in rats that lost their original Leydig cells after EDS treatment (Yang. 2015).

EDS injected rats are a good model to study the relationship of Leydig cells with their adjacent cell types and to further study alkylating and carcinogenic drugs, like busulfan. EDS is a valuable tool for the investigation of androgen-dependent reproductive toxicity and cell death by apoptosis as it eliminates both basal and luteinizing hormone (LH)- stimulated (described later in text) testosterone production in adult rat testes (Henriksén *et al.* 1995, Troiano *et al.* 1994, Woolveridge *et al.* 1999). Therefore, we might further exploit the EDS model to find ways of regulating testicular health and the amplitude of spermatogenesis.

While maintenance of Leydig cells and their function are clearly important for the synthesis of testosterone, the mechanistic pathways of how the Leydig cells are lost due to EDS treatment are not well understood. Some pathways are known to be involved in testicular apoptosis. For example: (a) the fibroblast-associated cell-surface (Fas) pathway has been proposed as a key regulator of the activation of germ cell apoptosis (Lee *et al.* 1999, Lee *et al.* 1997, Nandi *et al.* 1999, Riccioli *et al.* 2003, Taylor *et al.* 1999, Virve *et al.* 1999) and for Leydig cell apoptosis in some studies (Taylor *et al.* 1999) (Fig. 1), and (b) the tumor necrosis factor-alpha (TNF-α) pathway (TNF-α belongs to the same family as Fas and has a role in apoptosis and inflammation) also plays a role in apoptosis, but not much has been studied about the role of TNF-α in Leydig cell apoptosis after EDS-treatment (Bauda & Karinb. 2001, Riccioli *et al.* 2000) (Fig. 1). In our studies, expect that selective damage of the adult Leydig cells in EDS-treated rats may be due to the increased expression of TNF-α and its two receptors involved in apoptosis and inflammation (Fig. 1).

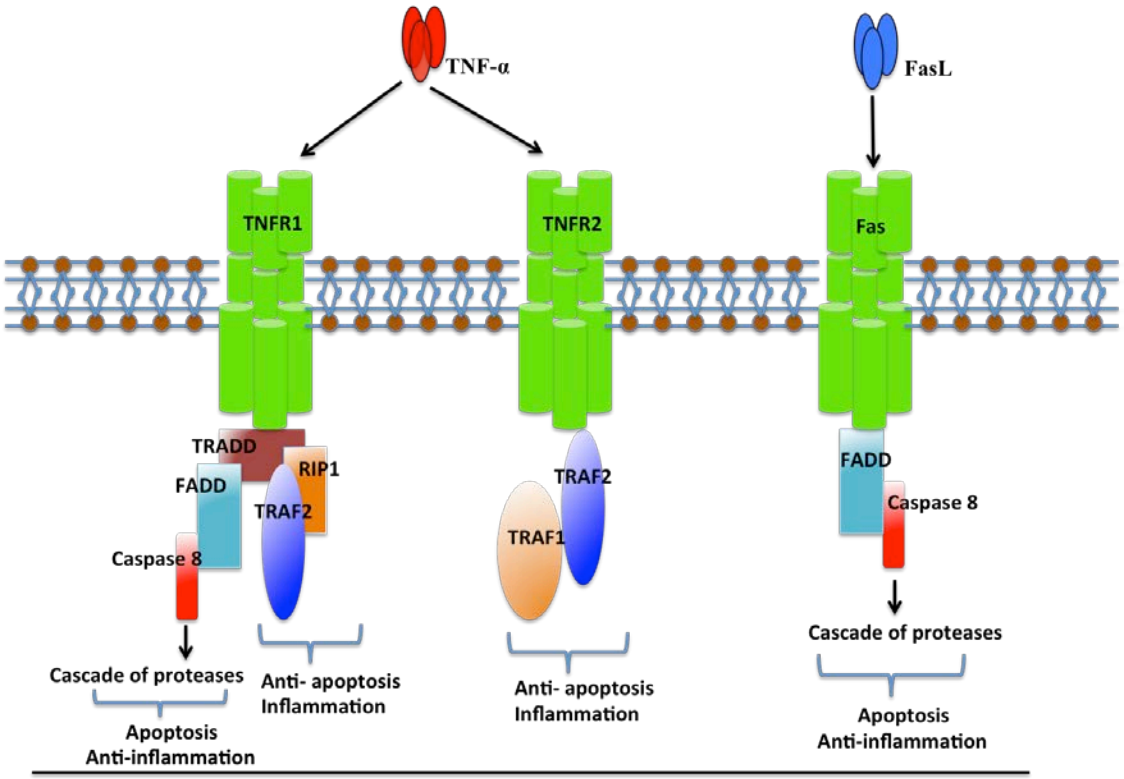

Adapted from Véronique, B., & Michael, M. (2001). Signal transduction by tumor necrosis factor and its relatives. *TRENDS of Cell Biology*, 11, 9. DOI: http://dx.doi.org/10.1016/S0962-8924(01)02064-5 and modified by Barkha Singhal

Figure 1
Fas and TNF-α mediated cell apoptosis and cell survival pathways. If TNF-α binds to TNFR1, it can initiate either apoptosis or anti-apoptosis, depending on the intermediate molecules (such as FADD, RIP1, TRAF2, caspase 8, proteases) involved in the pathway. On the other hand, if TNF-α binds to TNFR2, then it initiates cell-survival pathway by initiating adaptor molecules such as TRAF1 and TRAF2. FasL binds to its receptor, Fas, and destroys the cells by apoptosis through the activation of FADD, caspase 8 and downstream proteases. Figure labels: Fas – fibroblast-associated cell-surface receptor, FasL – fibroblast-associated cell-surface ligand, FADD – fibroblast-associated death domain, RIP1 – receptor interacting protein, TNF-α – tumor necrosis factor alpha, TNFR1 – tumor necrosis factor receptor type 1, TNFR2 – tumor necrosis factor receptor type 2, TRADD – tumor necrosis factor receptor type 1 associated death domain, TRAF1 – TNF receptor-associated factor 1 and TRAF2 – TNF receptor-associated factor 2.

Testes anatomy

In histological cross-section of mature rat testes, two compartments are identified: (a) the avascular seminiferous tubules (82.4% of testes volume), containing Sertoli cells that nurture the germ cells attached to them, is where germ cells finally

mature to form spermatozoa by the process of spermatogenesis. (b) the vascularized inter-tubular area (15.7% of testes volume) between the seminiferous tubules, comprised of blood vessels, nerve fibers and interstitial cells such as Leydig cells (2.7% of testes volume), immune cells including circulating monocytes, lymphocytes, neutrophils, natural-killer cells and macrophages (up to 25% of the total interstitial cell population) (Drut *et al.* 2006, Hardy *et al.* 1989, Kern *et al.* 1995, Mori & Christensen. 1980, Payne & Hardy. 2007, Sharpe. 1983) (Fig. 2). In seminiferous tubules, the tight junctions between Sertoli cells form the blood-testis barrier and provide a microenvironment for the germ cells to proliferate and mature to haploid spermatozoa. Sertoli cells can only support a limited number of germ cells; thus, increased germ cell numbers lead to germ cell apoptosis by the Fas pathway (Lagarrigue *et al.* 2011, Virve *et al.* 1999). The intertubular area, also called the interstitial compartment, contains interstitial fluid derived from circulating plasma and is important for the delivery of trophic hormones and cytokines to the Leydig cells and other cell types in the testes (Mori & Christensen. 1980) (Fig. 2). The interstitial fluid also serves as an exit path for testosterone distribution to the various body tissues (Jégou *et al.* 1982, Sharpe. 1983).

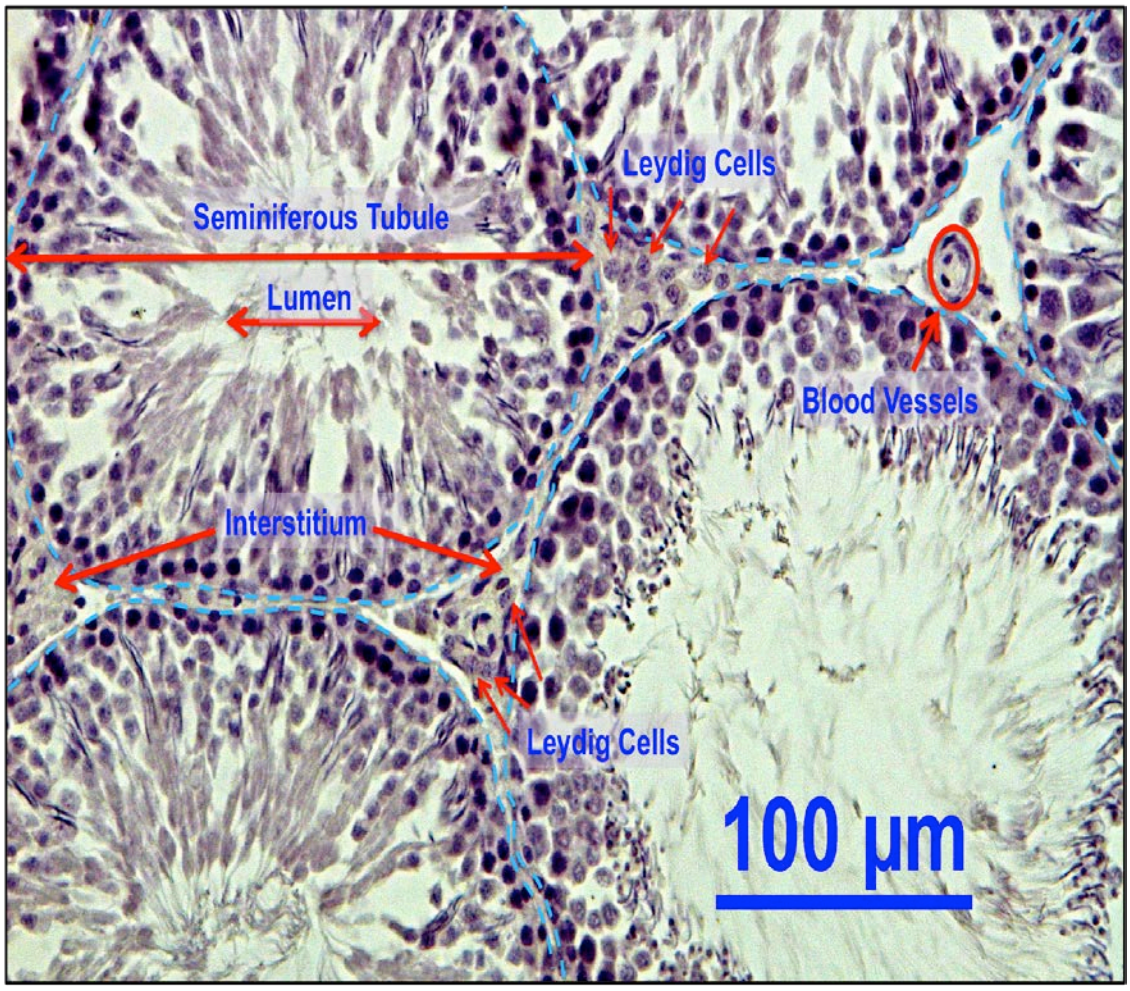

Figure 2
Histology of rat testes using hematoxylin. Spermatogenesis takes place within the seminiferous tubules (marked by blue colored broken lines) and mature spermatozoa are released in to lumen of the seminiferous tubules. Intertubular region surrounding the seminiferous tubules is called testicular interstitium. Interstitium is comprised of blood vessels, nerve fibers, Leydig cells, immune cells including circulating monocytes, lymphocytes, neutrophils, natural-killer cells and macrophages. Under normal conditions in testes, the immune cells provide a suitable microenvironment for steroidogenesis and spermatogenesis.

Basal testosterone production/ Leydig cell markers

In past, people used testosterone concentrations as an indicator of Leydig cell loss, but by measuring the amount of testosterone, it was not possible to identify the specific step that was affected in steroidogenesis. Thus, to study more targeted gene

and protein changes in steroidogenesis after EDS treatment, we used the molecular markers of Leydig cell. A constant supply of cholesterol is needed as a substrate for steroid hormone (testosterone) synthesis in steroidogenic tissues. Cholesteryl esters are the immediate endogenous source of cholesterol in steroidogenic cells. When the endogenous cholesterol pool is depleted, cholesterol is synthesized *de novo* and/or acquired from exogenous lipoproteins, such as high-density lipoprotein (HDL) and low-density lipoprotein (LDL) (Quinn *et al.* 1981). Leydig cells mostly synthesize their own cholesterol *de novo* (Payne & Hardy. 2007). Under normal physiological conditions, the pulsatile release of luteinizing hormone (LH) from the anterior pituitary into the peripheral circulation is the primary regulator of appropriate amounts of testosterone biosynthesis in the Leydig cells (Fig. 3). LH binds to and activates the luteinizing hormone receptor (LHR), a guanine (G-) nucleotide-binding protein coupled receptor (GPCR), localized mostly on the Leydig cell membrane. Activated GPCR, in turn, stimulates adenylyl cyclase for the production of cyclic adenosine monophosphate (cAMP) (Hsueh *et al.* 1977, Payne & Hardy. 2007) (Fig. 4). The equilibrium concentration of intracellular cAMP is maintained by the activity of two enzymes: (a) adenylyl cyclases, involved in cAMP production; and (b) cyclic nucleotide phosphodiesterases, involved in cAMP breakdown (Payne & Hardy. 2007).

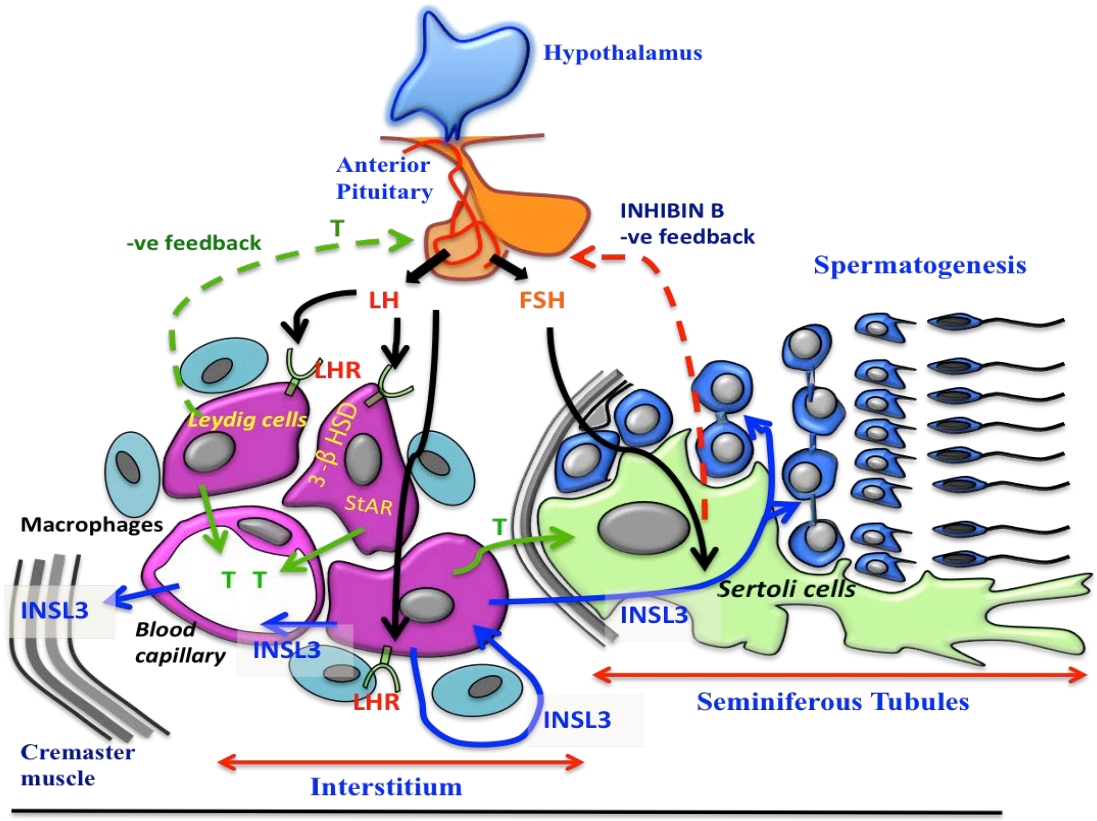

Adapted from Ivell, R., Heng, K., & Anand-Ivell, R. (2014). Insulin-Like Factor 3 and the HPG Axis in the Male. *Frontiers in Endocrinology*, *5*, 6. doi:10.3389/fendo.2014.00006 and modified by Barkha Singhal

Figure 3

Basal testosterone production in rat testes. There is a pulsatile release of luteinizing hormone (LH) from the anterior pituitary (AP), when stimulated by the hypothalamus. LH binds to LH receptors (LHR) localized in the Leydig cells and initiates steroidogenesis. Steroidogenic acute regulator protein (StAR) is the carrier protein that binds to the cholesterol and transports it from the outer to the inner membrane of Leydig cell mitochondria. In the inner mitochondrial membrane and smooth endoplasmic reticulum of Leydig cells, the steroidogenic enzymes, such as 3-β-hydroxyl steroid dehydrogenase (3β-HSD), process cholesterol to form testosterone as an end product. Testosterone is released into the interstitium and blood capillaries. Testosterone released in circulation contributes to serum testosterone levels and testosterone released in the interstitium has paracrine and autocrine interactions with the neighboring cells, such as macrophages. In the seminiferous tubules, testosterone binds to androgen receptors located in Sertoli cells, and maintains germinal epithelium and spermatogenesis. Testosterone can also have a negative feedback on the AP to regulate the release of LH. Insulin-like peptide 3 (INSL3) is a small peptide hormone synthesized by the Leydig cells and binds to their receptors on the cremaster muscle and initiates testicular descent in the inguinal region at birth or soon after birth. AP also releases follicle-stimulating hormone (FSH) that binds to its receptors localized on Sertoli cells and inititates spermatogenesis. An inhibitory protein, inhibin B, secreted by Sertoli cells has a negative feedback on the AP.

Increased intracellular cAMP induces cAMP- dependent protein kinase A (PKA) activity and phosphorylation of transcription factors that in turn regulate the expression of steroidogenic acute regulator (StAR) protein. The phosphorylation of PKA is an important regulator in LH-stimulated steroidogenesis because phosphorylated PKA can regulate the transcription of StAR. The StAR protein mediates the rate-limiting step in steroidogenesis; that is, translocation of dietary or stored cholesterol from the outer mitochondrial membrane to the inner mitochondrial membrane (Kotula-Balak *et al.* 2012, Lukyanenko *et al.* 1998, Luo *et al.* 2001, Payne & Hardy. 2007) (Fig. 4). The aqueous intermembrane space between the mitochondrial membranes restricts the free movement of hydrophobic cholesterol to the mitochondrial matrix. Therefore, only cholesterol bound to phosphorylated StAR is transported to the inner mitochondrial membrane where the P450 cholesterol side-chain cleavage (P450scc) enzyme is located (Lukyanenko *et al.* 1998, Luo *et al.* 2001). In the mitochondrial matrix, the side chain of 27-carbon cholesterol is cleaved by P450scc enzyme converting it to a 21-carbon product, pregnenolone, the first steroid synthesized in the steroidogenesis pathway for steroid hormones. Pregnenolone diffuses across the mitochondrial membrane to be further metabolized by the steroidogenic enzymes associated with the smooth endoplasmic reticulum (SER) (Kotula-Balak *et al.* 2012) (Fig. 5).

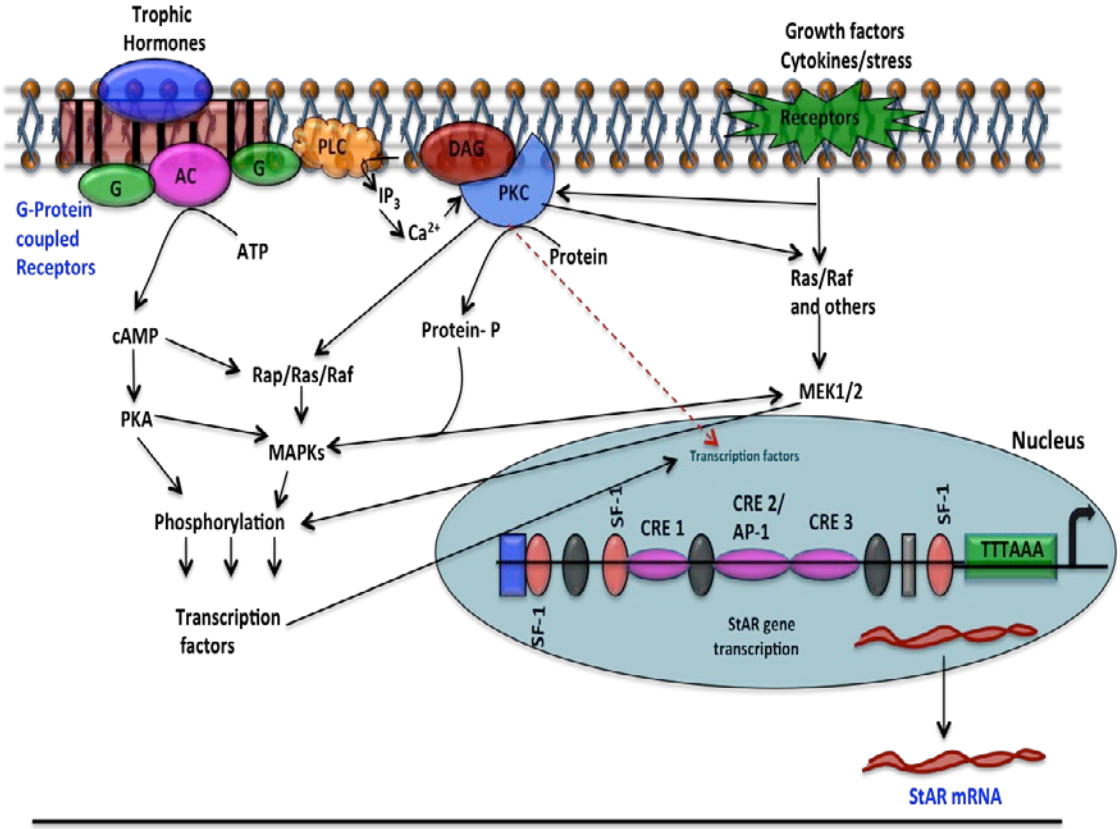

Adapted from Manna, P. & Stocco, D. (2011). The Role of Specific Mitogen-Activated Protein Kinase Signaling Cascades in the Regulation of Steroidogenesis *Journal of Signal Transduction*, vol. 2011, Article ID 821615, 13 pages, doi:10.1155/2011/821615 and modified by Barkha Singhal

Figure 4

Transcription regulation of StAR. Trophic hormones, such as luteinizing hormone bind, to the transmembrane G-protein coupled receptors and stimulate AC to produce cAMP. Other intermediary proteins, such as PKA, Ras, MAPKs; get phosphorylated by cAMP which in turn phosphorylate the transcription factors such as SF-1, to regulate transcription of StAR. Growth factors and a variety of hormones also stimulate hydrolysis of membrane phospholipid phosphatidylinositol by PLC to produce two distinct second messengers: (a) IP_3 – is released into the cytosol to signal the release of Ca^{+2} from intracellular stores, (b) DAG – activates members of PKC family. Some members of the PKC family require both Ca^{+2} and DAG for their activation. Activated PKC can phosphorylate other intermediate proteins that in turn can regulate the transcriptions factors that modulate downstream transcription machinery. Figure labels; AC – adenylyl cyclase, AP-1 – activation protein 1, ATP – adenosine triphosphate, cAMP – cyclic adenosine mono phosphate, CRE – cAMP response element-binding protein, DAG – diacylglycerol, G – guanine nucleotide-binding protein coupled receptor, IP_3 – inositol triphosphate, MAPKs – mitogen activated protein kinase, MEK1/2 – mitogen activated protein kinase kinase 1 and 2, PLC – phospholipase C, PKA – protein kinase A, PKC – protein kinase C, Protein-P – phosphorylated protein, RAP/Ras/Raf – small protein kinase, SF1 – steroidogenic factor 1 and StAR – steroidogenic acute regulator protein.

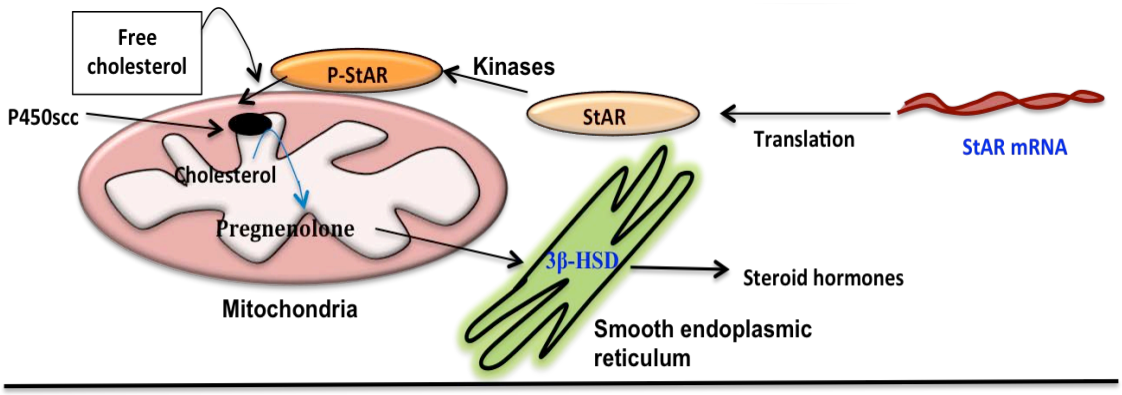

Adapted from Manna, P. & Stocco, D. (2011). The Role of Specific Mitogen-Activated Protein Kinase Signaling Cascades in the Regulation of Steroidogenesis *Journal of Signal Transduction*, vol. 2011, Article ID 821615, 13 pages, doi:10.1155/2011/821615 and modified by Barkha Singhal

Figure 5

StAR – dependent steroidogenesis. StAR mRNA is translated to functional carrier protein. StAR gets phosphorylated by the kinases and binds to the free cholesterol to transport it from the outer mitochondrial membrane to the inner mitochondrial membrane. In the mitochondrial matrix, the side chain of 27-carbon cholesterol is cleaved by P450scc enzyme converting it to a 21-carbon product, pregnenolone. Pregnenolone diffuses across the mitochondrial membrane to be further metabolized by the steroidogenic enzymes such as 3β-HSD, associated within the smooth endoplasmic reticulum (SER). Figure labels; 3β-HSD – 3-β-hydroxyl steroid dehydrogenase, P450scc – P450 cholesterol side-chain cleavage, P-StAR – phosphorylated steroidogenic acute regulator protein and StAR – steroidogenic acute regulator protein.

The two major classes of steroidogenic enzymes present in the SER of rat testis are: (a) the cytochrome P450 heme-containing proteins and (b) the hydroxyl steroid dehydrogenases (HSDs). These two classes convert pregnenolone to other weaker androgens, such as androstenedione and finally to testosterone, the most abundant androgen. 3β-hydroxyl steroid dehydrogenase (3β-HSD) catalyzes the synthesis of progesterone from pregnenolone. Cytochrome P450c17 (steroid 17 alpha-hydroxylase/17,20 lyase) is the single enzyme mediating both 17 alpha-hydroxylase (steroid 17 alpha-monooxygenase) and 17,20 lyase activities in the synthesis of androstenedione from progesterone (Chung. 1987). The enzyme 17β-hydroxysteroid dehydrogenases (17β-HSD), catalyzes dehydrogenation of androstenedione to

testosterone. Testosterone is released into the interstitial fluid and has paracrine action, after binding to the androgen receptors (ARs) on Sertoli cells, and an autocrine action, by binding to the ARs on the Leydig cell itself. Testosterone can be reduced in the target cells by 5α-reductase to dihydrotestosterone (DHT), which binds about three times better than testosterone to the androgen receptors (Windahl *et al.* 2011). Testosterone also has a negative feedback effect on the anterior pituitary when testosterone concentrations are increased above the basal level required to maintain spermatogenesis and other body functions (Fig. 3). The biosynthesis of testosterone is dependent on both acute (altering the steroidogenic enzyme activity) and chronic (impacting Leydig cell differentiation and gene expression) stimulation of Leydig cells by the anterior pituitary's luteinizing hormone (LH). Age-related reduced testosterone was found to result from reduced Leydig cell steroidogenesis, but not by their loss, while EDS causes the loss of adult Leydig cells (Payne & Hardy. 2007). Some testosterone is released into the blood capillaries present in the testicular interstitium and contributes to serum testosterone levels, which is also measured as an indicator of Leydig cell health.

Insulin-like peptide 3 (INSL3) is a small peptide hormone secreted by Leydig cells in testes and contributes to testicular hormone circulation. Other peripheral tissues may also secrete INSL3 but these do not contribute to testicular hormone circulation (Fig. 3). In mammals, both the fetal and the adult Leydig cells secrete INSL3. In the male fetus, the primary role of INSL3 is to induce the transabdominal phase of testicular descent after sex differentiation (Ivell *et al.* 2014). INSL3 binds to

relaxin/insulin-like family peptide receptor 2 (RXFP2), present on the gubernacular bulb, and initiates testicular descent in the inguinal region. Subsequent inguino-scrotal migration of testis requires androgens but not INSL3 (Ivell *et al.* 2014). Adult Leydig cells also secrete INSL3, but the function of INSL3 in adult testis remains unknown. It is believed that INSL3 may be a stabilizing factor to maintain Leydig cell capacity (Ivell *et al.* 2014, Payne & Hardy. 2007). INSL3 is considered a constitutive biomarker for both Leydig cell differentiation (maturity) and cell number. Thus measurement of INSL3 mRNA in testis or INSL3 as a secreted peptide circulating in blood proclaims the "functional capacity" of Leydig cells (Foresta *et al.* 2004, Ivell *et al.* 2013, Ivell *et al.* 2014) (Fig. 3). INSL3 is not under the acute and pulsatile LH regulation of the HPT-axis and has no feedback inhibitions on the anterior pituitary (Ivell *et al.* 2014). Anterior pituitary also releases follicle-stimulating hormone (FSH) that binds to follicle stimulating hormone receptors (FSHR) localized on the Sertoli cell surface and stimulate Sertoli cells. Sertoli cells secrete a dimeric protein, inhibin B that feeds back to inhibit the synthesis of FSH by the anterior pituitary (Ivell *et al.* 2014, Walker & Cheng. 2005).

LHR, 3β-HSD, StAR and INSL3 are the receptors, enzymes, transporter molecules and secretory products, respectively that are localized mainly to or secreted by the Leydig cells (Luo *et al.* 2001, Teerds *et al.* 1999). Therefore, the gene and protein expression of these molecules are good biomarkers to test for Leydig cell loss and functional capacity after EDS treatment in adult rats.

Testicular macrophages, pro-apoptotic and pro-inflammatory cytokines

Testes provide a unique immunoregulatory environment for the germ cells to differentiate and mature, as the testicular immune cells protects the germ cells from exogenous antigens, while still protecting the endogenous antigens of spermatogenesis (Nasr *et al.* 2005, Payne & Hardy. 2007, Winnall *et al.* 2011, Yang. 2015). The blood-testis barrier formed by the Sertoli – Sertoli cell interactions physically restricts the immune cells and other cell types from entering the seminiferous tubules during the development of spermatocytes; however, the testicular interstitium is freely accessible to the immune cells from the peripheral blood circulation. The immune cells present in testes include; monocytes, resident testicular macrophages, lymphocytes, neutrophils and natural killer cells, and these immune cells are mostly phagocytic (Frungieri *et al.* 2002). Monocytes are part of the innate immune system and play roles, such as: (a) replenishing resident macrophages under physiological conditions and (b) upon inflammation, the monocytes from the blood circulation are quickly recruited to the site of tissue infection and damage. At the site of infection, monocytes can divide/differentiate into macrophages and dendritic cells, to elicit an adaptive immune response. Macrophages plays a part in both adaptive and innate immunity and the cytokines secreted by them can further initiate adaptive immune response, as they activate other immune cells, such as lymphocytes. Neutrophils are a type of leukocytes that are essential for innate immunity and can be recruited quickly to the site of tissue infection. Natural killers cells are a part of both innate and adaptive immunity. Macrophages and neutrophils are also phagocytic in nature (Payne & Hardy. 2007).

Immune cells that find their way into the testis appear to be functionally modified to restrict their pro-inflammatory activity and provide an immunologically suppressed environment where immune responses are blunted and/or limited (Payne & Hardy. 2007). However, these suppressed immune cells can become inflammatory if needed to help protect testicular cells from toxicants and pathogens.

Intimate association of Leydig cells with the adjacent macrophages was first observed in the 1960s and has been a prime area of focus and investigation during past decades. The Leydig cells are inter-digitated with the surrounding resident macrophages. Mouse and rat studies show that the number of Leydig cells interacting with macrophages has a relatively fixed stoichiometry at about one macrophage for every four or five Leydig cells (Hardy *et al.* 1989, Niemi *et al.* 1986, Payne & Hardy. 2007). Various speculations have been made about a direct physical contact between Leydig cells and macrophages, such as: (a) macrophages metabolize the steroids secreted by Leydig cells, and (b) Leydig cells are induced with the steroidogenic molecules, pro-inflammatory molecules and cytokines secreted by macrophages (Payne & Hardy. 2007). The selective depletion of testicular macrophages prevents Leydig cell regeneration after EDS treatment, through unknown ways (Gaytan *et al.* 1994, Wang *et al.* 1994). Thus, there seems little doubt that macrophages play an important role in Leydig cell development. Heterogeneity of testicular macrophages (i.e. macrophages at different stages of differentiation as they evolve from monocytes) was seen after lipopolysaccharide (LPS) induction in rats and also in rats treated with EDS (Dijkstra, *et al.* 1985, Gerdprasert & 'et al.'. 2002, Wang, *et al.* 1994). The two types of

macrophages found in testis are inflammatory-infiltrating monocytes/newly arrived macrophage (also called subtype M1 and identified by antibody-ED1) and resident tissue macrophage (also called subtype M2 and identified by antibody-ED2) (Suescun *et al.* 2003). As the inflammatory-infiltrating monocytes/macrophage (identified as, $ED1^{+}ED2^{-}$) convert to resident tissue macrophages, they stain less for $ED1^{+}$ and more for $ED2^{+}$ and finally become $ED1^{-}ED2^{+}$, resident macrophages.

Antibody-ED1 recognizes cluster of differentiation 68 (CD68), located on monocytes (O'Reilly & Greaves. 2007, Suescun *et al.* 2003). Expression level of CD68 is a marker for inflammatory-infiltrating monocytes/newly arrived macrophages. Antibody-ED2 recognizes the cluster of differentiation 163 (CD163) present on resident macrophages (Hedger. 2002, Kern *et al.* 1995, Onofre *et al.* 2009, Suescun *et al.* 2003, Yee & Hutson. 1985). Monocytes divide into macrophages and dendritic cells, but CD163 is expressed only on macrophages and not on dendritic cells, such as Langerhans cells (Buechler *et al.* 2000). Therefore, CD163 can differentiate macrophages from both monocytes and dendritic cells. Due to the restricted expression of CD163 on monocytic lineage cells, CD163 is considered a marker for tissue resident macrophages (Davis & Zarev. 2005). CD163 is associated with homeostasis and anti-inflammatory activity (Onofre *et al.* 2009). In previous studies of rat skeletal muscle, it was observed that $ED1^{+}$ cells were phagocytic and were found around degenerating muscle fibers, while $ED2^{+}$ macrophages were abundant throughout the tissue but not at the site of muscle degeneration (McLennan. 1993). This suggests that upon infection

more monocytes were infiltrated at the site of damage while resident macrophages may be secreting cytokines.

Macrophages play a complex diametric role in testis by releasing both Leydig cell stimulatory and inhibitory factors into the interstitial area. For example, activated testicular monocytes and macrophages secrete pro-inflammatory cytokines, such as tumor necrosis factor (TNF-α) and interleukin-1 (IL-1) (Frungieri *et al.* 2002). Elevated TNF-α and IL-1 levels in human patients have been associated with critical illness, burn trauma, sepsis and rheumatoid arthritis, and as a correlate, these patients experience depressed gonadal function with low serum testosterone (Aderka *et al.* 1998, Calandra *et al.* 1990, Spooner *et al.* 1992, Spratt *et al.* 1992, Vasanthi *et al.* 2007).

Administration of TNF-α to healthy human males and rats also causes a decrease in serum testosterone levels (Hong *et al.* 2004). Elevated TNF-α and IL-1β play a significant role in certain testicular pathologies like testicular torsion and autoimmune orchitis (Lysiak. 2004, Theas *et al.* 2008). Elevated levels of TNF-α affect the HPT-axis at multiple levels and may be involved in direct or indirect reduction in circulatory testosterone levels in systemic illnesses (Van der Poll *et al.* 1993). TNF-α and IL-1 are known to inhibit steroidogenesis of Leydig cells mainly at the transcriptional level by altering the expression of different steroidogenic-enzymes (Lukyanenko *et al.* 1998, Morales *et al.* 2003). For example, in primary cultures of mouse Leydig cells, TNF-α reduced the expression of steroidogenic enzymes, $P450_{scc}$, P450c17 and HSD-3β, and, in primary cultures of porcine Leydig cells, TNF-α reduced

the expression of the StAR mRNA transcripts (Hong *et al.* 2004, Lysiak. 2004, Xiong & Hales. 1993) (Fig. 4). TNF-α inhibits 17 α -hydroxylase/c17-20 lyase gene expression in primary Leydig cell cultures of mouse (Li *et al.* 1995). Thus, we can say that the upregulation of TNF-α in testes can negatively alter steroidogenesis, by regulating the expression of steroidogenic enzymes. Many cell types produce IL-1, but activated monocytes and macrophages are the major producers of secreted IL-1. In mouse, human and rat testes, the receptors for IL-1β are reported to be localized on Sertoli cells, Leydig cells, testicular macrophages, and germ cells suggesting both autocrine and paracrine functions (Gomez *et al.* 1997, Lysiak. 2004, Payne & Hardy. 2007).

The IL-1 family cytokine subtype, interleukin-1 beta (IL-1β), is synthesized as a 31-33 kDa inactive precursor protein that is activated to a 17 kDa form by the action of proteases, such as IL-1 converting enzyme/caspase-1. IL-1β induced acute inflammatory-like changes in testicular microcirculation when injected locally in the adult rats (Bergh *et al.* 1990). IL-1β inhibits LH/human chorionic gonadotropin (hCG) and/or cAMP stimulated testosterone production (Hales. 1992, Hales *et al.* 1992, Hales. 2002, Verhoeven *et al.* 1988). In mouse and rat primary cultures of Leydig cells, IL-1 inhibits cholesterol side-chain cleavage cytochrome P450 ($P450_{scc}$) expression, whereas the gene expression and protein synthesis of StAR are unaffected (Lin *et al.* 1991, Lin *et al.* 1998). Thus, in the presence of IL-1, even if StAR transports cholesterol to Leydig cell mitochondria, not much testosterone will be produced due to the inhibition of first rate-limiting step in steroidogenesis, i.e. cleavage

of cholesterol side chain by enzyme $P450_{scc}$. Secretory capacity of testicular macrophages depends on their paracrine interaction with the surrounding gonadal cells (Frungieri *et al.* 2002). The pro-inflammatory cytokines also have important roles in normal testicular homeostasis because an elevation of their expression can lead to testicular dysfunctions (Diemer *et al.* 2003, Lysiak. 2004).

Apoptotic pathways

Apoptosis is one of the most conserved cell death signaling pathways in all mammals. The two theories that explain the direct initiation of apoptosis of Leydig cells are: (a) Fas/FasL mediated model and (b) TNF/TNFR mediated model. The two models are discussed below in detail.

Fas pathway

Fas ligand (FasL/CD95L), a type II transmembrane protein, belongs to the same family as tumor necrosis factor. Sertoli cells synthesize FasL (D'Abrizio *et al.* 2004, Xiong *et al.* 2009). FasL binds to Fas receptor (Fas), a type I transmembrane receptor protein (i.e. transmembrane proteins with a single stretch of hydrophobic polypeptide with amino terminal facing the outside of the cell and carboxy terminal facing the cell cytoplasm), that are localized on germ cells and triggers the death of cells expressing Fas (Nandi *et al.* 1999, Waring & Müllbacher. 1999). Fas acts through the Fas associated death domain (FADD) motif in their cytoplasmic regions and activates initiator caspases, such as caspase-8. Active caspase-8 cleaves the executioner caspases, such as caspase-3, and directly initiates apoptosis or activates the intrinsic apoptotic pathway (McIlwain *et al.* 2013). The loss of testosterone cause Fas mediated

germ cell and Leydig cell apoptosis in adult rat testis after EDS administration (Nandi *et al.* 1999, Taylor *et al.* 1999, Woolveridge *et al.* 1999).

Tumor necrosis factor alpha (TNF-α) pathway

TNF-α/CD120 is a 17kDa glycosylated polypeptide primarily synthesized by activated monocytes and macrophages. TNF-α is synthesized as a monomeric cytokine, but in order to be active and bind to its receptors, TNF-α needs to trimerize. In mammalian testes, TNF-α is also secreted by round spermatids, pachytene spermatocytes and germ cells (Lysiak. 2004). TNF-α transduces its effects through receptor trimerization of two distinct TNFα receptors (TNFRs): (a) TNFR type I (TNFR1/ CD120a/TNFRSF1A − which can initiate both apoptotic and an anti-apoptotic signaling), are found on Sertoli, Leydig cells and all other testicular cells, such as macrophages (Fig. 1). (b) TNFR type II (TNFR2/CD120b/TNFRSF1B − which activates an anti-apoptotic pathway), are expressed mostly on the immune cells, but also on Leydig cells and endothelial cells (Aggarwal. 2000, Bauda & Karinb. 2001, Darnay & Aggarwal. 1999, Lysiak. 2004, MacEwan. 2002) (Fig.1). TNFR1 induce cell death through a motif in their cytoplasmic regions called the death domain. In contrast, the death domains are absent from TNFR2 (see Fig.1). TNFR1 associated death domain (TRADD) is a death domain motif that binds to the downstream adaptor molecules, such as FADD, and initiate apoptosis through caspase-8 and caspase-3 mediated pathways directly or through the activation of intrinsic apoptotic pathway. In contrast, TNFR1 can bind to the other adaptor protein molecules like TNF receptor associated factor-2 (TRAF-2) and initiate cell proliferation through one of the cell

survival pathways like nuclear factor kappa-light-chain-enhancer of activated B cells (NF-κB) or c-Jun N-terminal kinases (JNKs) pathway (Bauda & Karinb. 2001). TNF-α regulates different cellular processes pertinent to spermatogenesis including steroidogenesis, germ cell apoptosis, cell survival, growth hormone function and inflammation (Li *et al.* 2006, Pentikainen *et al.* 2001, Suominen *et al.* 2004). TNF-α also stimulates the release of IL-1 and IL-6 from activated monocytes and macrophages, and the synthesis and release of IL-1 and IL-6 is enhanced by interferon gamma (IFN-γ) secreted from activated T-lymphocytes (Spooner *et al.* 1992). Thus, cytokines, such as TNF-α can induce additive or synergistic effects by initiating the production of other cytokines, such as IL-1. TNF-α is a major protective cytokine as it recruits and activates neutrophils, macrophages and lymphocytes when attacked by external toxicants and due to exogenous antigen action. The secretion and degradation of TNF-α and other cytokines orchestrate the mechanism of cell survival and cell death. The half-life of these cytokines might also be important in defining their activity in the cells. Cytokines are usually expressed for short times and degrade soon after initiating a cellular response. For example, TNF-α mRNA has a half-life of 44 - 46 min in mouse macrophage cell lines and TNF-α protein has a half-life of 2.5 hr (Aderka *et al.* 1998, Mijatovic *et al.* 2000). In primary human monocytes, the mRNA for TNF-α has a short half-life of 20 - 30 min (MacKenzie *et al.* 2002).

Tumor necrosis factor beta (TNF-β)

TNF-β, now named as lymphotoxin, is a N-glycosylated protein of 171 amino acids. TNF-β is secreted by leukocytes. TNF-β binds to the same receptors as TNF-α

but is less potent than TNF-α and has mostly a paracrine role (Spahn *et al.* 2005). The presence and role of TNF-β has not been well studied in testis.

Inhibition of TNF-α

TNF-α play a central part in the host immune response to parasitic infections. Although, TNF-α is crucial to the protective immune response, it also plays a role in the pathogenesis of both infectious and autoimmune diseases (Corral & Kaplan. 1999, Corral *et al.* 1999). Increased concentration of TNF-α also triggers the lethal effects in patients with septic shock syndrome. In patients with tuberculosis, cancer, rheumatoid arthritis and many other acute and chronic diseases, the inhibition of TNF-α by thalidomide, alleviate the symptoms related to such disease (Corral & Kaplan. 1999, Saito *et al.* 2007). In past studies, neutralization of TNF-α by anti-TNF-α antibodies led to a dramatic reduction in disease activity of patients suffering with rheumatoid arthritis and inflammatory bowel disease, such as Crohn's disease. Along with TNF-α, there was also a reduction in IL-1 levels (Maini *et al.* 1995, Saito *et al.* 2007, Van Dullemen. 1995). Thus, it was felt important to reduce TNF-α concentrations in an effort to prevent Leydig cell loss caused after EDS treatment.

TNF-α inhibitory compounds, such as thalidomide; is an immunomodulatory drug that has a number of side effects. For example, it causes birth defects when taken during early pregnancy. Therefore, lenalidomide (Revlimid), analogue of thalidomide, has been designed which has increased anti-TNF-α activity but reduced toxicities (Armoiry *et al.* 2008, Corral *et al.* 1999, Muller. 1999). Lenalidomide has a neuroprotective effect in lateral sclerosis as it destabilizes the mRNA expression of

TNF-α, suggesting this to be the mechanism of action of lenalidomide (Kiaei *et al.* 2006).

Hypotheses

In the present study, we investigated the molecular mechanism of Leydig cell apoptosis in the adult rat testis at 6, 15 and 24 hours after EDS administration. We chose these time points since there was no Leydig cell apoptosis until 6 hr after a 85 mg/kg intraperitoneal injection of EDS in adult rats while maximum Leydig cell apoptosis was observed at 24 hr after EDS treatment (Nandi *et al.* 1999). Considering a mid point close to 24 hr, we selected 15 hr as the intermediate time point to study the effect of EDS. Fas proteins were tested in the previous studies to cause Leydig cell and germ cell apoptosis after EDS treatment; therefore, we tested for the changes in gene expression of Fas and FasL after EDS treatment (Nandi *et al.* 1999, Rommerts *et al.* 1988). We also tested for the potential involvement of TNF-α pathway, in Leydig cell apoptosis. Thus, our hypothesis are; (1) to test for the loss of Leydig cells- we selected various Leydig cell gene markers; (2) to observe and quantify increased DNA fragmentation in testicular interstitium- we performed TUNEL assay; (3) to test the changes in immune cells within testes- we selected the gene markers for monocytes and tissue resident macrophages; (4) to test the increase in pro-apoptotic and inflammatory cytokines and ligands- we tested for the gene and protein expression of cytokines and ligands, such as TNF-α and FasL. Along with testing for the change in cytokines and ligands, we also tested for the change in cytokine and apoptotic receptors, such as TNFRs and Fas, using gene expression; and (5) to test if inhibition of

TNF-α can prevent loss of Leydig cells, caused after EDS treatment- we used lenalidomide treatment. We postulated that:

(1) **There will be an increased expression of tissue resident macrophage receptors:** This was tested by evaluating the changes in gene expression of molecular markers for monocytes (CD68) and tissue resident macrophages (CD168).

(2) **There will be an activation of the pro-apoptotic and pro-inflammatory cytokines/ligands initiator genes after EDS treatment:** This was tested by evaluating the changes in gene expression of molecular markers for pro-apoptotic and inflammatory cytokines/ligands, such as FasL, IL-1β, TNF-α and TNF-β.

(3) **There will be an increased expression of the apoptotic receptor genes after EDS treatment:** TNFR1 is involved in apoptosis and anti-apoptosis, and TNFR2 is involved in anti-apoptotic pathways. We hypothesis that, the imbalance or increased apoptotic and decreased anti-apoptotic receptors may lead to Leydig cell loss. Therefore, we tested our hypothesis by measuring the mRNA expression of the two TNF receptors (TNFR1 and TNFR2). To test the increased expression of other apoptotic markers, we analyzed mRNA expression of Fas and TNFRSF11a (data not shown).

(4) **TNF-α antagonist will inhibit Leydig cell loss after EDS treatment:** In an effort to prevent Leydig cell loss caused after EDS treatment, we tested if lenalidomide (TNF-α release blocker) in combination with EDS, can upregulate the gene expression of Leydig cell markers, such as 3β-HSD and INSL3.

CHAPTER II

MATERIALS AND METHODS

Drugs

Ethylene dimethane sulfonate (EDS) was synthesized in our laboratory using previously published methods (Jackson & Jackson, 1984) as it is not commercially available. EDS (75 mg/kg) was dissolved in 25% dimethylsulfoxide (DMSO from Amresco) and 75% deionized water. Lenalidomide (Selleckchem) (50 mg/kg) was dissolved using 25% DMSO and 75% propylene glycol.

Animal model

Adult male Sprague-Dawley rats (age 90 ± 20 day, weight > 300 gm) were purchased from Charles River Laboratories and were housed and maintained in the TWU vivarium under controlled temperature (23 °C) and a 14L : 10D photoperiod. Standard laboratory chow and drinking water were provided *ad libitum* and rats were acclimated for 5−10 days before any treatment. All the experimental procedures involving animals were carefully performed and approved by Texas Woman's University's Institutional Animal Care and Use Committee (IACUC) and adhere to Public Health Services (PHS) guidelines.

EDS treatment paradigm

The three time points tested for EDS treatment paradigm were 6, 15 and 24 hr. Based on similar body weight, the rats were assigned into three groups (n = 6/group) for each time point. The treatment groups were as described in table 1. All the animals

were injected intraperitoneally. After the animals were anesthetized with Isoflurane®, disposable syringes and 23-gauge needles were used to inject group specific chemicals. The animals were euthanized at 6, 15 or 24 hr after treatment and samples were collected.

Table 1 EDS treatment paradigm

NT (Non - treated)	**Veh** (Vehicle - treated)	**EDS** (Ethylene dimethane sulfonate -treated)
Non-treated	25% DMSO (75% deionized water)	75 mg/kg EDS dissolved in 25% DMSO (75% deionized water)

Lenalidomide treatment paradigm

The only time point tested for lenalidomide treatment paradigm was 24 hr. Based on similar body weight, the rats were assigned into five groups (n = 3/group). The treatment groups were as described in table 2. All the animals were injected intraperitoneally. After the animals were anesthetized with Isoflurane®, they were injected with group specific chemicals. All animals were euthanized 24 hr after treatment and samples were collected.

Table 2 Lenalidomide treatment paradigm

NT (Non - treated)	**Veh** (Vehicle - treated)	**EDS** (Ethylene dimethane sulfonate - treated)	**Leno** (Lenalidomide -treated)	**EDS + Leno** (Ethylene dimethane sulfonate and lenalidomide - treated)
Non - treated	(a) 25% DMSO (75% deionized water)	(a) 75 mg/kg EDS dissolved in 25% DMSO (75% deionized water)	(a) 50 mg/kg lenalidomide dissolved in 25% DMSO (75% propylene glycol)	(a) 75 mg/kg EDS dissolved in 25% DMSO (75% deionized water)
	(b) 25% DMSO (75% propylene glycol)	(b) 25% DMSO (75% propylene glycol)	(b) 25% DMSO (75% deionized water)	(b) 50 mg/kg lenalidomide dissolved in 25% DMSO (75% propylene glycol)

Collection of tissue

Rats were anesthetized with Isoflurane® and sacrificed by decapitation at 6, 15 and 24 hr after treatment. Testes were excised and washed in 1X cold phosphate buffered saline (PBS; 137 mM NaCl, 2.7 mM KCl, 10 mM Na_2HPO_4 and 2 mM KH_2PO_4, pH 7.4 were q.s. to 1.0 lt., using deionized water). Testes were trimmed of excess connective and fatty tissue and weighed. The right testis (#1) was used for total RNA and protein extraction and the left testis (#2) was fixed in modified Davidson's Fluid (mDF; 30% formaldehyde, 15% ethanol and 5% glacial acetic acid, pH 3.2) for 24 hr at 4 °C for histological analysis and TUNEL assay. After being anesthetized

with Isoflurane®, the samples from lenalidomide experiments were collected at 24 hr after treatment. Samples from lenalidomide experiments were used for RNA extraction only.

RNA extraction and quantification

Total RNA was extracted after careful removal of the tunica albuginea from each right testis (#1). Testicular tissue was processed for total RNA extraction using TRIzoL® (Invitrogen) in accordance with the manufacture's protocol. For the extraction of total RNA, approximately 200 mg tissue from each animal of a treatment group was homogenized in 2.0 ml TRIzol using an Ultra-Turrax tissumizer from Tekmar for one min in a 15 ml polypropylene tube. Homogenizer was set to generate a torque of 2300 rotations/min, recorded by IKA-TRON Drehzahlmesser DZM 5 tachometer. The homogenate was incubated for 15 min in a 30 °C water bath. Following incubation at 30 °C, 0.20 ml of chloroform/ml of TRIzol were added to homogenates and vortexed vigorously. The chloroform containing homogenate was incubated at room temperature for 15 min followed by centrifugation at 9000 X G for 15 min at 4 °C. Centrifugation resulted in separation of homogenate into two distinct phases, a clear (aqueous) phase on top of a red layer (organic phase). The aqueous phase (containing total RNA) was carefully transferred to a new 2 ml polypropylene tube and the organic phase was discarded into chemical waste. An equal volume of 100% isopropanol was added to the aqueous phase; tubes were vortexed and incubated at -20 °C for 30 min to facilitate the precipitation of total RNA. Tubes were centrifuged at 9000 x G for 20 min at 4 °C and the alcohol content was discarded. The

total RNA was collected as a white pellet at the bottom of each tube. One milliliter of 75% ethanol for each milliliter of TRIzol was added to the tube and vortexed thoroughly to wash any phenol residue from the RNA pellet. The total RNA was centrifuged again at 9000 x G for 20 min at 4 °C. The supernatant of ethanol was decanted and the pellet air-dried for 20 min at room temperature. The RNA pellets were dissolved in 500 µl Tris-EDTA (1.0 mM Tris, 0.1 mM EDTA, pH 7.2) and stored at -20 °C for further analysis.

Quantification and intactness of total RNA

The extracted total RNA was diluted 100-fold in Tris-EDTA to determine the extraction yield, purity and intactness using UV160U uv-visible recording spectrophotometer (Shimadzu). The purity of RNA was assessed by the A_{260nm}/A_{280nm} ratio ranging between 1.8-2.0. The extinction coefficient of 25 A_{260nm}/mg of RNA was used to calculate total RNA concentration for each extract. The RNA stocks were diluted to a concentration of 0.5 µg/µl and stored at -20 °C for later gene analysis. Three micrograms of RNA were subjected to 1.5% agarose gel electrophoresis and stained with 0.5 µg/ml of ethidium bromide for one hour to verify the quality and intactness of RNA. The gel picture was captured with the help of Alpha Innotech Fluor Chem® HD2 imager and stored using Alpha Ease Fluor Chem HD2 gel imaging software.

Reverse transcription-polymerase chain reaction (RT-PCR)

Total RNA extracts were used to make complementary DNA (cDNA) using Super Script III™ First-Strand Synthesis System kit for RT (Invitrogen) in accordance

to the manufacture's protocol. The reaction took place in a thermo cycler (PTC-100 from MJ Research or BIO- RAD CFX 96^{TM} Real-Time System). For synthesis of cDNA, 2.0 μg of total RNA were mixed with 1.0 μl of 50 μM oligo $(dT)_{20}$ (to target the poly A tail of mRNA) and 1.0 μl of dNTP set containing 20 mM each dNTP. The reaction mix was heated to 65 °C for 5 min to denature the secondary structures of the RNA. To that RNA mix, 10 μl of cDNA synthesis mix [2.0 μL of 10 X RT buffer, 1.6 μL of 25 mM $MgCl_2$, 2.0 μL of 0.10 M DTT, 1.0 μL of RNaseOUT (40 U/μL), and 1.0 μL of Superscript III® Reverse Transcriptase (200 U/μL) + 2.40 μL of deionized H_2O] were added and incubated for 50 min at 48 °C for synthesis of cDNA. Denaturing the reverse transcriptase at 85 °C for 5 min terminated the cDNA synthesis reaction. From the resultant RNA/DNA hybrid, RNA was digested with 1.0 μL of RNase H at 37 °C for 40 min. The 21 μL final volume of cDNA was diluted 25-fold with 25 μg/mL acetylated-BSA (Invitrogen) for quantitative polymerase chain reaction (qPCR).

Primer design

Selected gene markers (*Hsd3b2, Lhr*, *Insl3, Star, Tnfα*, *Tnfβ, Il1β, Tnfrsf1a*, *Tnfrsf1b*, *Cd68*, *Cd163* and *Gapdh*) were targeted using specifically designed gene primers of 25 − 35 bases for both (+) and (-) strands of DNA encoding the gene. Primer sequences for this study are listed in Table 3. Since DNA polymerase requires an open 3'−OH group for strand extension, primers are required to initiate DNA synthesis. To keep the cycle time short and to ensure the completion of dsDNA fragments, the primers were designed to achieve short dsDNA products with 3' specific

primer sets. Every primer had a Tm of 64 − 66 °C and a GC content of 40 − 60%. The product length of the amplified cDNAs was kept to approximately 210 − 300 bp to have comparable cycle numbers for all the genes to be analyzed. The primer sets for the targeted regions of the genes were picked from two different exons to assure that the amplified cDNA is only from the original cDNA and not from genomic DNA that might be present as a contaminant from the RNA extraction procedure. If genomic DNA is amplified, then the product lengths will be longer than the ones designed (210 − 300 bp) because they will include both parts of the exons and the intron. All the primers were designed using Invitrogen's Vector NTI® Advance V.11 software and checked using NCBI's Primer-BLAST. Desired primers were synthesized by Biosynthesis (Lewisville, TX). The synthesized primers were made to a stock concentration of 10 μM with 25 μg/ml of acetylated-BSA (Invitrogen) and stored at −20 °C until use. The working stocks of primer sets were prepared by combining 100 μL of 10 μM forward primer and 100 μL of 10 μM reverse primer in 800 μL of 25 μg/ml acetylated-BSA (Invitrogen).

Table 3 Primer sequences of genes of interest and quantification cycle (Cq) value

Genes of Interest	Gene Bank® Accession Code	Primer Sequence (With respect to the accession code)	Product Length	Cq value
Lhr	NM_012978.1	**Forward + 1370** 5'- TGCGGTGCAGCTGGCTTCTTTACTG -3' **Reverse – 1605** 5'- ATGGGGAGGCAGATGCTGACCTTC -3'	236 bp	25
Insl3	NM_053680.1	**Forward + 185** 5'- TGCAGTGGCTGGAGCAACGACATC -3' **Reverse – 449** 5'- TTCATTGGCACAGCTGTNAGGTGGG -3'	265 bp	19
Hsd3b2	NM_001042619.1	**Forward + 1020** 5'- CTGCTCTACTGGCTTGCCTTCCTGCTG -3' **Reverse – 1258** 5'- TCCAGTGTCTCCCTGTGCTGCTCCA -3'	239 bp	20
Star	NM_031558.3	**Forward + 519** 5'- TGAAGAACTGGTGGACCGCATGGAG -3' **Reverse – 744** 5'- CATCTCCCCAAAGTGTGTGGCCATG -3'	226 bp	21
Cd 68	NM_001031638.1	**Forward + 712** 5'- AATGTGTCCTTCCCACAAGCAGCACAG -3' **Reverse – 946** 5'- GAGGCAGCAAGAGAGATTGGTCACTGG -3'	235 bp	25
Cd163	NM_001107887.1	**Forward + 3105** 5'- ATGAGTCTTCCCTGTGGGATTGTCCTGC -3' **Reverse – 3317** 5'- TCTGTCGTCGCTTCAGAGTCCACAAGA -3'	213 bp	26
Il1β	NM_031512.2	**Forward + 803** 5'- CCTAGGAAACAGCAATGGTCGGGACA -3' **Reverse – 1042** 5'- TGTCAGAGGCAGGGAGGGAAACACA -3'	240 bp	31
Tnfα	NM_012675.3	**Forward + 426** 5'- CGTCGTAGCAAACCACCAAGCGGA -3' **Reverse – 675** 5'- GCTCTTGATGGCAGAGAGGAGGCTGAC -3'	250 bp	30
Tnfβ	NM_080769.2	**Forward + 616** 5'- GCTACAAGGACCGTGGGTACGCTCAAT -3' **Reverse – 856** 5'- GGCTATTTTGGTTGGGAAGGCTGGAG -3'	241 bp	30
Tnfrsf1a	NM_013091.1	**Forward + 1639** 5'- TCAGGAACGGGACTCGAAGGACCATC -3' **Reverse – 1857** 5'- TGTCTGGGAGCAGATGGCACACTTCC -3'	219 bp	24
Tnfrsf1b	NM_130426.4	**Forward + 2302** 5'- CTGTACTCGCTGTGACCCAAGTGCATG -3' **Reverse – 2535** 5'- CTGTGAGCATGGCATCCAAGCACC -3'	234 bp	27
Gapdh	NM_017008.4	**Forward + 740** 5'- TGAACGGGAAGCTCACTGGCATGG -3' **Reverse - 973** 5'- CAATGCCAGCCCCAGCATCAAAG-3'	234 bp	18

Quantitative real-time polymerase chain reaction (qPCR)

To quantify mRNA abundance in the testicular tissue, we used 3.0 μg of the cDNA preparation for q-PCR using Roche's Fast Start SYBR Green Master Mix (Rox) kit in accordance with the manufacture's protocol. MJ Opticon Monitor 3.1 software on the Opticon 2 real-time PCR system or BIO- RAD CFX 96^{TM} Real-Time System using Bio-Rad CFX Manager 2.1 were used to quantify the amplified dsDNA by detecting the cycle numbers (Cq). A 3.0 μL working stock of the primer sets were added to the PCR tubes and to this 22.0 μL of the reaction mixture [13.0 μL Roche's Fast Start SYBR Green Master Mix, 6.0 μL of the diluted cDNA (1:25) and 3.0 μL of deionized H_2O] were added. The cycles were set at 95 °C for 10 min for hot start of the Taq polymerase, followed by 40 cycles of template denaturation at 94 °C for 30 sec, primer annealing at 60 °C for 25 sec and primer extension at 72 °C for 25 sec. The temperature was increased to 78 °C and, after a 9.0 sec pause, the fluorescence of the bound SYBR Green was measured. After 40 cycles, the temperature was ramped slowly to obtain the melting curve of the amplified dsDNA product to establish the quality and accuracy of the dsDNA synthesis. The qPCR products were also assessed for dsDNA product quality by agarose gel (1.5%) electrophoresis. For each gene, one band is expected in each lane of their respective product size. Reactions with no template were run concurrently as negative controls and glyceraldehyde 3-phosphate dehydrogenase (*Gapdh*) was used as the housekeeping gene. Comparison of differences in quantity of the mRNA expressions between the treatments was analyzed

using the $2^{-\Delta\Delta C(q)}$ method (Vermeulen. 2009). Each qPCR sample was run in duplicate and all the experiments were repeated 3 to 6 times.

Cleaning the qPCR products and sequencing

The qPCR products were cleaned of excess primers and nucleotides using HT ExoSAP-IT® High-Throughput PCR Product Clean Up kit (Affymetrix). The dsDNA product was sequenced at GENEWIZ using the Sanger DNA sequencing method. The acquired sequences were checked for specificity using BLAST (NCBI).

Preparation of the fixative

The modified Davidson's fixative (mDF, pH 3.2 − 3.4) was prepared by mixing 30 ml of 37% formalin (11% formaldehyde) (Fisher), 15 ml of absolute ethanol (15%) and 5 ml of 0.9 M glacial acetic acid (Sigma) in 50 ml of de-ionized water. Modified Davidson's fixative was prepared 3-5 days in advance of usage since methylene hydrate (the reactive form of formaldehyde in water) is formed slowly at a lower pH.

Preparation of slides

Untreated glass slides cannot hold the tissue sections for extended procedures and proteinase K digestion; therefore, slides were thoroughly processed and coated (subbed). Glass slides (Fisher) were thoroughly cleaned by soaking in soap and tap water for 20 min each, followed by soaking in an acid-alcohol solution [1N HCl (EM Science) & isopropanol (Pharmaco-Aaper) (1:3)] for 20 min. The slides were rinsed with tap water and finally with de-ionized water. Slides were air-dried and subbed with a chromate-collagen subbing mixture, prepared by boiling 0.50 gm bovine gelatin (EM Science, Gibbstown, NJ, USA) and 0.50 ml Hi-pure liquid gelatin (cod fish,

Norland Products, North Brunswick, NJ, USA) in 80 ml of de-ionized water. Upon cooling, 0.20 gm of chrome alum [$CrK(SO4)_2 \cdot 12H_2O$] (EM Science) was added to the subbing mixture. Subbed slides were air-dried overnight at room temperature and stored in slide boxes at 4 °C until use. The slides were brought to room temperature before placing the tissue sections to avoid any moisture collection between the tissue sections and the subbed surface.

Tissue fixation and paraffin wax embedding

The left testes (#2) were carefully trimmed to remove any extra tissue and were soaked in modified Davidson's fixative (mDF) at a tissue to fixative ratio of 1:10 (weight by volume ratio). The testes were carefully pierced several times using a 23-gauge needle to facilitate permeation of the fixative inside the tissue and stored at 4 °C. After two hours of incubation, the testes were sliced horizontally into three pieces using a sharp razor blade. The three pieces were again immersed in mDF for 24 hr in the refrigerator. The fixed testes were dehydrated at 4 °C in ascending concentrations of 70%, 90% and 100% ethanol (Pharmaco-Aaper) for 2 hr each. Post-dehydration, the testes were cleared at room temperature by xylene-ethanol immersion (2 hr in 50:50 mix of xylene and ethanol). The solution was replaced with two exchanges of 100% xylene (Fisher Scientific) for 2 hr incubation each at room temperature. The testes were incubated for 1 hr at 60 °C in 50 : 50 mix of wax and xylene for removal of any xylene left in the tissue and to fill the empty tissue spaces with the paraffin wax. Wax-xylene mix was replaced with three changes of pure molten wax for 1 hr each at 60 °C. The three pieces of testis were placed into separate stainless steel molds for paraffin

wax embedding. The 7.0 μm thick sections were cut from each tissue block using a rotary microtome (Reichert Histo STAT). The wax ribbons were spread on a 40 °C water bath, carefully placed on subbed slides, and heated on a slide warmer to allow the sections to adhere to the slides. The slides with adhered sections were stored in slide boxes and refrigerated until use.

Hematoxylin and eosin (H&E) staining

The H&E staining procedure was performed at room temperature (Fischer *et al.* 2008). Sections on slides were de-waxed in xylene (Fisher Scientific) for 20 min each and replaced with fresh xylene at least five times. The sections were air dried for 15 min. each between the xylene washes and rehydrated in the descending series of 100%, 90% and 70% ethanol (Pharmaco-Aaper) for 15 min each. Modified Mayer's hematoxylin (American Mater Tech) was diluted 1:1 with de-ionized water and applied to rehydrated testes sections for 3 min. The sections were then counterstained for 3 min with eosin (0.10% Eosin Y; 0.50% glacial acetic acid v/v dissolved in 1.0 L of 70% ethanol). For coverslip mounting, the sections were dehydrated by soaking slides for 5 min each in 70%, 90% and 100% ethanol (Pharmaco-Aaper) and finally for 5 min in xylene. A few drops of permount were added and the sections were mounted with a coverslip. All the experiments were repeated three times.

In situ localization of fragmented DNA by TUNEL

Terminal deoxynucleotidyl transferase dUTP nick end-labeling (TUNEL) assay was used to individually stain the cells showing fragmented DNA, a hallmark of apoptosis. TUNEL staining of the mDF fixed testis sections was performed using the

ApopTag® Peroxidase *In Situ* Apoptosis Detection Kit (Millipore) in accordance to manufacturer's instructions with minor changes. The sections were de-waxed in 100% xylene and rehydrated in the descending series of 100%, 90% and 70% ethanol (Pharmaco-Aaper) for 15 min. each at room temperature. After rehydration in de-ionized water for 5 min, the sections were washed in PBS (pH 7.4) for 5 min. For better accessibility of the 3'− OH ends of the fragmented DNA in apoptotic cells, the sections were subjected to 3.0 µg/ml of proteinase K (Amresco) for 3 min. at room temperature. In order to reduce non-specific TUNEL staining, loss of antigenic sites and the destruction of tissue architecture, the recommended working strength (20 µg/ml) of the proteinase K. Based on testing, the time (15 min) of incubation was reduced to 3.0 µg/ml and 3 min, respectively. Endogenous peroxidase activity was blocked by quenching the sections with 3% H_2O_2 for 10 min at room temperature. The sections were incubated with terminal deoxynucleotidyl transferase (TdT) at 37 °C for one hr in a humidified chamber to enzymatically label the 3'-OH ends of the fragmented DNA with digoxigenin-conjugated and unconjugated nucleotides (negative control). The nucleotides randomly incorporated by TdT, form an oligomer composed of digoxigenin-conjugated nucleotide and unlabeled nucleotide. Stop buffer provided in the kit was added to the sections to terminate TdT activity. Peroxidase conjugated anti-digoxigenin antibody was applied and the sections were incubated in a humidified chamber for 30 min at room temperature. Digoxigenin-conjugated nucleotide bound by peroxidase conjugated anti-digoxigenin antibody was detected by incubating the sections with peroxidase chromogenic substrate 3,3'-diaminobenzidine (DAB), a

precipitable brown stain. For stain of normal nuclei, the sections were counter stained with Immunomaster's Hematoxylin (American MasterTech, diluted 1:10 with de-ionized water) for 10 min at room temperature. The sections containing no TdT enzyme were processed in parallel as negative controls. All the experiments were repeated three times.

Tissue imaging and cell counting

All the images were captured using the Nikon's eclipse 90i digital microscope. The interstitial apoptotic cells were counted using Nikon's NIS-Element Basic Research version 3.1 software's count tool. For TUNEL positive cell counting; (a) fields were selected randomly for sample analysis; (b) to have non-overlapping sampling, the apoptotic cells were counted in a minimum of 11 to a maximum of 27 different fields; (c) prior to final TUNEL positive cell counting, the parameters for counting were established by working out a subset of images with at least one apoptotic cell in the field; and (d) the computerized counted fields were rechecked visually to remove the wrong ones counted. For counting we selected the six-point circle to standardize the threshold with a lower limit of 26 – 30 and an upper limit of 130 – 150. Mean intensity was selected with a lower limit of 60 and an upper limit of 120 – 140. Circularity of the interstitial cell nucleus was selected between 0.7 – 1.0 and the area of the TUNEL positive cells ranged between 30 and 200. Six iterations were performed on the binary images to remove any non-specific background and 16 iterations were performed to smooth the contours on the binary image. Adobe Photoshop CC was used to adjust the brightness and contrast of the images for visual

presentation. To reduce bias in evaluation, all the slide labels were covered during TUNEL positive cell counting.

Total tissue protein extraction and quantification using BCA assay

Total protein was extracted from frozen testicular tissue (~200 mg) using 2.0 ml of lysis buffer (20 mM Tris, 154 mM NaCl, 10% glycerol, 5 mM EDTA, 0.1% Triton-X100, 0.1% NP-40, 100 μM PMSF, 50 μM NaF, 1 mM ortho-vanadate and 10 mM Na-butyrate Q.S. to 100 ml in deionized water; pH 7.9) in a 15 ml polypropylene tube. The tissue was kept on ice and homogenized for one minute using the Ultra-Turrax tissumizer from Teckmar. The homogenizer was set at 2300 rotations/min as recorded by IKA-TRON Drehzahlmesser DZM 5. After clearing of the big tissue chunks by centrifugation, the supernatant was transferred to a 5 ml polypropylene tube and stored at -20 °C until use. We estimated the total protein concentration using Thermo Scientific™ Pierce™ BCA Protein Assay kit in accordance with the manufacturer's protocol. The protein samples were diluted (1:4) with de-ionized water to fit within the limits of the standard curve. The absorbance was read at 660 nm using a BIO-TEK Synergy HT reader and KC4™ version 3.4, software. The standard curve and the total protein concentrations were calculated using 5- or 4-parameter logistics curve-fitting algorithm in MasterPlex® ReaderFit curve-fitting software for ELISA analysis. Both the standards and the samples were run in duplicate. The BCA assay was repeated four times.

Enzyme-linked immuno sorbent assay (ELISA)

The concentration of TNF-α in the treatment groups was evaluated using BioLegend® Rat TNF-α ELISA MAX™ Deluxe kit following the manufacturer's instruction. The 96 well ELISA plate included in the kit was incubated with pre-titrated capture antibody (diluted 1:200 in 1X Coating buffer). The plate was sealed and incubated overnight at 4 °C. The next day, the plate was washed four times with 300 µl of wash buffer (1X PBS at pH 7.4 and 0.05% Tween-20) in each well. The plate was then incubated with 200 µl 1X Assay diluent (diluted using 1X PBS) to block non-specific protein binding. The plate was sealed and incubated at room temperature for 1 hr with shaking at 200 rpm on a plate shaker. After blocking, the plate was washed 4 times with wash buffer and then incubated with 50 µl of 1X Assay diluent added to each wells. These wells were overlaid with either a 50 µl standard to standard well or 50 µl sample (diluted in 1X Assay diluent) to each sample well. The plate was sealed and incubated at room temperature for 2 hr with shaking. After incubation, the plate wells were washed 4 times each with wash buffer and 100 µl of pre-titrated biotinylated detection antibody (diluted 1:200 in 1X Assay diluent) was added to each well. The plate was sealed and incubated for one hr while shaking at room temperature. Following incubation the plate wells were washed 4 times with the wash buffer. Then 100 µl of Avidin-HRP (diluted 1:1000 in 1X Assay diluent) was added to each well and the plate was incubated for 30 min while shaking at room temperature. After 5 washes, the wells were overlaid with 100 µl of TMB substrate solution (1:1 mix of substrate solution A and substrate solution) and then incubated for 25 min in the

dark. Stop solution (2N H_2SO_4) was added and the absorbance was read at 450 nm and 570 nm within 30 min using a BIO-TEK Synergy HT reader and KC4^{TM} version 3.4, software. The standard curve and the TNF-α concentrations were calculated using 5- or 4-parameter logistics curve-fitting algorithm in MasterPlex® ReaderFit curve-fitting software for ELISA analysis. Both the standards and the samples were run in duplicate. We calculated the ratio of TNF-α to the total protein concentration of that sample (ng TNF-α/ μg total protein). Each ELISA sample was run in duplicate and all the experiments were repeated four times.

Statistical analysis

Data from PCR and ELISA with treatment and time as independent factors were compared by two-way analysis of variance (ANOVA) on Graph-Pad PRISM Version 6.01 software. Analysis was done to compare: (a) the difference between treatments (NT, Veh and EDS- treated), (b) the effect of time points (6, 15 and 24 hr) and (c) the interactions between time and treatment. Post-hoc comparisons were performed with the Sidak's multiple comparison tests with p-value ≤ 0.05 considered to be statistically significant.

The PCR data for lenalidomide inhibition experiments were analyzed using one-way analysis of variance (ANOVA) on Graph-Pad PRISM Version 6.01 software. Analysis was done to compare the differences between treatments at 24 hr. Post-hoc comparisons were performed with the Dunnett's multiple comparison tests and p-value ≤ 0.05 was considered statistically significant. We used t-test to compare NT and Veh-

treated groups in the inhibition assay, with p-value ≤ 0.05 considered to be statistically significant.

CHAPTER III

RESULTS

The potential effect of EDS in Leydig cells was determined by detecting the changes in various gene and protein markers for Leydig cells, monocytes/macrophages, and pro-apototic/pro-inflammatory cytokines and their receptors. The objectives of these studies were: (a) to detect the earliest time where an EDS effect could be identified on Leydig cells- therefore, we tested for loss of *Lhr*, *Insl3*, *Hsd3b2* and *Star* at 6, 15 and 24 hr after EDS, (b) to test the increase in tissue resident macrophage and their activation after EDS treatment- detected by changes in expression of *Cd68* and *Cd163*, (c) to test the increased expression of pro-apoptotic and pro-inflammatory cytokines and ligands- we analyzed the expression of *Fasl*, *Il1β*, *Tnfα* and *Tnfβ* using RT and qPCR; we also tested for the increase in protein expression for TNF-α using ELISA, (d) to test the increased expression of apoptotic receptors- we analyzed the expression of *Fas*, *Tnfrsf1a* and *Tnfrsf1b*, and (e) to test if lenalidomide can inhibit the loss of Leydig cells caused by EDS treatment; we analyzed the expression of Leydig cell markers, *Hsd3b2* and *Insl3* at 24 hr after treatments.

Change in *Lhr, Insl3, Hsd3b2* and *Star* expression in rat testis after EDS treatment

To determine the minimum time when Leydig cells were lost after EDS treatment, we tested for the loss/downregulation in Leydig cell biomarkers. The levels of two Leydig cell-specific mRNAs, luteinizing hormone receptor and insulin-like peptide 3 (*Lhr* and *Insl3*), were quantified using RT and qPCR. These findings

demonstrated a significant treatment effect on *Lhr* ($F_{1, 30} = 71.84$, $p \leq 0.0001$) but no effect of time or the interaction between time and treatment ($p > 0.05$). *Lhr* of EDS-treated rats was significantly reduced by 64%, 80% and 88% at 6, 15 and 24 hr, respectively (Fig. 6).

In contrast to *Lhr*, an EDS-induced change in mRNA for Insl3 did not occur until 15 hr after treatment. There was a significant effect of treatment ($F_{1, 27} = 31.99$, $p \leq 0.0001$), time ($F_{2, 27} = 8.964$, $p \leq 0.0010$), and the interaction between time and treatment ($F_{2, 27} = 7.861$, $P \leq 0.0020$) on *Insl3*. *Insl3* of EDS-treated rats was significantly reduced by 18% and 87% at 15 and 24 hr respectively, but not at 6 hr (Fig. 7).

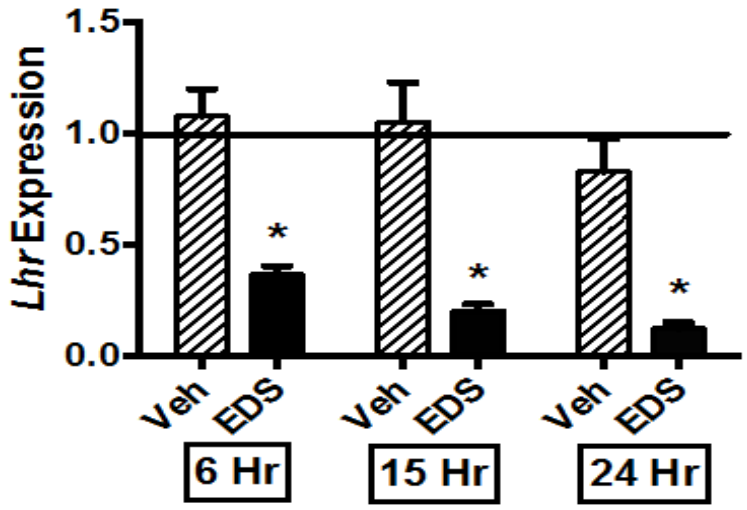

Figure 6
The expression of *Lhr* relative to *Gapdh* as the reference gene. The horizontal line is the normalized value for non-treated (NT) rats. Error bars represent SEM with n = 6 and (*) indicates a significant difference between EDS and vehicle (Veh)-treated rats within the same time of treatment.

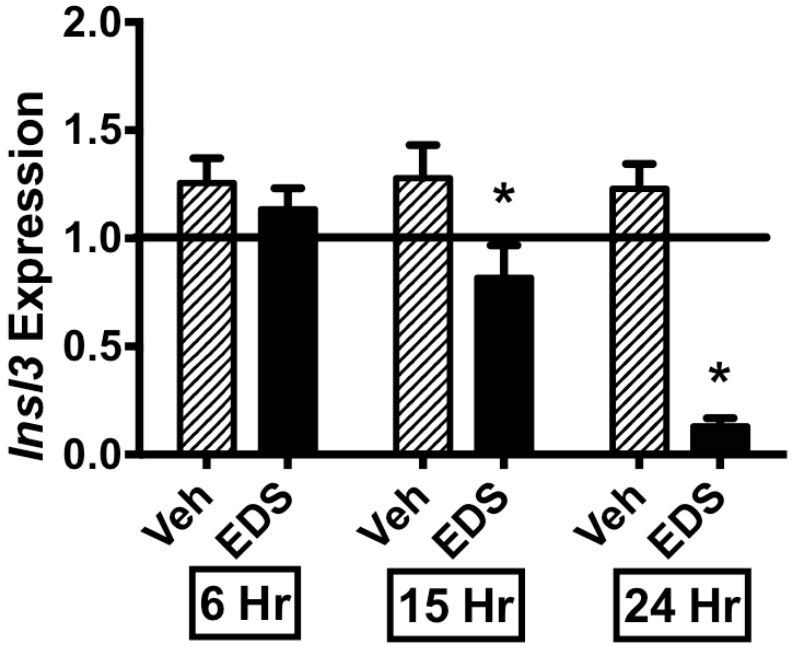

Figure 7
The expression of *Insl3* relative to *Gapdh* as the reference gene. The horizontal line is the normalized value for the non-treated (NT) rats. Error bars represent SEM with n = 6 and (*) indicates a significant difference between EDS and vehicle (Veh)-treated rats within the same time of treatment.

We also examined the potential changes in mRNA for the Leydig cell specific enzyme, 3-beta-hydroxyl steroid dehydrogenase (*Hsd3b2*)- involved in steroidogenesis, and Leydig cell specific transporter protein, steroidogenic acute regulatory protein (*Star*)- involved in cholesterol transfer between mitochondrial membranes; mRNA were quantified by RT and qPCR to further confirm the degree of Leydig cell loss. These findings demonstrate a significant effect of treatment ($F_{1, 29} = 23.99$, $p \leq 0.0001$), time ($F_{2, 29} = 11.82$, $p \leq 0.0002$) and the interaction ($F_{2, 29} = 5.945$, $P \leq 0.0069$) on

Hsd3b2. *Hsd3b2* of EDS-treated rats was significantly reduced by 73% and 96% at 15 and 24 hr, respectively, but not at 6 hr (Fig. 8).

There was a significant treatment effect on *Star* ($F_{1, 27} = 32.24$, $p \leq 0.0001$) but no effect of time or the interaction between time and treatment ($p > 0.05$). The *Star* expression of EDS-treated rats was significantly reduced by 52%, 69% and 75% at 6, 15 and 24 hr, respectively (Fig. 9).

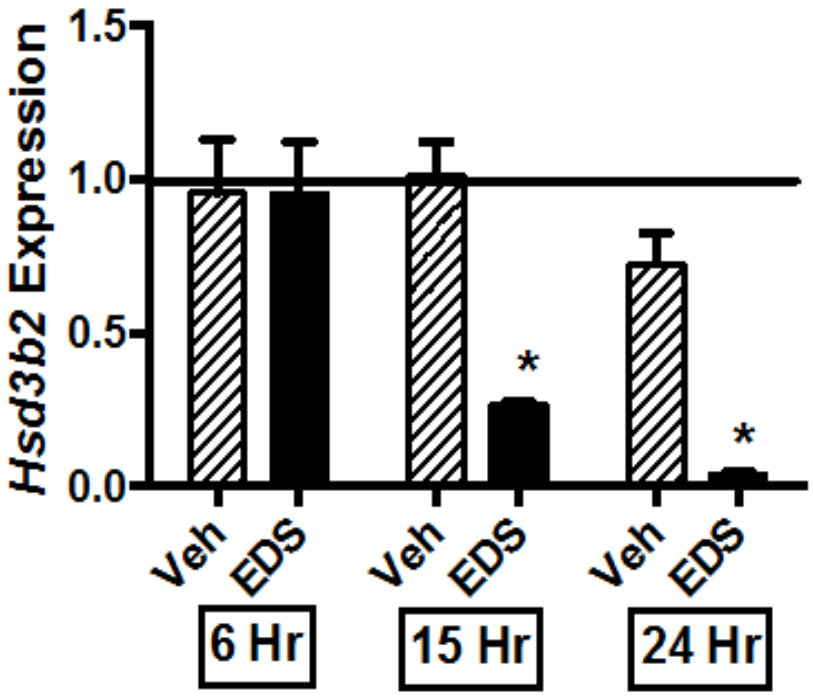

Figure 8
The expression of *Hsd3b2* relative to *Gapdh* as the reference gene. The horizontal line is the normalized value for the non-treated (NT) rats. Error bars represent SEM with n = 6 and (*) indicates a significant difference between EDS and vehicle (Veh)-treated rats within the same time of treatment.

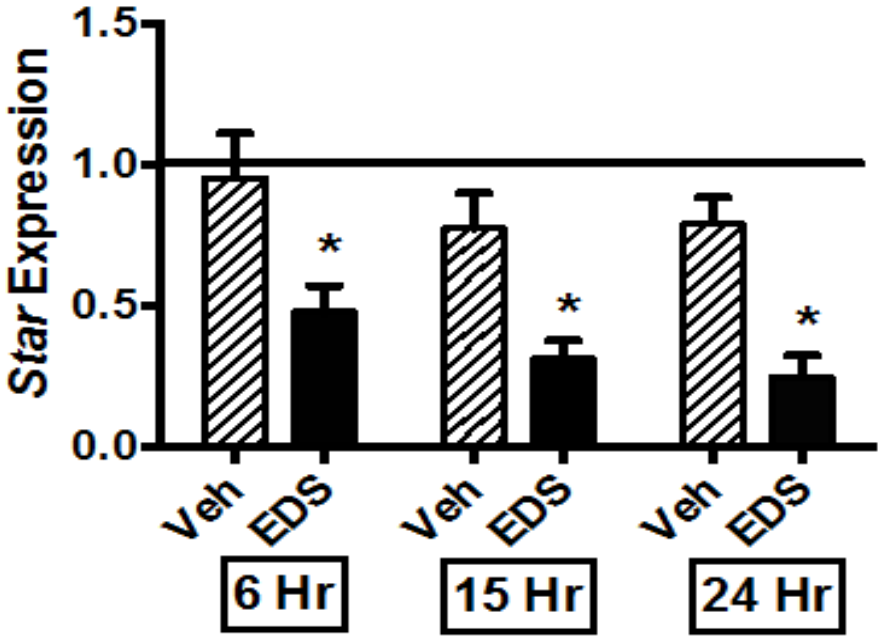

Figure 9
The expression of *Star* relative to *Gapdh* as the reference gene. The horizontal line is the normalized value for the non-treated (NT) rats. Error bars represent SEM with n = 6 and (*) indicates a significant difference between EDS and vehicle (Veh)-treated rats within the same time of treatment.

Histological and morphological evaluation of testicular cross sections

Potential loss of testicular interstitial cells was determined by hematoxylin and eosin staining of testes cross-section (Fig. 10 –13). Hematoxylin stains the nucleus and eosin stains the cell cytoplasm. These studies demonstrated that following EDS treatment, there was an observable cell loss (as indicated by arrows) in testicular intersitium at 15 (Fig. 11C, 11F and 13C) and 24 hr (Fig. 12C, 12F and 13D) but not at 6 hr (Fig 10C, 10F and 13B). No such changes were present across time in vehicle-treated rats. However, with simple microscopy, it was not possible to detect which particular cells in the interstitium were undergoing degradation.

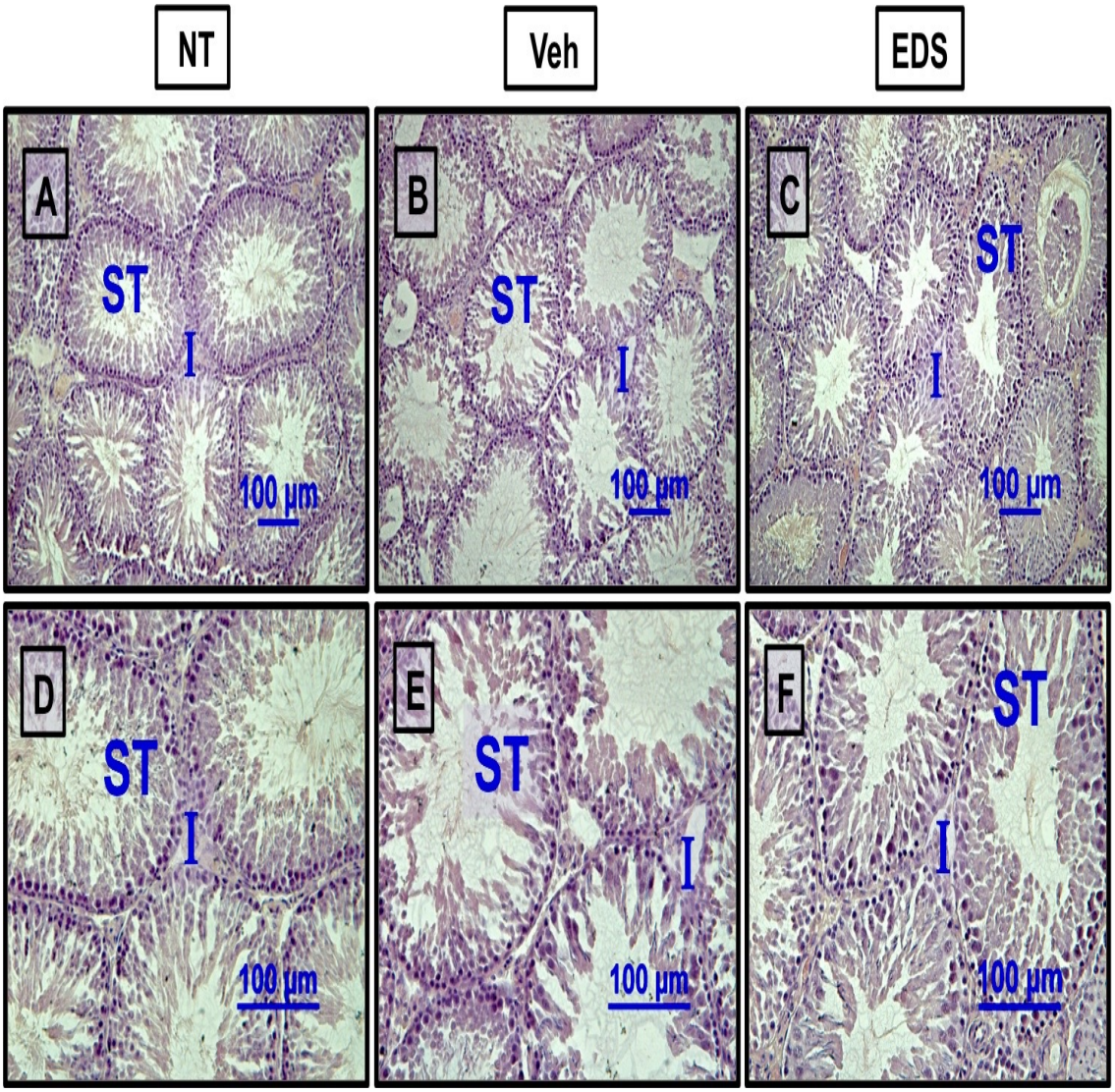

Figure 10

Hematoxylin and eosin stained rat testicular tissue with EDS treatment at 6 hr. A, B and C represent NT, Veh and EDS- treated rats and D, E, F are their photographic magnifications, respectively. Column labels: NT – non treated, Veh – vehicle-treated and EDS – received EDS. Figure labels: ST – seminiferous tubules and I – interstitial. All the experiments were repeated thrice and above images are representative of microscopic observations.

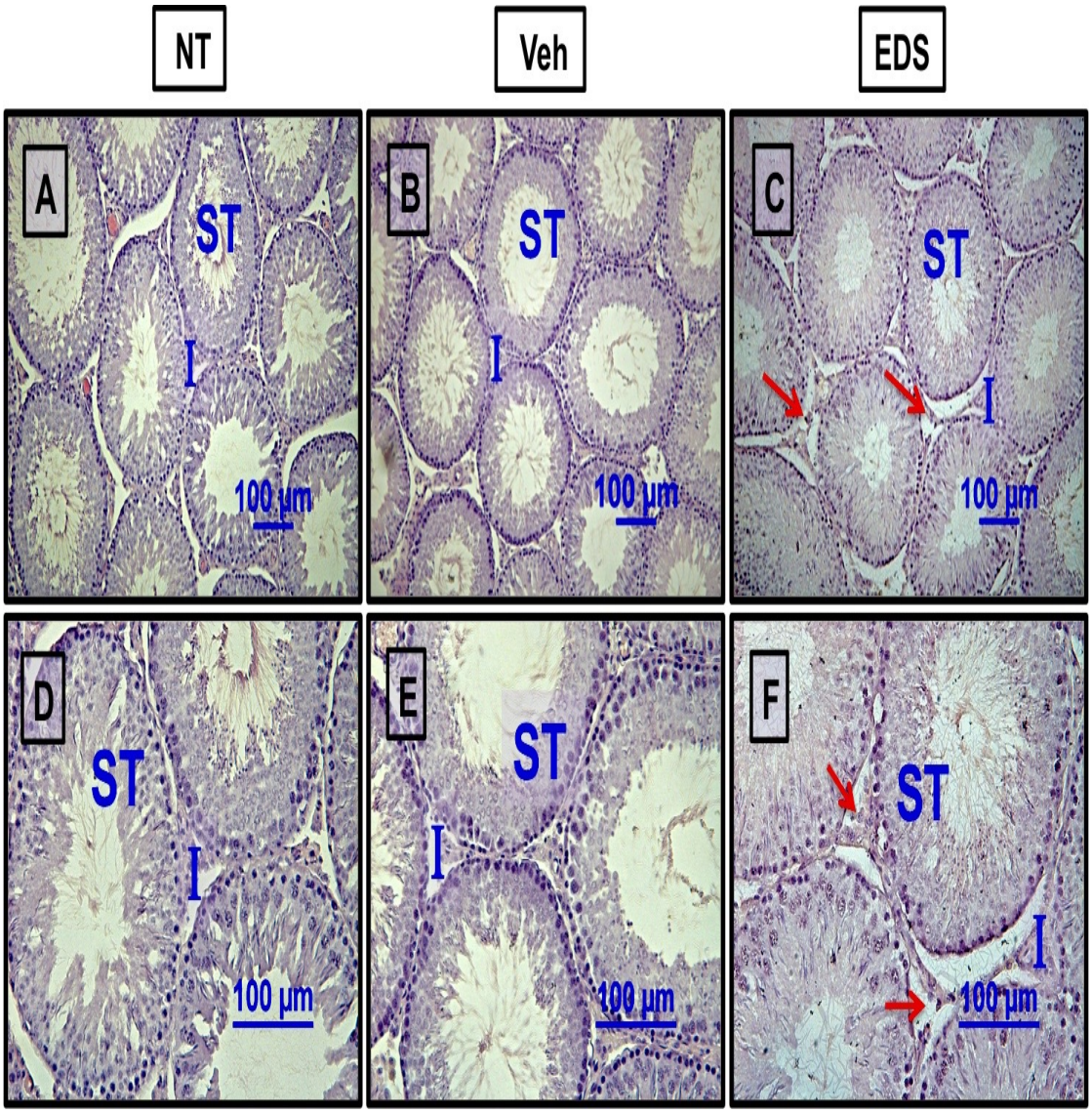

Figure 11

Hematoxylin and eosin stained rat testicular tissue with EDS treatment at 15 hr. A, B and C represent NT, Veh and EDS- treated rats and D, E, F are their photographic magnifications, respectively. Column labels: NT – non treated, Veh – vehicle-treated and EDS – received EDS. Figure labels: ST – seminiferous tubules, I – interstitial and red arrows – mark areas with loss of intersititial cells. All the experiments were repeated thrice and above images are representative of microscopic observations.

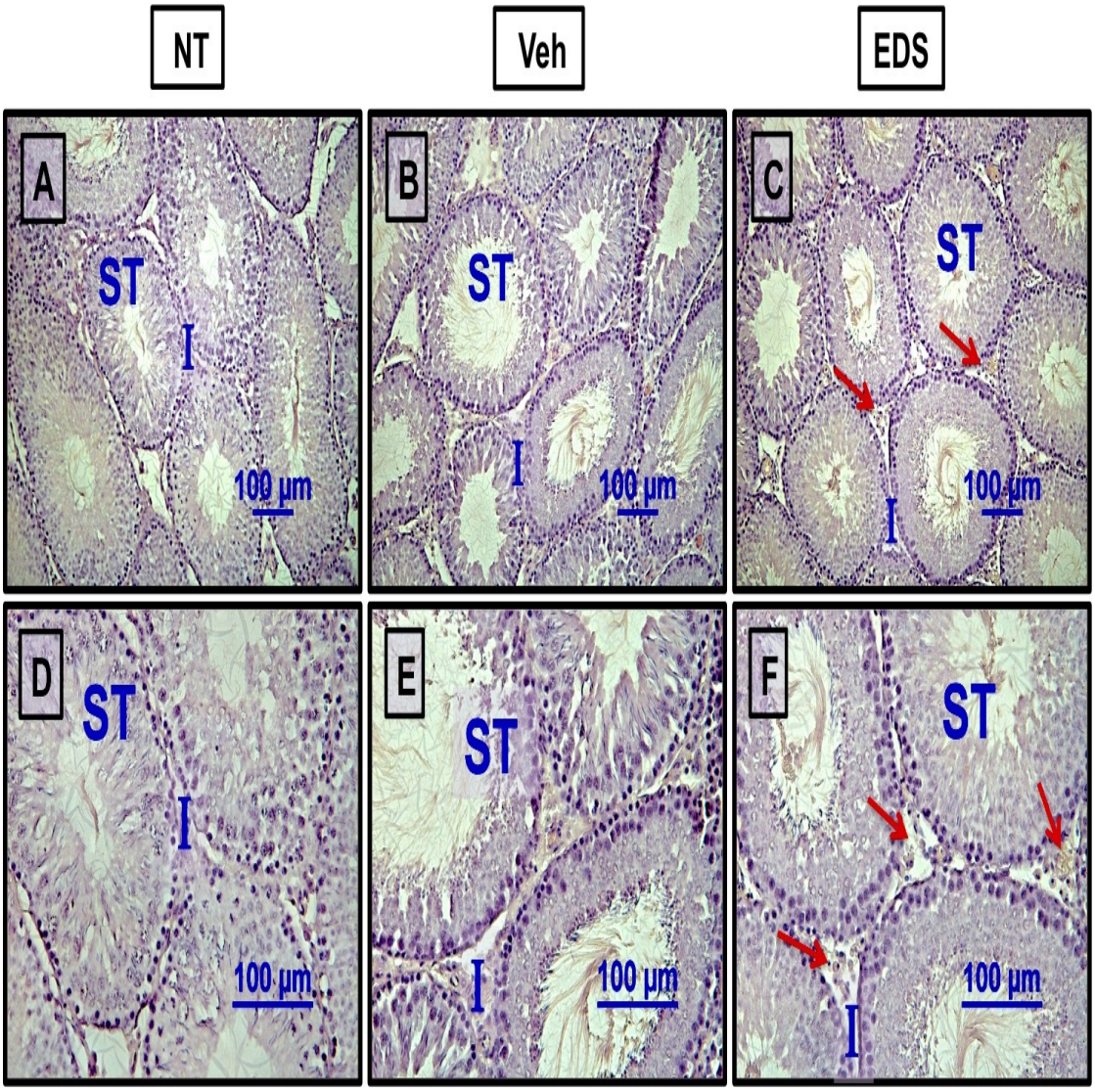

Figure 12

Hematoxylin and eosin stained rat testicular tissue with EDS treatment at 24 hr. A, B and C represent NT, Veh and EDS- treated rats and D, E, F are their photographic magnifications, respectively. Column labels: NT – non treated, Veh – vehicle-treated and EDS – received EDS. Figure labels: ST – seminiferous tubules, I – interstitial and red arrows – mark areas with loss of intersitital cells. All the experiment were repeated thrice and above images are representative of microscopic observations.

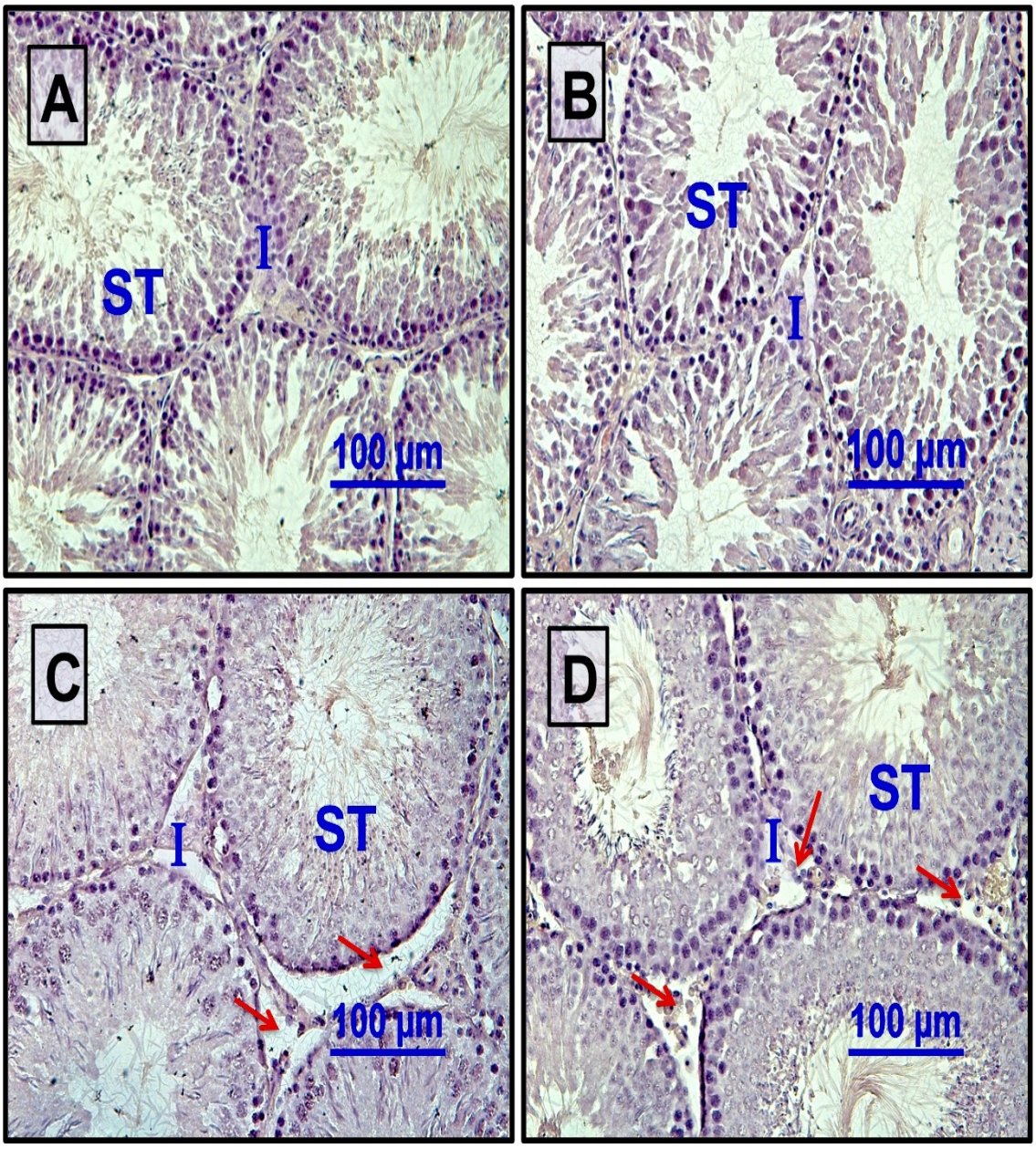

Figure 13
Hematoxylin and eosin stained rat testicular tissue with EDS treatment. (A) Control (NT), (B) 6 hr-, (C) 15 hr-, and (D) 24 hr-EDS treated rat testicular tissue, respectively. Figure labels: ST – seminiferous tubules, I – interstitial tissue and red arrows – mark areas with loss of intersititial cells (C and D). All the experiments were repeated thrice and above images are representative of microscopic observations.

Testicular interstitium apoptosis detected by TUNEL assay

Increased DNA breakage is mostly observed in cells undergoing apoptosis. Thus, to detect the effect of EDS in intersitial cell apoptosis, we labelled the 3'-OH terminus of broken DNA using TUNEL assay. Apoptotic cells in testis cross-section (as indicated by arrow head) are shown in fig. 14 – 17. Apoptotic cells were not observed at 6 hr of EDS treatement, compared to NT and Veh at 6 hr (Fig. 14 and 17B). In 15 and 24 hr EDS-treated rats, apoptotic cells (dark-brown colored cells) were observed (indicated using the arrow head) in the interstitium compared to NT and Veh at 15 and 24 hr, respectively (Fig. 15 and 16, respectively, indicated by arrow). There appeared to be more apoptotic cells at 24 hr (Fig. 16J and 17D) post-EDS treatment compared to 6 (Fig. 14J and 17B) and 15 hr (Fig. 15J and 17C) of EDS-treated rats. However, with simple microscopy, it was not possible to detect which particular cells in the interstitium were undergoing apoptosis.

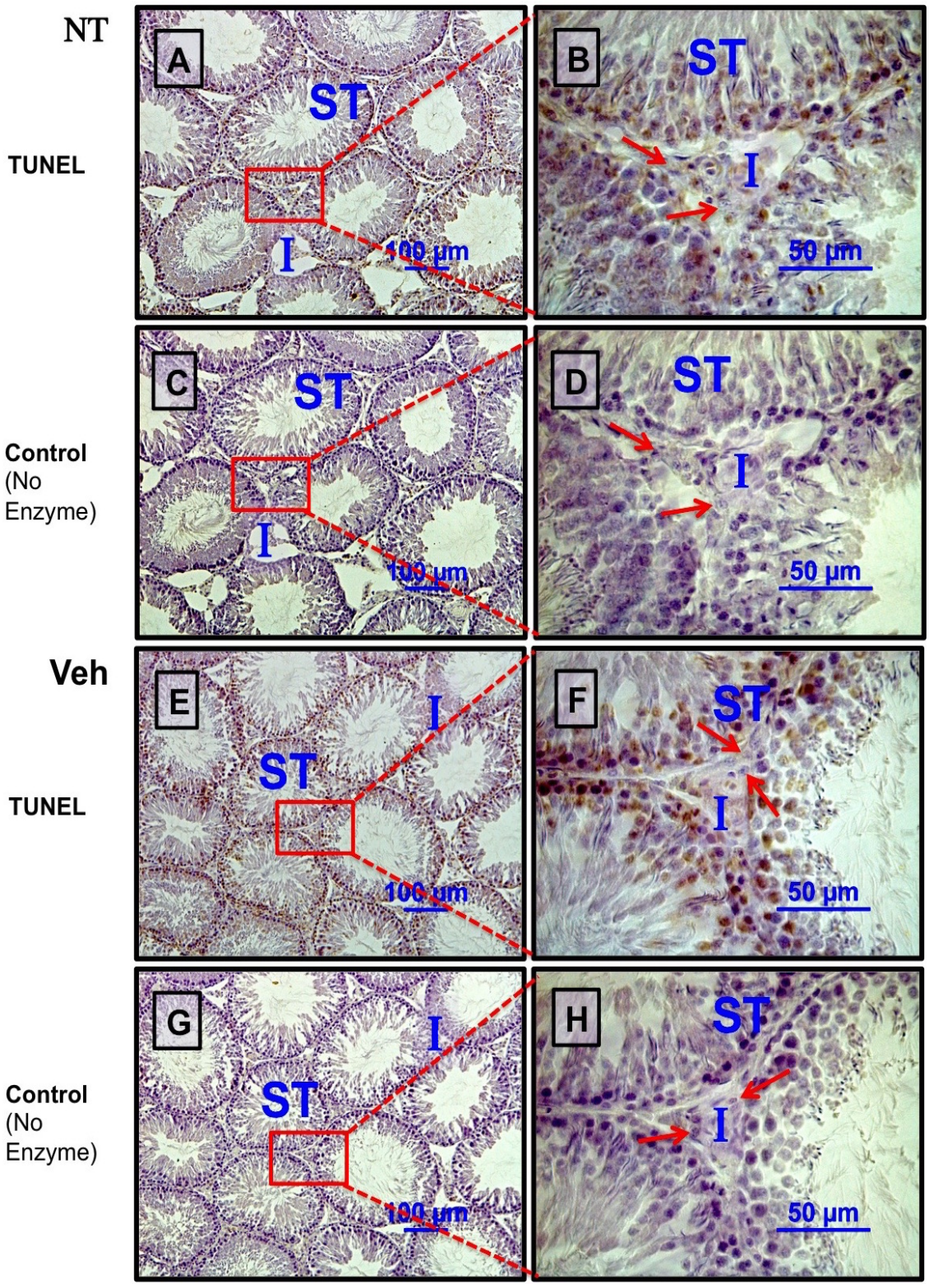
NT
TUNEL
A
ST
I
100 µm
B
ST
I
50 µm
Control
(No
Enzyme)
C
ST
I
100 µm
D
ST
I
50 µm
Veh
TUNEL
E
I
ST
100 µm
F
ST
I
50 µm
Control
(No
Enzyme)
G
I
ST
100 µm
H
ST
I
50 µm

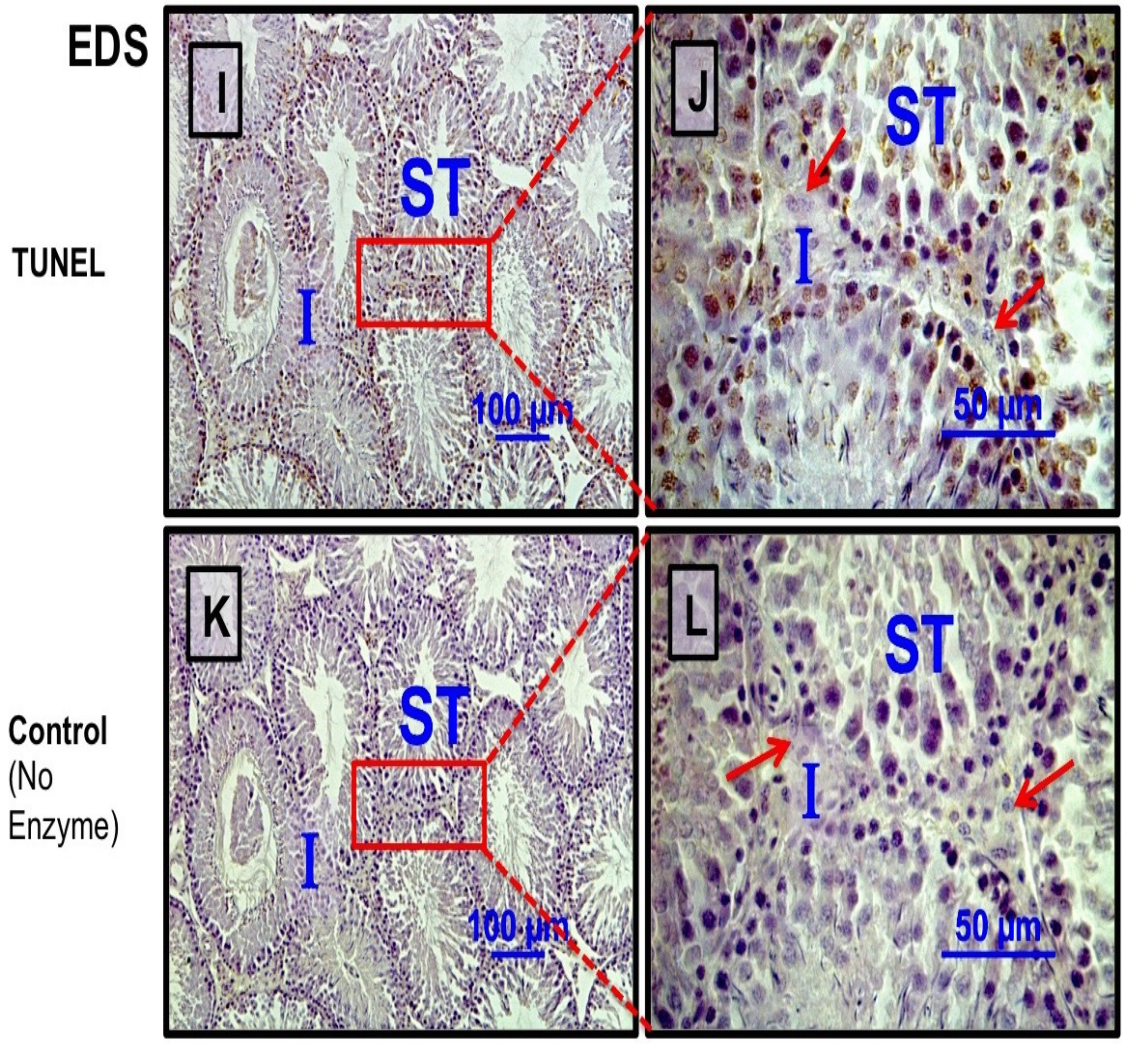

Figure 14
TUNEL analysis for 6 hr EDS-treated rat testes. TUNEL positive – A and B are NT (non-treated), E and F are Veh (vehicle-treated), and I and J are EDS (EDS-treated). Control (without terminal deoxynucleotidyl transferase, TdT) – C and D are NT, G and H are Veh, and K and L are EDS. Figure labels: ST – seminiferous tubules, I – interstitial tissue and red arrows – mark normal interstitial cells. Images of TUNEL positive and control (no enzyme) are from the adjascent tissue sections on the same slide. All the experiments were repeated thrice and above images are representative of microscopic observations.

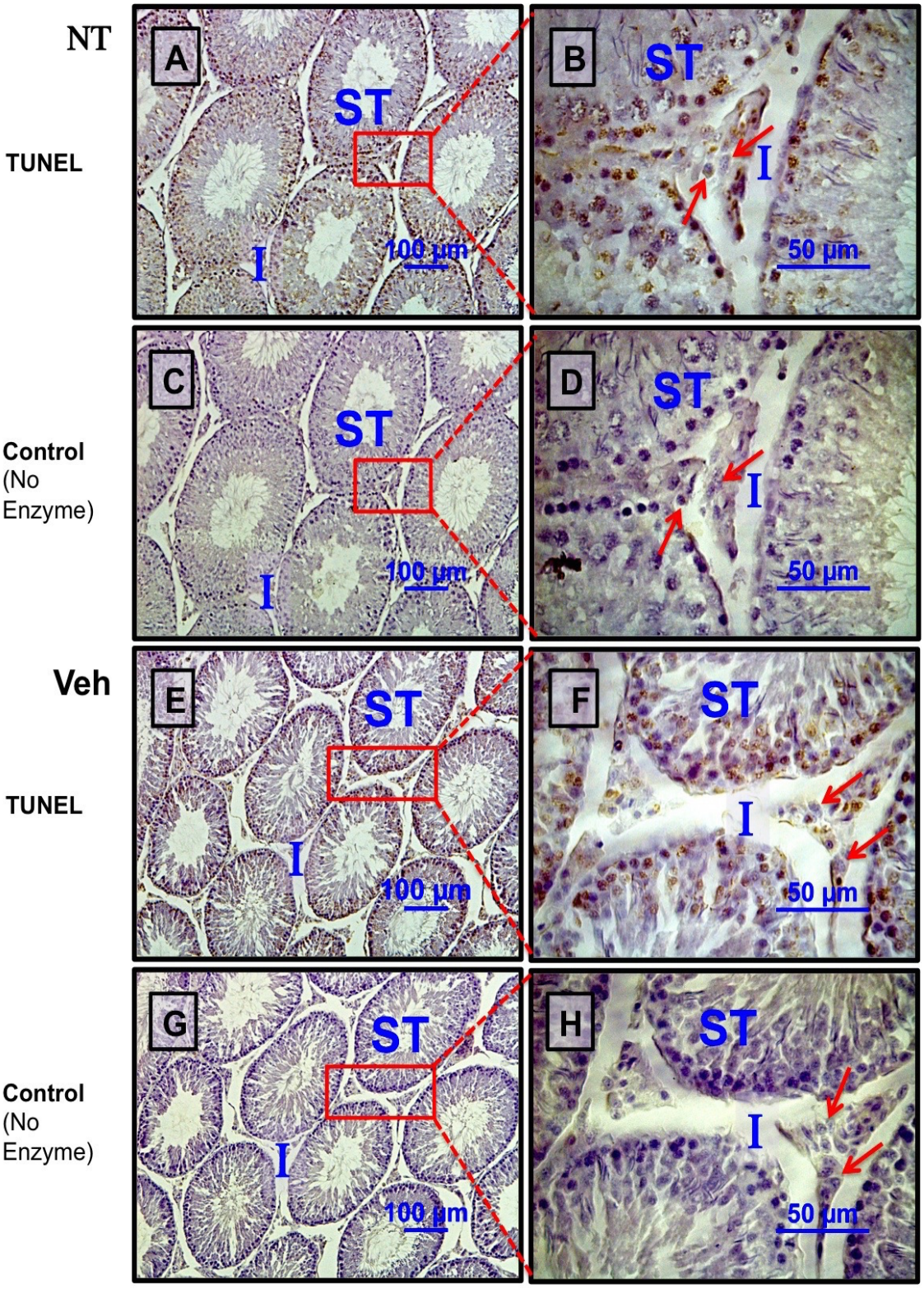
NT
TUNEL
A
ST
I
100 µm
B
ST
I
50 µm
Control
(No
Enzyme)
C
ST
I
100 µm
D
ST
I
50 µm
Veh
TUNEL
E
ST
I
100 µm
F
ST
I
50 µm
Control
(No
Enzyme)
G
ST
I
100 µm
H
ST
I
50 µm

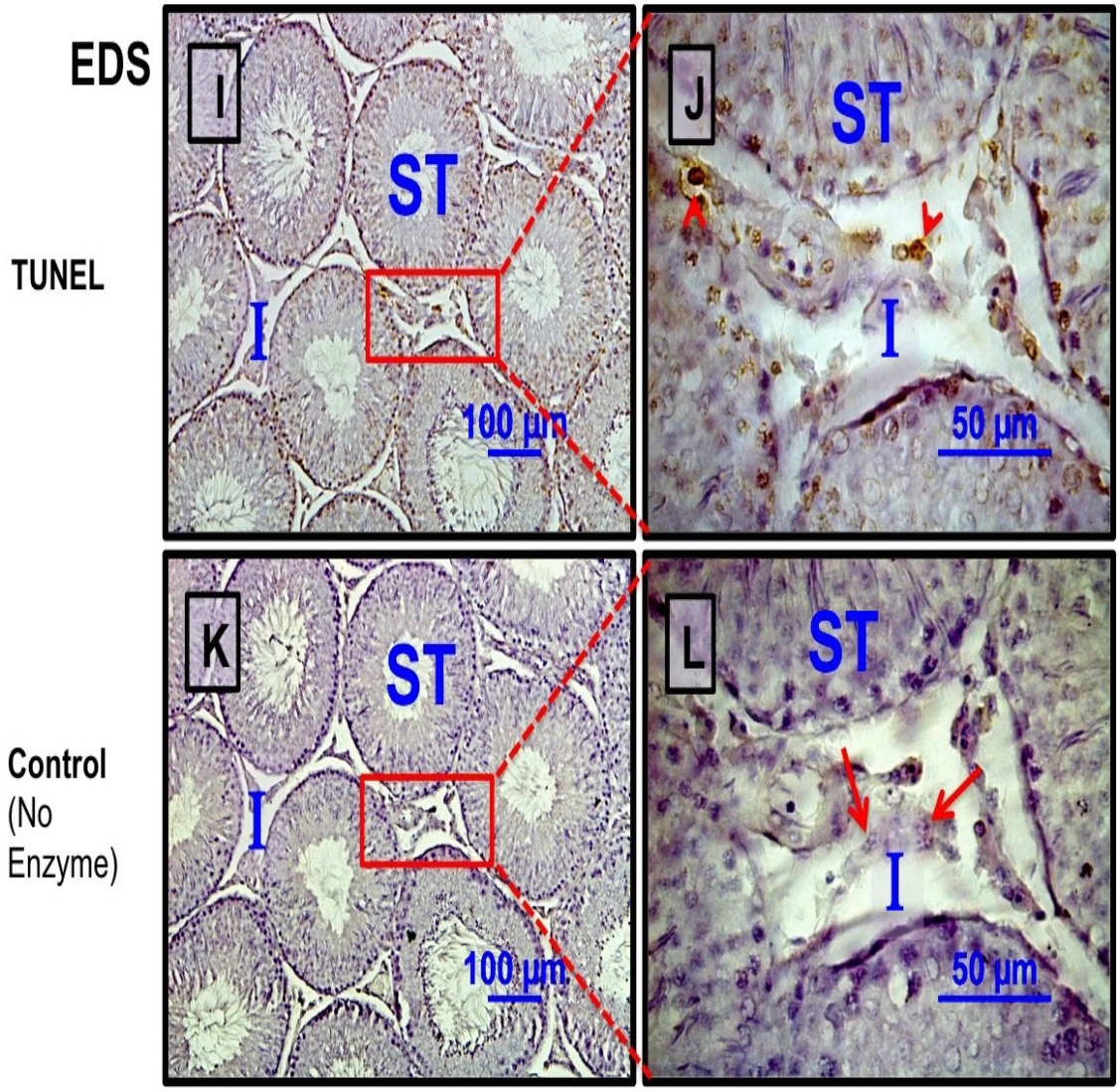

Figure 15
TUNEL analysis for 15 hr EDS-treated rat testes. TUNEL positive – A and B are NT (non-treated), E and F are Veh (vehicle-treated), and I and J are EDS (EDS-treated). Control (without terminal deoxynucleotidyl transferase, TdT) – C and D are NT, G and H are Veh, and K and L are EDS. Figure labels: ST – seminiferous tubules, I – interstitial tissue, red arrows – mark normal interstitial cells and red arrow head – mark TUNEL positive cells, showing DNA fragmentation. Images of TUNEL positive and control (no enzyme) are from the adjascent tissue sections on the same slide. All the experiments were repeated thrice and above images are representative of microscopic observations.

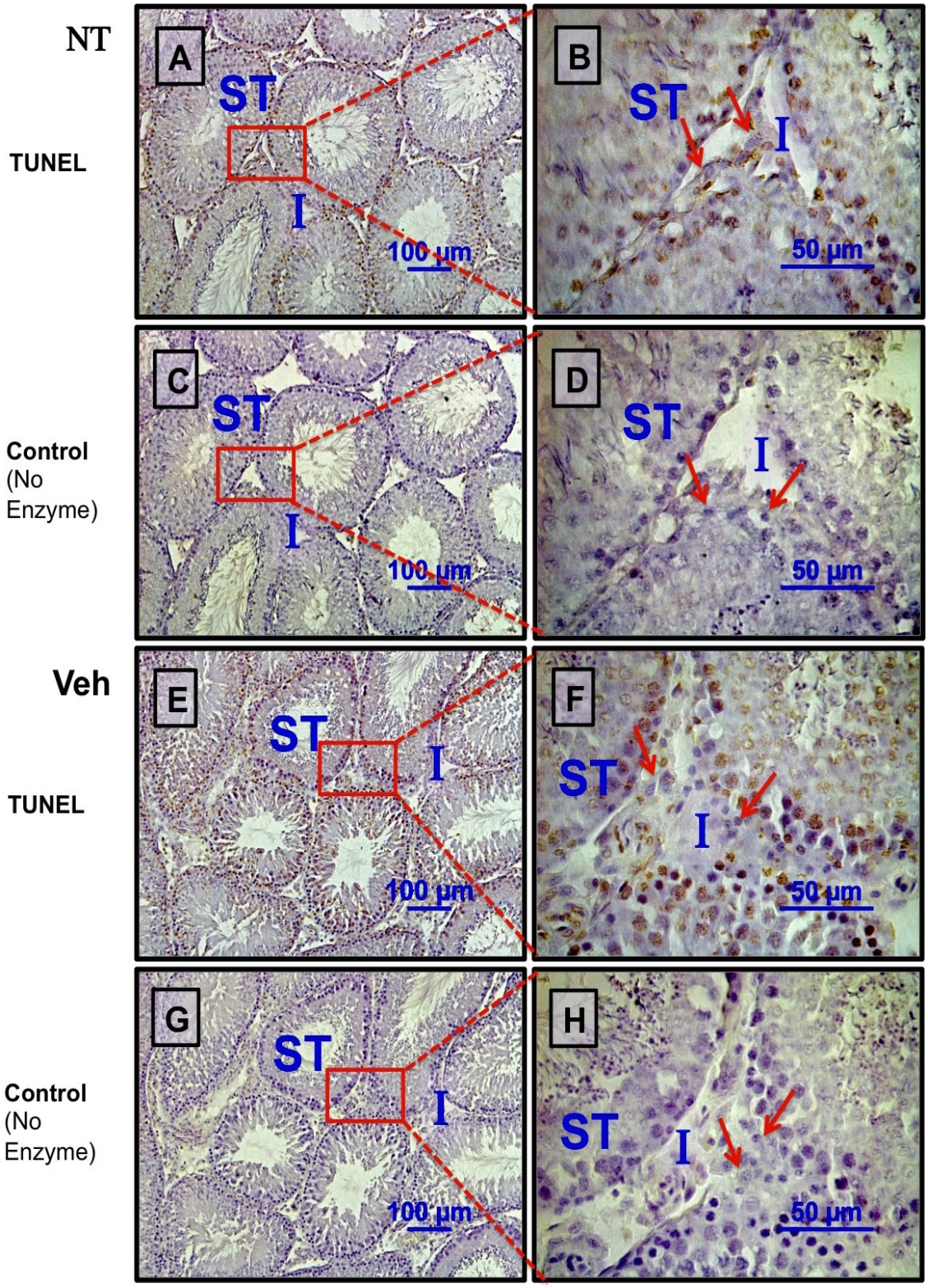
NT
TUNEL
A
ST
I
100 µm
B
ST
I
50 µm
Control
(No
Enzyme)
C
ST
I
100 µm
D
ST
I
50 µm
Veh
TUNEL
E
ST
I
100 µm
F
ST
I
50 µm
Control
(No
Enzyme)
G
ST
I
100 µm
H
ST
I
50 µm

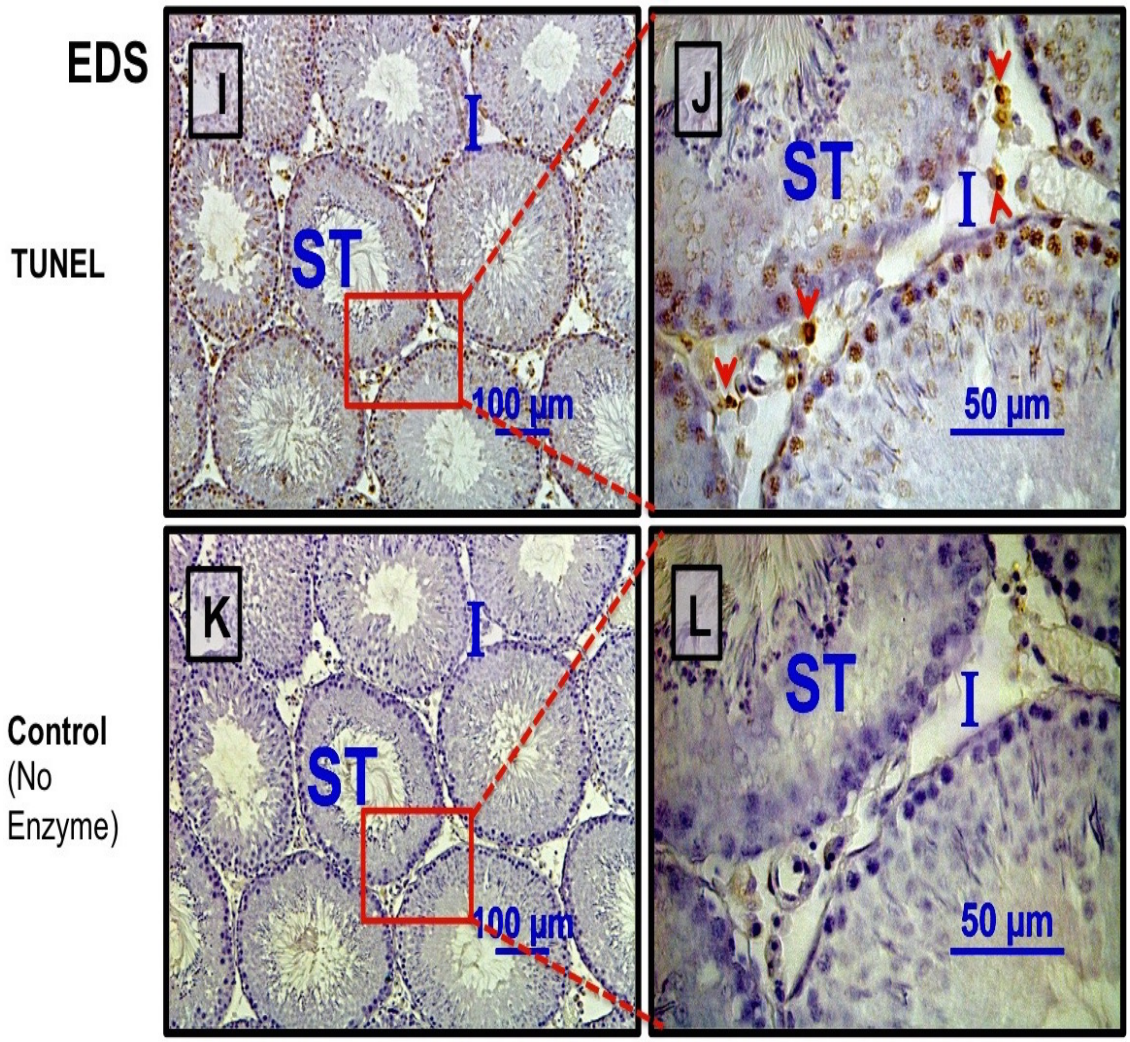

Figure 16
TUNEL analysis for 24 hr EDS-treated rat testes. TUNEL positive – A and B are NT (non-treated), E and F are Veh (vehicle-treated), and I and J are EDS (EDS-treated). Control (without terminal deoxynucleotidyl transferase, TdT) – C and D are NT, G and H are Veh, and K and L are EDS. Figure labels: ST – seminiferous tubules, I – interstitial tissue, red arrows – mark normal interstitial cells and red arrow head – mark TUNEL positive cells, showing DNA fragmentation. Images of TUNEL positive and control (no enzyme) are from the adjascent tissue sections on the same slide. All the experiments were repeated thrice and above images are representative of microscopic observations.

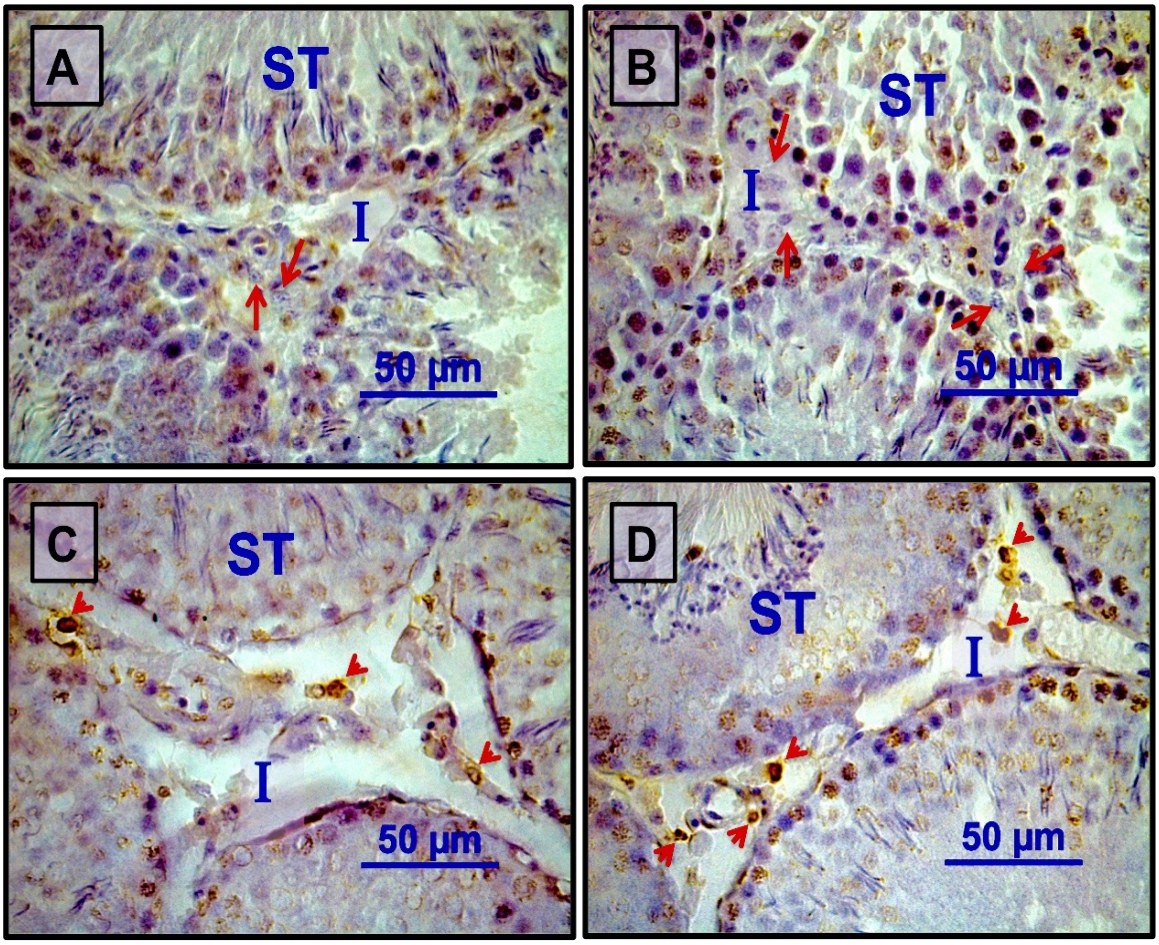

Figure 17

TUNEL analysis for EDS-treated rat testes. (A) Control (NT), (B) 6 hr EDS-treated, (C) 15 hr EDS-treated and (D) 24 hr EDS treated, rat testicular tissue. Figure labels: ST – seminiferous tubules, I – interstitial tissue, red arrows – normal Leydig cells (A and B), and red arrow head – TUNEL positive cells, showing DNA fragmentation (C and D). All the experiments were done in triplicate and above images are representative of microscopic observations.

Quantification of apoptotic cells in the interstitium

When apoptotic cells (indicated by the arrow head in Fig. 14 – 17) were quantified, there was a significant effect of treatment ($F_{2, 18} = 87.85$, $p \leq 0.0001$), time ($F_{2, 18} = 11.33$, $p \leq 0.0007$) and interaction of time and treatment ($F_{4, 18} = 15.11$, $P \leq$

0.0001). Apoptosis for EDS-treated rats was significantly increased by 3- and 5- fold at 15 and 24 hr, respectively, but not at 6 hr (Fig. 18).

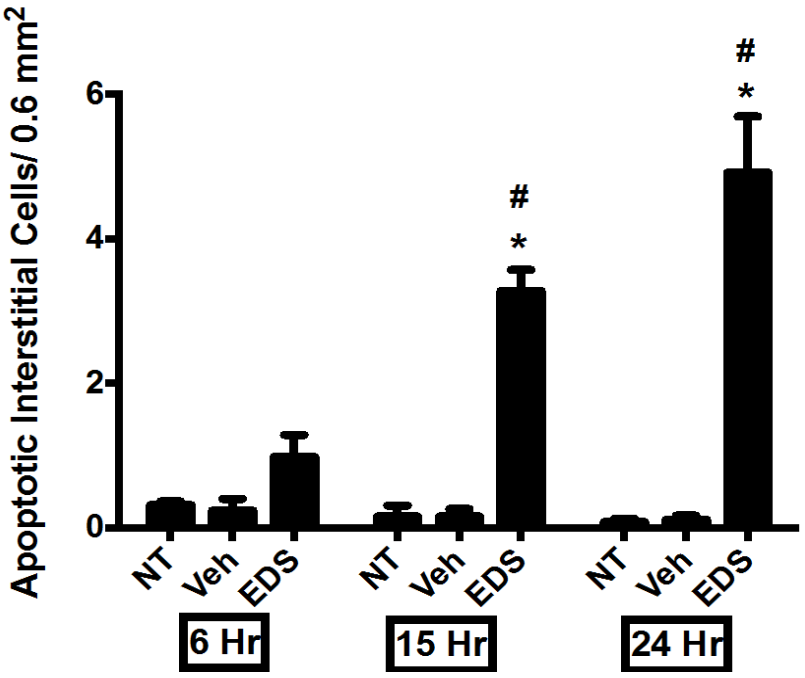

Figure 18
Apoptotic cells in the rat testicular interstitium. Data are for the number of apoptotic cells as determined with the TUNEL assay from non-treated (NT), vehicle-treated (Veh) and EDS-treated animals (n = 3) at 6, 15 and 24 hr post-treatments. The bars represent the mean number of apoptotic cells per 0.6 mm^2 area. Counts are from a minimum of 11 fields. Error bars represent SEM and the symbols (#) and (*) indicates significant difference between EDS and NT and between EDS and Veh-treated rats, respectively, within the same time of treatment.

Fas and Fas ligand (*FasL*) expression in rat testis after EDS treatment

Fas/FasL signaling is one of the major apoptotic pathways. The potential change in Fas and FasL mRNA after EDS treatments was determined by RT and qPCR. There was no significant effect of treatment, time or their interaction ($p > 0.05$) on *Fas* (Fig. 19) or on *Fasl* (Fig. 20).

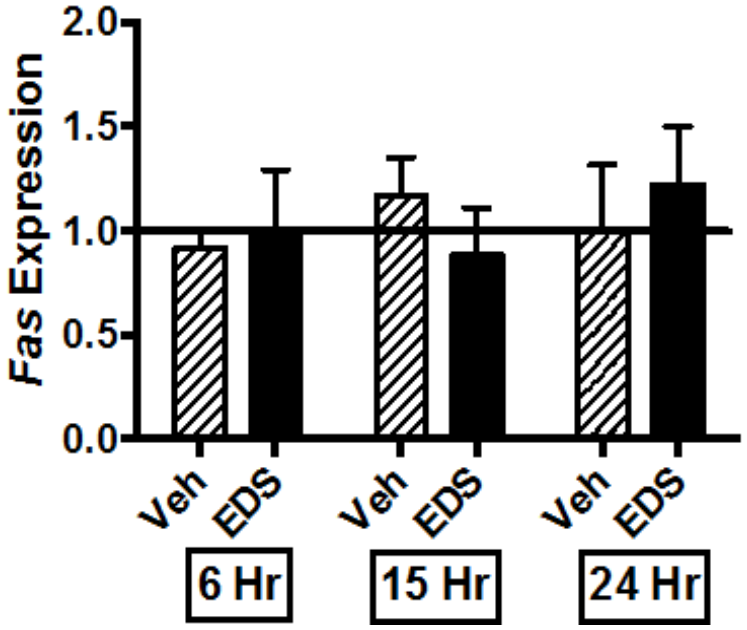

Figure 19
The expression of *Fas* relative to *Gapdh* as the reference gene. The horizontal line is the normalized value for the non-treated (NT) rats. Error bars represent SEM with n = 6.

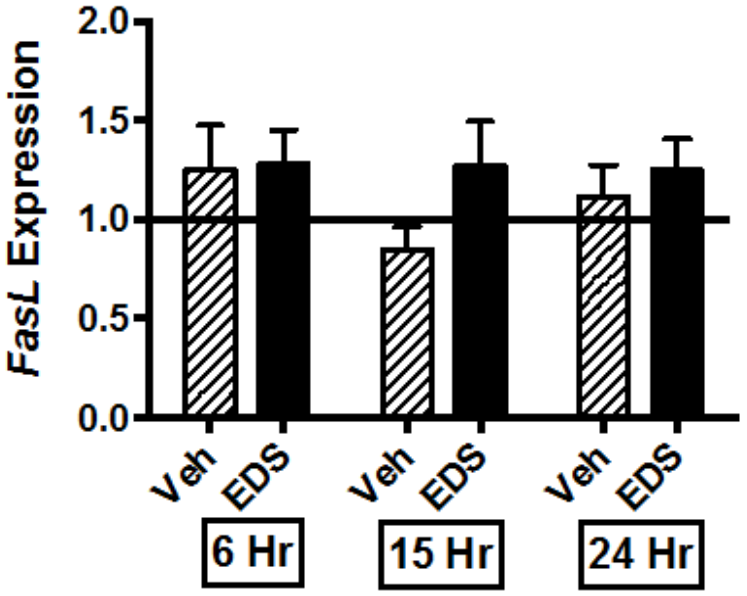

Figure 20
The expression of *FasL* relative to *Gapdh* as the reference gene. The horizontal line is the normalized value for the non-treated (NT) rats. Error bars represent SEM with n = 6.

Expression of proinflammatory/ apoptotic cytokine markers

The potential increase in pro-inflammatory and pro-apoptotic cytokines was determined. There was a significant treatment effect on *Tnfα* ($F_{1, 16} = 13.11$, $p \leq 0.0023$) but no effect of time or the interaction between time and treatment ($p > 0.05$). *Tnfα* of EDS-treated rats was significantly increased by 2.69-fold at 15 hr but not at 6 and 24 hr (Fig 21). There was no significant effect of treatment, time or their interaction ($p > 0.05$) on *Tnfβ* (Fig. 22).

We found a significant effect of treatment ($F_{1, 26} = 58.68$, $p \leq 0.0001$), time ($F_{2, 26} = 6.378$, $p \leq 0.0056$) and their interaction ($F_{2, 26} = 4.494$, $P \leq 0.0211$) on *Il1β*. *Il1β* of EDS-treated rats was significantly increased by 5.03-, 3.25- and 2.44- fold at 6, 15 and 24 hr, respectively, as shown in Fig. 23.

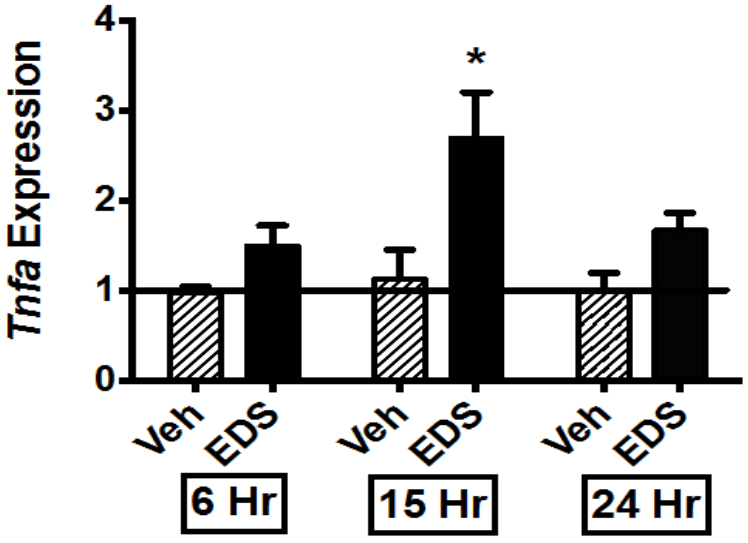

Figure 21
The expression of *Tnfα* relative to *Gapdh* as the reference gene. The horizontal line is the normalized value for the non-treated (NT) rats. Error bars represent SEM with n = 4 and (*) indicates a significant difference between EDS and vehicle (Veh)-treated rats within the same time of treatment.

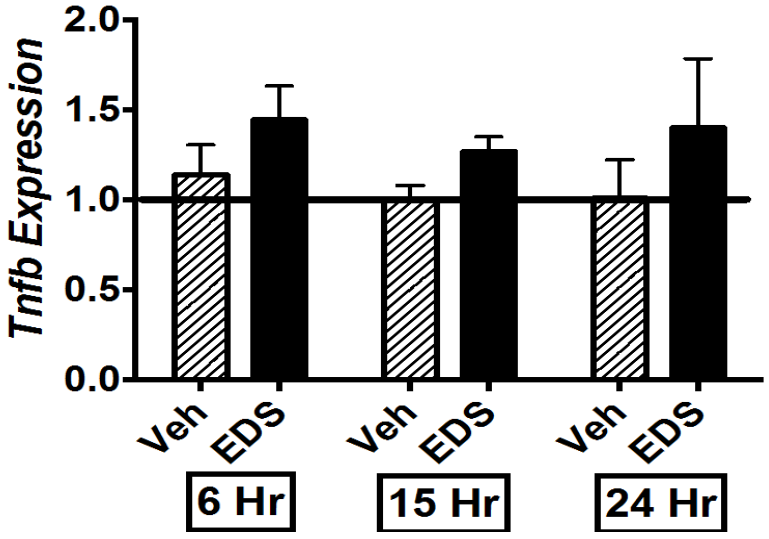

Figure 22
The expression of *Tnfβ* relative to *Gapdh* as the reference gene. The horizontal line is the normalized value for the non-treated (NT) rats. Error bars represent SEM with n = 6.

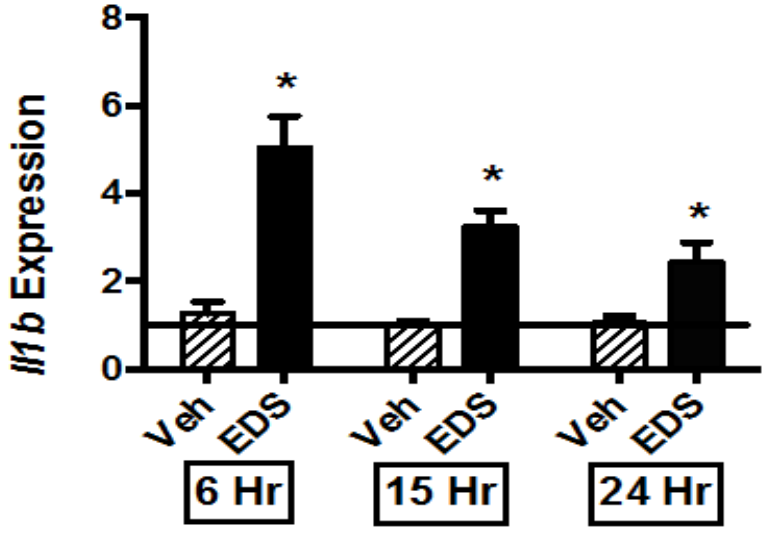

Figure 23
The expression of *Il1β* relative to *Gapdh* as the reference gene. The horizontal line is the normalized value for the non-treated (NT) rats. Error bars represent SEM with n = 6 and (*) indicates a significant difference between EDS and vehicle (Veh)-treated rats within the same time of treatment.

Change in TNF-α expression using ELISA

Since there was a prominent increase in TNF-α mRNA levels at 15 hr following EDS treatment but not at 6 and 24 hr post-EDS treatment (Fig. 21), we analyzed the levels of TNF-α protein by sandwich ELISA. When TNF-α protein was calculated with respect to the total testicular protein concentration of the sample (pg/mg), we found a significant effect of EDS treatment ($F_{2, 25} = 6.958$, $p \leq 0.0040$) with respect to NT, but there was no significant effect of time or their interaction ($p > 0.05$). TNF-α protein of EDS-treated rats was significantly increased by 0.8- fold at 15 hr, but did not change at 6 and 24 hr, as shown in Fig. 24.

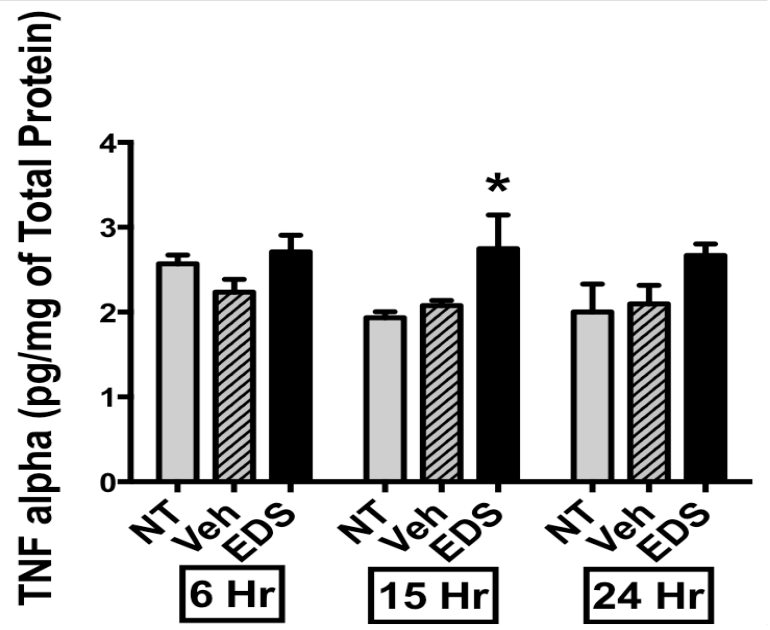

Figure 24
TNF-alpha (TNF-α) protein per total testicular protein (pg/mg). Data are for TNF-α /total testicular protein from non-treated (NT), vehicle-treated (Veh) and EDS-treated (EDS) rats at 6, 15 and 24 hr after EDS treatment. Error bars represent SEM with n = 4 and (*) indicates a significant difference between EDS and NT rats within the same time of treatment.

Relative changes in the mRNA for tumor necrosis factor receptors

The potential increase in pro-apoptoic and inflammatory receptors was determined. The two TNF-α receptors, TNFR1 and TNFR2, are involved in different cellular pathways. TNFR1 initiates apoptotic and/or anti-apoptotic signaling while TNFR2 initiates the anti-apoptotic pathway. The relative expression of mRNA for these receptors is illustrated in fig. 25 and 26. There was a significant effect of treatment ($F_{1, 26} = 60.14$, $p \leq 0.0001$), time ($F_{2, 26} = 30.90$, $p \leq 0.0001$) and the interaction ($F_{2, 26} = 35.91$, $P \leq 0.0001$) on *Tnfrsf1a*. *Tnfrsf1a* of EDS-treated rats was significantly increased by 1.89- and 3.83-fold at 15 and 24 hr, respectively, but not at 6 hr (Fig. 25).

These findings demonstrated a significant treatment ($F_{1, 26} = 6.081$, $p \leq 0.0206$) and time ($F_{2, 26} = 4.649$, $p \leq 0.0188$) effect on *Tnfrsf1b* but no interaction between time and treatment ($p > 0.05$). *Tnfrsf1b* of EDS-treated rats was significantly reduced by 66% at 6 hr but not at 15 and 24 hr (Fig. 26).

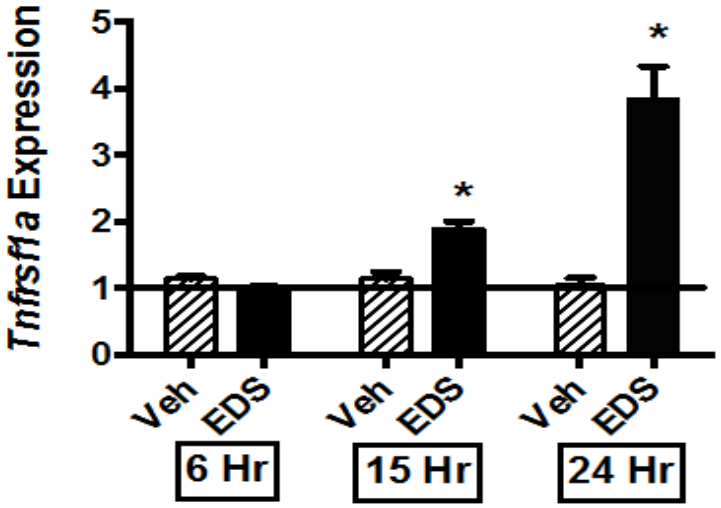

Figure 25

The expression of *Tnfrsf1a* relative to *Gapdh* as the reference gene. The horizontal line is the normalized value for the non-treated (NT) rats. Error bars represent SEM with n = 6 and (*) indicates a significant difference between EDS and vehicle (Veh)-treated rats within the same time of treatment.

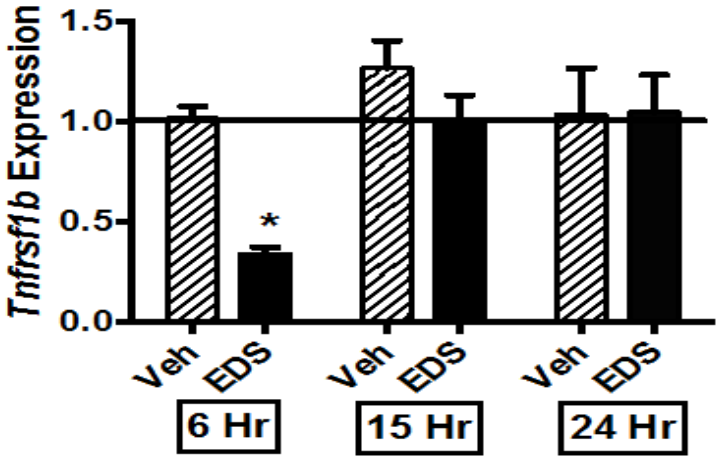

Figure 26

The expression of *Tnfrsf1b* relative to *Gapdh* as the reference gene. The horizontal line is the normalized value for the non-treated (NT) rats. Error bars represent SEM with n = 6 and (*) indicates a significant difference between EDS and vehicle (Veh)-treated rats within the same time of treatment.

Cluster of differentiation 68 (*Cd68*) and 163 (*Cd163*) expression after EDS treatment

Quantification of the mRNA expression for CD68 and CD163 was used as an index of the conversion of monocytes (present in blood circulation or tissue) into tissue resident macrophages and also the activation/differentiation of macrophages. These findings demonstrated no significant effect of treatment, time or their interaction ($p > 0.05$) on the monocyte marker, *Cd68* (Fig. 27). In contrast, there was a significant effect of treatment ($F_{1, 27} = 14.86$, $p \leq 0.0006$), time ($F_{2, 27} = 3.983$, $p \leq 0.0305$) and their interaction ($F_{2, 27} = 4.150$, $p \leq 0.0268$) on the macrophage marker, *Cd163*. *Cd163* of EDS-treated rats was significantly increased by 2.9- fold at 15 hr, but not at 6 and 24 hr (Fig. 28).

The ratio of *Cd163* to *Cd68* (*Cd163*/*Cd68*) represents proliferation of testicular resident macrophages (TRMs), and/or tissue invasion by activated macrophages/monocytes and localization of these monocytes to form more specific TRMs. There was a significant effect of treatment ($F_{1, 27} = 8.081$, $p \leq 0.0084$), time ($F_{2, 27} = 3.923$, $p \leq 0.0319$) and interaction ($F_{2, 27} = 4.875$, $P \leq 0.0156$) on *Cd163/Cd68*. *Cd163/Cd68* of EDS-treated rats was significantly increased by 2.2- fold at 15 hr, but not at 6 and 24 hr (Fig. 29).

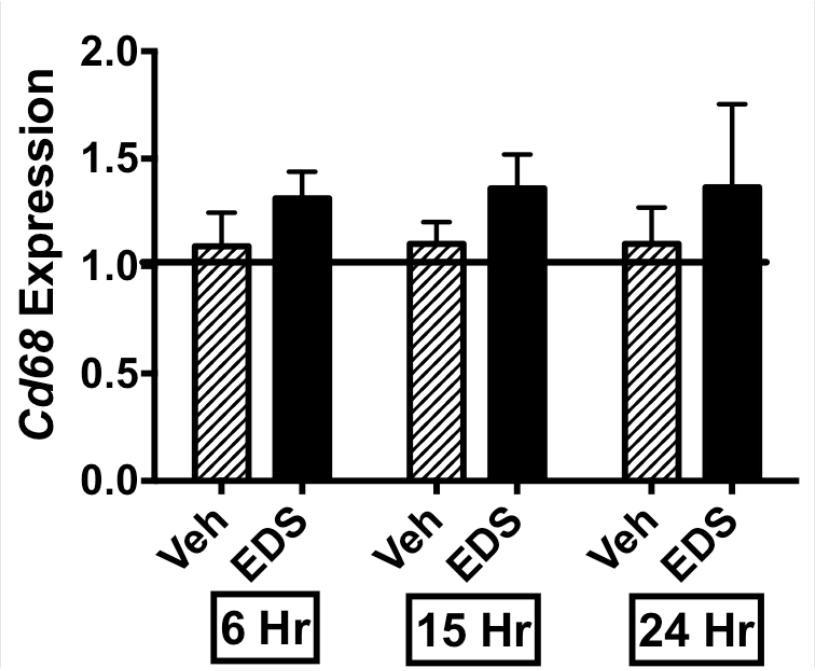

Figure 27
The expression of *Cd68* relative to *Gapdh* as the reference gene. The horizontal line is the normalized value for the non-treated (NT) rats. Error bars represent SEM with n = 6.

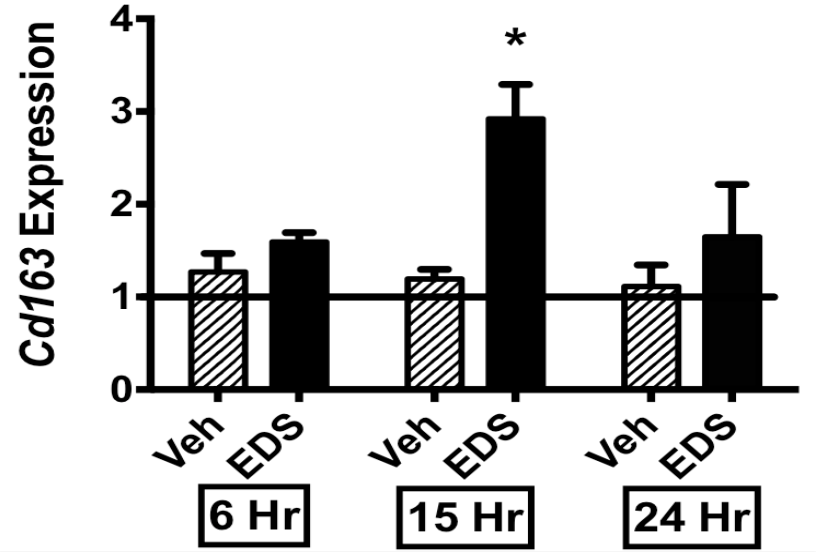

Figure 28
The expression of *Cd163* relative to *Gapdh* as the reference gene. The horizontal line is the normalized value for the non-treated (NT) rats. Error bars represent SEM with n = 6 and (*) indicates a significant difference between EDS and vehicle (Veh)-treated rats within the same time of treatment.

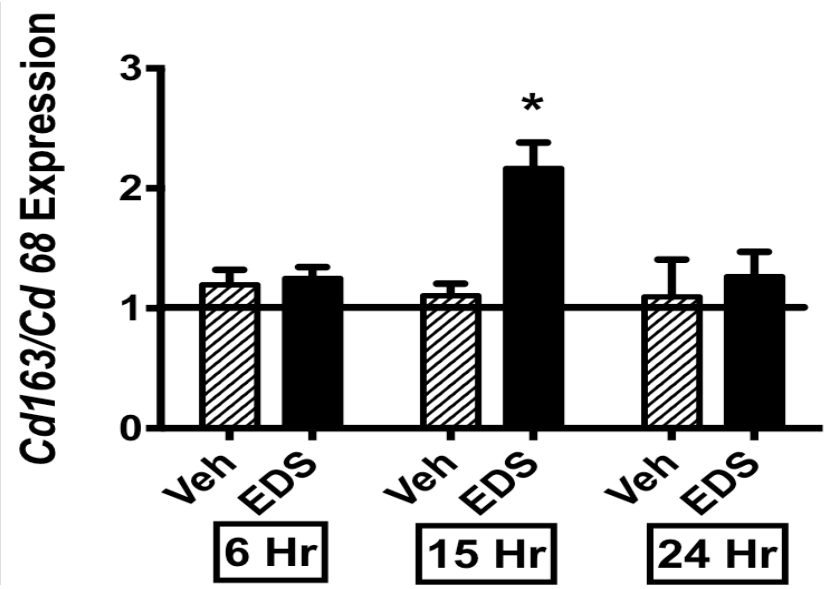

Figure 29
The expression of *Cd163/Cd68*. The horizontal line is the normalized value for the non-treated (NT) rats. Error bars represent SEM with n = 6 and (*) indicates a significant difference between EDS and vehicle (Veh)-treated rats within the same time of treatment.

Lenalidomide inhibition assay

To determine if blocking the release of TNF-α by lenalidomide can prevent the loss of Leydig cells, we tested for the Leydig cell marker genes, *Hsd3b2* and *Insl3,* using RT and qPCR at 24 hr after treatment with EDS or EDS plus lenalidomide (EDS + Leno). There was a decline in Hsd3b2 mRNA by 93% ($F_{4, 10} = 11.95$, $p \leq 0.0008$) with EDS treatment and this loss was not prevented by lenalidomide ($p > 0.05$). Lenalidomide alone had no effect ($p > 0.05$) (Fig. 30).

Similar results were obtained for *Insl3* (Fig. 31). There was a decline in Insl3 mRNA by 91% ($F_{4, 10} = 14.74$, $p \leq 0.0003$) with EDS treatment and this loss was not prevented by lenalidomide ($p > 0.05$). Lenalidomide alone had no effect ($p > 0.05$).

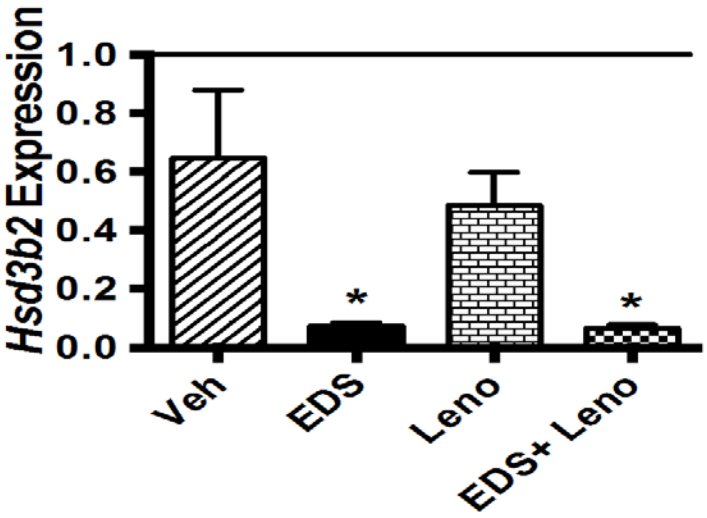

Figure 30
The expression of *Hsd3b2* relative to Gapdh as the reference gene. The horizontal line is the normalized value for the non-treated (NT) rats. Error bars represent SEM with n = 3 and (*) indicates a significant difference (p-value ≤ 0.05) from vehicle (Veh)-treated rats at 24 hr after EDS treatment.

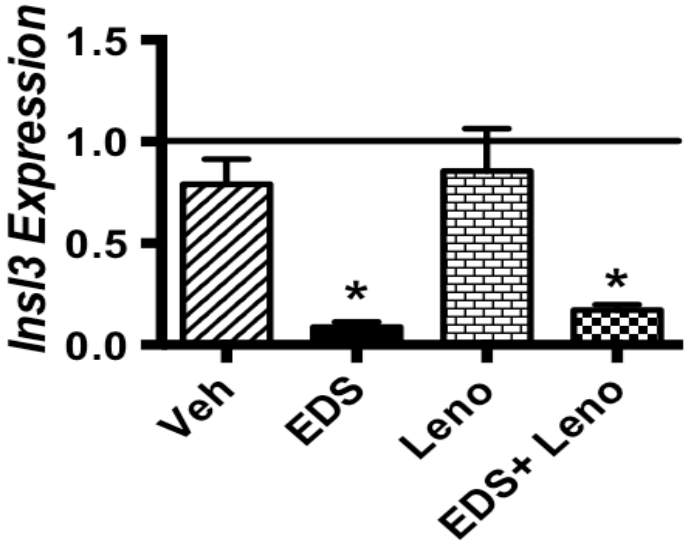

Figure 31
The expression of *Insl3* relative to Gapdh as the reference gene. The horizontal line is the normalized value for the non-treated (NT) rats. Error bars represent SEM with n = 3 and (*) indicates a significant difference (p-value ≤ 0.05) from vehicle (Veh)-treated rats at 24 hr after EDS treatment.

CHAPTER IV

DISCUSSION

We have investigated EDS induced apoptosis in Leydig cells to evaluate a possible selective mechanism of an extrinsic pathway(s) for this targeted deletion of cells. That is, EDS causes apoptosis of adult Leydig cells in the rat testis through as yet, an unidentified pathway. The primary function of Leydig cells is the synthesis and secretion of androgens in the testis. The amount of androgens produced by these cells depends on both the number of Leydig cells present in the testis and the capacity of these cells to produce steroids. Leydig cell depletion after 3 and 7 days post-EDS has been used to study the need of testosterone for germ cell maintenance via Sertoli cells (Nandi *et al.* 1999). In studies where intratesticular testosterone is maintained in the control range after EDS deletion of Leydig cells, little alteration of spermatogenesis in only a few seminiferous tubules is observed (Sprando *et al.* 1990). Thus, testosterone is clearly needed for the normal maintenance and progression of normal spermatogenesis. Since it is known that serum testosterone levels are very low at 3 days post- EDS, it is clear that Leydig cells are being lost early on. However, serum levels of testosterone as a measure of Leydig cell loss has the complicating features of testosterone turnover in the serum by mechanisms that involve availability of serum binding proteins, testosterone use in the somatic tissues, modifications in the liver and clearance of these modified steroids through the urine. Thus, in this work more immediate and timely markers were needed to study Leydig cell loss.

For investigation of Leydig cell loss after EDS, we selected different Leydig cell markers to measure the loss of Leydig cells. Since, mRNA very rapidly turns over in cells; we chose to use loss of selective mRNAs as a measure of Leydig cell loss. Four Leydig cell markers were chosen since they are fairly abundant in Leydig cells and have been studied by other investigators - LHR, INSL3, 3β-HSD and StAR (Abney & Zhai. 1998, Dong. 2011, Hsueh *et al.* 1977, Luo *et al.* 2001, Teerds *et al.* 1999). Since 6 hr and 24 hr post-EDS have been used previously, we chose these time points and further selected 15 hr post-EDS as an intermediate time point between these two time points studied earlier in Leydig cell loss.

The downregulation of mRNA for LHR and StAR at 6 hr suggests, that gene expression of these mRNAs are early markers to observe loss of Leydig cells and steroidogenesis after EDS treatment. In contrast to LHR and StAR mRNA, we found no loss of 3β-HSD and INSL3 mRNA until 15 hr after EDS administration (Table 4). Therefore, we suggest 3β-HSD and INSL3 genes to be late markers to detect EDS action. Thus, these markers are more acute in detection of Leydig cells that are in the process of apoptosis, and not dependent upon the turnover of testosterone in circulation. A large reduction (> 75%) of the selected Leydig cell marker mRNAs for LHR and StAR by 24 hr suggests that these markers are primarily expressed in the Leydig cells. More than 87% downregulation/ loss of the mRNA for 3β-HSD and INSL3 at 24 hr suggests that these markers may be expressed specifically in the Leydig cells. These findings are consistent with previous reports that 3β-HSD and INSL3 are located in and are secreted specifically by the Leydig cells, respectively (Ivell *et al.*

2013, Ivell *et al.* 2014, Teerds *et al.* 1999). No previous studies have reported the four Leydig cell marker genes - LHR, StAR, 3β-HSD and INSL3, in one study. Therefore, our findings give a better understanding of which mRNA markers are good to study for early and late Leydig cell apoptosis after EDS treatment. Cycle number (Cq) of the genes also reveals the abundance of mRNAs in total rat testes and is more meaningful as markers for Leydig cells, since Leydig cells are less than 3% of the total cell numbers (Table 3). Thus, we suggest that StAR, 3β-HSD and INSL3, are not only Leydig cell specific biomarkers but are also highly abundant in Leydig cells, with the Cq values for StAR, 3β-HSD and INSL3 mRNAs at 10 to 50% of the Cq for GAPDH found in 80% plus of total testicular cells.

Using hematoxylin and eosin staining for detection of histological and morphological changes in the rat testis, we observed visual cell loss and cell lysis in the interstitium at 15 and 24 hr after EDS treatment. This was supported by increased interstitial cell damage with increased time after EDS administration (Fig. 18). However, with simple microscopy, it was not possible to detect which particular cells in the interstitium were undergoing apoptosis or damage.

The Leydig cell gene expression analysis, and the histology analysis- using hematoxylin and eosin staining, and TUNEL staining are consistent with the suggestion that a dose of 75 mg/kg EDS is effective in destroying the rat Leydig cells without overall toxicity. These observations also support previous studies where rats were injected with a single 85 mg/kg intraperitoneal dose of EDS at 0 hr to 10 day.

Table 4 Change in gene expression levels at 6, 15 and 24 hr after EDS treatment

Leydig Cell Markers				
	mRNA	6 Hour	15 Hour	24 Hour
1	*Lhr*	**EDS < Veh**	**EDS < Veh**	**EDS < Veh**
		-64%	-80%	-88%
2	*Insl3*	**EDS = Veh**	**EDS < Veh**	**EDS < Veh**
		0%	-18%	-87%
3	*Hsd3b2*	**EDS = Veh**	**EDS < Veh**	**EDS < Veh**
		0%	-73%	-96%
4	*StAR*	**EDS < Veh**	**EDS < Veh**	**EDS < Veh**
		-52%	-69%	-75%
Apoptotic and Inflammatory Cytokine Ligands				
	mRNA	6 Hour	15 Hour	24 Hour
6	*Fasl*	**EDS = Veh**	**EDS = Veh**	**EDS = Veh**
		0%	0%	0%
7	*Tnfa*	**EDS = Veh**	**EDS > Veh**	**EDS = Veh**
		0%	+269% (2.69 – fold)	0%
8	*Tnfb*	**EDS = Veh**	**EDS = Veh**	**EDS = Veh**
		0%	0%	0%
9	*Il1b*	**EDS > Veh**	**EDS > Veh**	**EDS > Veh**
		+503% (5.03 – fold)	+325% (3.25 – fold)	+244% (2.44 – fold)
Apoptotic and Inflammatory Receptors				
	mRNA	6 Hour	15 Hour	24 Hour
10	*Fas*	**EDS = Veh**	**EDS = Veh**	**EDS = Veh**
		0%	0%	0%
11	*Tnfrsf1a*	**EDS = Veh**	**EDS > Veh**	**EDS > Veh**
		0%	+189% (1.89 – fold)	+383% (3.83 – fold)
12	*Tnfrsf1b*	**EDS < Veh**	**EDS = Veh**	**EDS = Veh**
		-66%	0%	0%
Monocyte and Macrophage Markers				
	mRNA	6 Hour	15 Hour	24 Hour
13	*Cd68*	**EDS = Veh**	**EDS = Veh**	**EDS = Veh**
		0%	0%	0%
14	*Cd163*	**EDS = Veh**	**EDS > Veh**	**EDS > Veh**
		0%	+292% (2.92 – fold)	0%

In the above table "–" means downregulation/loss and "+" means upregulation/increase in the mRNA expression with the EDS treatment. Zero percentage means no change.

The previous results were: (a) there was a significant DNA damage at 24 hr but no significant DNA damage was observed before or after 24 hr of EDS treatment; (b) no significant Leydig cell apoptosis was seen at 6 hr but apoptosis was increased at 12 hr with a peak at 24 hr. Leydig cell apoptosis was still significantly higher at 2 day but was reduced compared to 24 hr; later it was undetectable until 10 day, as most of the Leydig cells were already depleted from the testes (Nandi *et al.* 1999, Payne & Hardy. 2007). However in our studies, we did not test for DNA fragmentation after 24 hr. Therefore, we cannot say that DNA fragmentation in the interstitium peaked at 24 hr after EDS. In the early studies with 85 mg/kg EDS, it was observed that both maximum Leydig cell apoptosis and significant DNA fragmentation occurred at 24 hr. Thus, our findings with about 75-96% loss in mRNA for Leydig cell markers and a significantly increased interstitial cell apoptosis at 24 hr after 75 mg/kg EDS, encourage us to say that Leydig cells may be the primary cells undergoing apoptosis (Fig. 32). Though, we cannot confirm that other testicular cells were not undergoing apoptosis. With the TUNEL assay, we observed some apoptosis within the seminiferous tubules but in this study we counted only the apoptotic cells present in the interstitium.

From our macrophage studies after EDS administration, we find an increased *Cd163*/*Cd68* mRNA ratio at 15 hr, but not at 6 and 24 hr. We suggest that EDS action involves invasion of monocytes ($CD68^{+}$) across the vascular endothelium where monocytes are converted to testicular resident macrophages (TRMs) ($CD163^{+}$) and

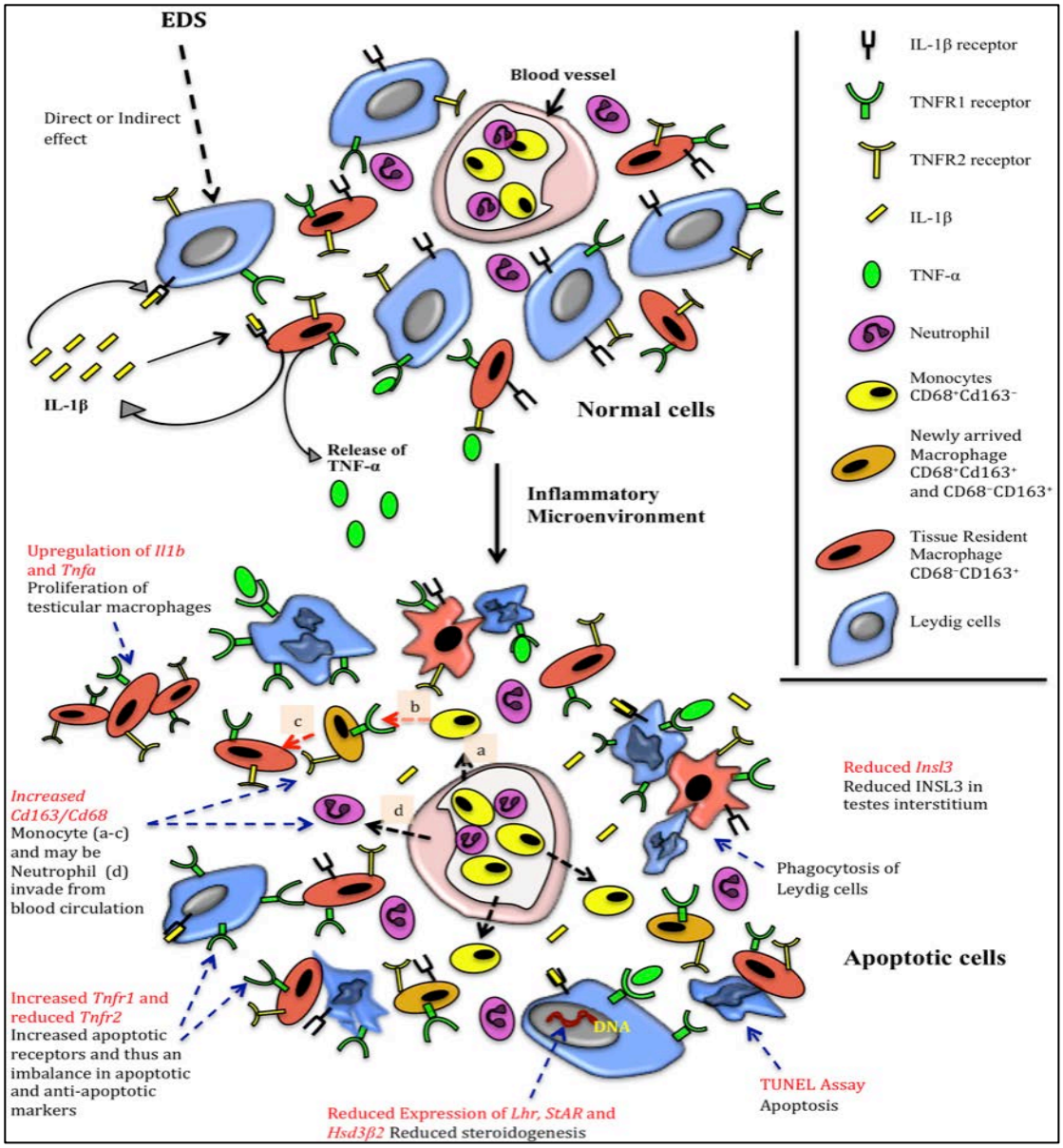

Figure 32

Model for Leydig cell apoptosis after EDS treatment. EDS may directly or indirectly alter testicular resident macrophages (TRMs) to secrete IL-1β, which binds to IL-1β receptors localized in TRMs and Leydig cells. Thus, proliferation of TRMs may take place and they secrete TNF-α. Upregulation of cytokines create an inflammatory microenvironment in the interstitium. Therefore, monocyte and neutrophil (step d) invade from blood circulation and monocytes mature to form more TRMs (step a − c). TNF-α receptors (TNFRs) are altered and create an imbalance of TNFR1 and TNFR2. TNF-α and IL-1β reduce the expression of LHR, StAR and HSD-3β after binding to TNFR1 and IL-1β receptor, respectively. TNF-α also induces Leydig cell apoptosis after binding to TNFR1 and finally Leydig cells undergo phagocytosis. Due to Leydig cell apoptosis, INSL3 is reduced or lost completely.

dendritic cells and also activate the TRMs already present in the testes to perhaps produce cytokines and inflammatory molecules, such as IL-1β and TNF-α (Hedger. 2002, Kern *et al.* 1995, Suescun *et al.* 2003) (Fig. 32).

Monocytes and macrophages are the major source of the pro-inflammatory cytokine, IL-1β, and can stimulate the production of numerous pro-inflammatory proteins such as inducible nitric oxide synthase (iNOS), cyclooxygenase 2 (COX-2), IL-6 and TNF-α (Lysiak. 2004, Payne & Hardy. 2007). In humans, IL-1β has also been localized in isolated Leydig and Sertoli cells (Lysiak. 2004). During inflammation and immune surveillance as seen in ischemic reperfusion (IR), IL-1β mediates a role in neutrophil and monocyte migration across the vascular endothelium by the activation of JNK and NF-κB pathway and upregulation of endothelial cell adhesion molecules, such as intercellular adhesion molecules (ICAMs), Vascular cell adhesion protein 1 (VCAM-1) and E-selectin (Lysiak. 2004, Lysiak *et al.* 2003, Parry *et al.* 1998). IL-1β can amplify its own production and can also stimulate TRMs to proliferate, synthesize and release cytokines, such as TNF-α (Lysiak. 2004). In this study, we observed increased expression of IL-1β mRNA at 6 hr which declined at 15 and 24 hr but was still significantly higher than the basal expression. Based on our mRNA data it is reasonable to hypothesize either a direct or an indirect activation of TRMs by EDS to release IL-1β at 6hr. Knowing that IL-1β mediates a chemo attractive role in neutrophil and monocyte migration from blood circulation, we suggest that increased IL-1β at 6 hr led to increased monocyte invasion and/or proliferation of TRMs in the interstitium, as seen by increased CD163/CD68 mRNA

ratio at 15 hr after EDS (Fig. 32). Most of the cytokines are expressed for a short duration and return to the basal levels after activating the cytokine receptors. Thus, we suggest a reduced expression of IL-1β mRNA at 15 and 24 hr after EDS, compared to 6 hr may be due to the same reason.

Another cytokine, TNF-α, is a pleotropic cytokine and is primarily secreted by testicular macrophages upon activation. Macrophages isolated without collagenase treatment, do not constitutively release TNF-α but release TNF-α when exposed to LPS, indicating that TNF-α could play a role in paracrine regulation of testicular steroidogenesis (Lysiak. 2004). TNF-α is secreted only during special conditions, such as inflammation and in response to LPS (Hutson. 1993, Moore & Hutson. 1994, Xiong & Hales. 1993b). In addition to IL-1β, TNF-α also plays a role in monocyte invasion after inflammation, resulting in an increased expression of TNF-α mRNA and protein at 15 hr after EDS; it is thus reasonable to hypothesize that TRMs and other immune cells release TNF-α that leads to an increase in monocyte invasion and thus increased CD163/Cd68 mRNA ratio. No change in TNF-β mRNA suggest, there is no involvement of TNF-β in EDS action in Leydig cell loss or that 6, 15 and 24 hr were not appropriate time points to detect a change in TNF-β mRNA (see Table 4).

Other than mediating a role in neutrophil and monocyte invasion, IL-1β and TNF-α, are also known to downregulate the expression of LHR, StAR and HSD-3β. Previous groups reported that in primary cultures of mouse Leydig cells, TNF-α reduced the expression of P450scc, P450c17 and HSD-3β, and in primary cultures of porcine Leydig cells, TNF-α reduced the expression of the StAR mRNA transcripts

(Hong *et al.* 2004, Lysiak. 2004, Mauduit *et al.* 1998, Xiong & Hales. 1993a). These early TNF-α study are reflective of our mRNA data for LHR, StAR and HSD-3β (Table 4 and Fig. 32).

IL-1β is known to inhibit LH/human chorionic gonadotropin (hCG) and/or cAMP stimulated testosterone production (Hales. 1992, Hales *et al.* 1992, Hales. 2002, Verhoeven *et al.* 1988) but in the presence of 22R-hydroxycholesterol or other steroid intermediates, the inhibitory action of IL-1 was not observed, suggesting that action of IL-1 is predominantly exerted through the decrease in cholesterol availability in the Leydig cell mitochondria for steroid hormone synthesis (Mauduit *et al.* 1992). In primary cultures of mouse Leydig cells, IL-1 inhibited cholesterol side-chain cleavage cytochrome P450 expression (Lin *et al.* 1991, Lin *et al.* 1998). In rat testes, the receptors for IL-1β are reported to be localized on Sertoli cells, Leydig cells, and testicular macrophages suggesting both an autocrine and a paracrine function of IL-1β (Gomez *et al.* 1997, Lysiak. 2004, Payne & Hardy. 2007). It is reasonable to hypothesize that IL-1β led to a reduced expression of LHR and StAR, which may lead to further reduced expression of HSD-3β and INSL3, as detected by our RT- and qPCR results (Table 4 and Fig. 32). Inhibition of TNF-α and IL-1β, together or individually, may further confirm our findings and their role in altering Leydig cell steroidogenesis and apoptosis.

TNF-α can bind to two distinct receptors, TNFR1 (apoptotic and anti-apoptotic receptor) is localized on all cell types in testes, and TNFR2 (anti-apoptotic receptor), expressed mostly by the immune cells, but also expressed on Leydig cells and

endothelial cells (Aggarwal. 2000, Bauda & Karinb. 2001, Darnay & Aggarwal. 1999, Lysiak. 2004, MacEwan. 2002). Based on our results examining mRNA we can only state an overall downregulation of TNFR2 and an upregulation of TNFR1, but the results do not indicate exactly which cell population in testes showed these changes (Table 4 and Fig. 32). To further confirm these results, TNFR1 and TNFR2 expression should be tested in isolated cell population or using receptor specific antibodies. However, we know that imbalances between apoptotic and anti-apoptotic gene expression can decide the fate of cells. Thus, TNF-α and TNFRs may play a potential role in Leydig cell apoptosis.

To further test for the involvement of Fas/FasL in Leydig cell apoptosis we looked for change in their mRNA expression. In a previous study on rats, injected with a single 85 mg/kg EDS, intraperitoneally, no change in testicular Fas protein until 24 hr was observed, but a significant increase in Fas was seen at 48 hr and at later times (Nandi *et al.* 1999, Payne & Hardy. 2007). Similarly, we found no changes in the mRNA for Fas and FasL at 6, 15 and 24 hr after 75 mg/kg of EDS treatment. With information from previous studies and our findings, we know that Leydig cells are already undergoing apoptosis at the initial time points (12 – 24 hr), times before Fas and FasL expression is upregulated at the mRNA level (Kim *et al.* 2000, Matsui. 2009, Nandi *et al.* 1999, Woolveridge *et al.* 1999). Therefore, the protein and mRNA results for Fas are consistent with the suggestion that there was no direct involvement of Fas in Leydig cell apoptosis. However, the germ cells may be undergoing apoptosis through Fas signaling as shown previously (Nandi *et al.* 1999, Woolveridge *et al.*

1999). Not having the data for time points after 24 hr, we cannot confirm if Fas will change with 75 mg/kg of EDS treatment at later timepoints.

We also tested a drug, lenalidomide (Revlimid) used in therapy of patients with multiple myeloma (MM) (Armoiry *et al.* 2008). The exact mechanism of action for lenalidomide is not well understood but lenalidomide is known to destabilize the mRNA expression of TNF-α and other cytokines like IL-1β (Kiaei *et al.* 2006). Lenalidomide also directly triggers apoptosis in drug resistant MM cells and is more potent with dexamethasone (Hideshima *et al.* 2008). With the treatment of lenalidomide in rats treated with EDS, we expected to find an upregulation in the mRNA profile of Leydig cell markers, 3β-HSD and INSL3. In contrast to our expectations, we did not find an upregulation in the mRNA for 3β-HSD and INSL3 after EDS and lenalidomide (EDS + Leno) treatment at 24 hr (Fig. 30 and 31).

Effect of lenalidomide has mostly been observed in patients with multiple myeloma (MM) and lymphoma. In healthy volunteers with a single oral-dose, two-thirds of lenalidomide is eliminated unchanged through urinary excretion and the half-life for elimination is 3 hr. Also, the exposure of lenalidomide is 57% higher in MM patients, compared to healthy volunteers (Armoiry *et al.* 2008, Hideshima *et al.* 2008). Since lenalidomide works actively in cancer patients and is quickly eliminated from healthy individuals, it may explain the results we achieved in our inhibition experiments. We injected rats with a single 50 mg/kg intraperitoneal injection of lenalidomide and a single 75 mg/kg intraperitoneal injection of EDS at 0 hr. However, since the half-life of lenalidomide elimination is 3 hr and TNF-α was upregulated at 15

hr, we also assume that lenalidomide may no longer be present in rats body to destabilize the mRNA of TNF-α and/or IL-1β. Effect of lenalidomide may also be species, age and cell specific. Also, we may have missed the effects of lenalidomide due to low sample size (n = 3) or the dose we selected. However, since TNFR1 may play a role in both apoptosis and anti-apoptosis, we cannot deny the possibility that upregulation of TNF-α and TNFR1 after EDS-treatment may actually be a cell survival mechanism to overcome the effects of EDS rather than an apoptotic mechanism. Perhaps for this reason, lenalidomide did not alleviate the Leydig cell loss caused after EDS administration. Another possibility is that TNF-α and IL-1β separately or in combination have a role in altering steroidogenesis but were not directly involved in Leydig cell apoptosis. In addition, there was no change in Fas, FasL mRNA, but there was a significant increase in TNF-α and TNFR1 mRNA, and TNF-α protein after EDS, we suggest a possible role of TNF-α in rat Leydig cell apoptosis. However, *in vitro* analysis and specific inhibition analysis in rats are needed to confirm the results of these findings.

If we can understand exactly how EDS signals Leydig cells to undergo apoptosis, then we can design drugs that are more targeted to tumor cells with parallel pathways and have fewer or limited side effects. This information should contribute to our understanding of male infertility problems arising from chemotherapeutic agents used in leukemia and other cancer treatments. By further study, it may also be possible to design better male contraceptives with reduced side effects.

REFERENCES

Abney T & Zhai J 1998 Gene expression of luteinizing hormone receptor and steroidogenic enzymes during leydig cell development. *Journal of Molecular Endocrinology* **20** 119-127.

Aderka D, Sorkine P, Abu-Abid S, Lev D, Setton A, Cope AP & Klausner J 1998 Shedding kinetics of soluble tumor necrosis factor (TNF) receptors after systemic TNF leaking during isolated limb perfusion. relevance to the pathophysiology of septic shock. *Journal of Clinical Investigation* **101** 650-659.

Aggarwal BB 2000 Tumour necrosis factors receptor associated signalling molecules and their role in activation of apoptosis, JNK and NF-κB. *Annals of the Rheumatic Diseases* **59** i6-i16.

Armoiry X, Aulagner G & Facon T 2008 Lenalidomide in the treatment of multiple myeloma: A review. *Journal of Clinical Pharmacy and Therapeutics* **33** 219-226.

Bartlett JMS, Kerr JB & Sharpe RM 1986 The effect of selective destruction and regeneration of rat leydig cells on the intratesticular distribution of testosterone and morphology of the seminiferous epithelium. *Journal of Andrology* **7** 240-253.

Bauda V & Karinb M 2001 Signal transduction by tumor necrosis factor and its relatives. *Trends in Cell Biology* **11** 372-377.

Bergh A & 'et al.' 1990 Interleukin-1β, but not interleukin-1α, induces acute inflammation-like changes in the testicular microcirculation of adult rats. *Journal of Reproductive Immunology* **17** 155-165.

Bishop JB & Wassom JS 1986 Toxicological review of busulfan (myleran). *Mutation Research/Reviews in Genetic Toxicology* **168** 15-45.

Bucci LR & Meistrich ML 1987 Effects of busulfan on murine spermatogenesis: Cytotoxicity, sterility, sperm abnormalities, and dominant lethal mutations. *Mutation Research/Fundamental and Molecular Mechanisms of Mutagenesis* **176** 259-268.

Buechler C, Ritter M, Orsó E, Langmann T, Klucken J & Schmitz G 2000 Regulation of scavenger receptor CD163 expression in human monocytes and macrophages by pro- and antiinflammatory stimuli. *Journal of Leukocyte Biology* **67** 97-103.

Calandra T & et al 1990 Prognostic values of tumor necrosis factor/cachectin, interleukin-l, interferon-α, and interferon-γ in the serum of patients with septic shock. *Journal of Infectious Diseases* **161** 982-987.

Chen GF, Ronis MJJ, Ingelman-Sundberg M & Badger TM 1999 Hormonal regulation of microsomal cytochrome P4502E1 and P450 reductase in rat liver and kidney. *Xenobiotica* **29** 437-451.

Chung BC'a' 1987 Cytochrome P450c17 (steroid 17 alpha-hydroxylase/17,20 lyase): Cloning of human adrenal and testis cDNAs indicates the same gene is expressed in both tissues. *Proceedings of the National Academy of Sciences of the United States of America* **84** 407-411.

Corral L & Kaplan G 1999 Immunomodulation by thalidomide and thalidomide analogues. *Annals of the Rheumatic Diseases*, **58** I107-I113.

Corral L & 'et.al' 1999 Differential cytokine modulation and T cell activation by two distinct classes of thalidomide analogues that are potent inhibitors of TNF-α. *The Journal of Immunology* **163** 380-386.

D'Abrizio P & 'et.al.' 2004 Ontogenesis and cell specific localization of fas ligand expression in the rat testis. *International Journal of Andrology* **27** 304-310.

Darnay BG & Aggarwal BB 1999 Signal transduction by tumour necrosis factor and tumour necrosis factor related ligands and their receptors. *Annals of the Rheumatic Diseases* **58** I2-I13.

Davis BH & Zarev PV 2005 Human monocyte CD163 expression inversely correlates with soluble CD163 plasma levels. *Cytometry Part B: Clinical Cytometry* **63B** 16-22.

Diemer T, Hales DB & Weidner W 2003 Immune-endocrine interactions and leydig cell function: The role of cytokines. *Andrologia* **35** 55-63.

Dijkstra CD, Döpp EA, Joling P & Kraal G 1985 The heterogeneity of mononuclear phagocytes in lymphoid organs: Distinct macrophage subpopulations in the rat recognized by monoclonal antibodies ED1, ED2 and ED3<*br* />. *Immunology* **54** 589-599.

Dong Lea 2011 Steroidogenic acute regulatory protein is a useful marker for leydig cells and sex-cord stromal tumors. *Applied Immunohistochemistry & Molecular Morphology* **19** 226-232.

Drut R, Wludarski S, Segatelli V, de Oliveira E, Barbosa A, Matheus A & Bacchi C 2006 Leydig cell tumor of the testis with histological and immunohistochemical features of malignancy in a 1-year-old boy with isosexual pseudoprecocity. *International Journal of Surgical Pathology* **14** 344-348.

Elmore S 2007 Apoptosis: A review of programmed cell death
. *Toxicologic Pathology* **35** 495-516.

Fijak M & Meinhardt A 2006 The testis in immune privilege. *Immunological Reviews* **213** 66-81.

Fischer AH, Jacobson KA, Rose J & Zeller R 2008 Hematoxylin and eosin staining of tissue and cell sections. *Cold Spring Harbor Protocols* **2008** pdb.prot4986.

Foresta C, Bettella A, Vinanzi C, Dabrilli P, Meriggiola MC, Garolla A & Ferlin A 2004 A novel circulating hormone of testis origin in humans. *Journal of Clinical Endocrinology & Metabolism* **89** 5952-5958.

Frungieri M & et al. 2002 Number, distribution pattern, and identification of macrophages in the testes of infertile men. *Fertility and Sterility* **78** 298-306.

Gaytan F & 'et.al.' 1994 Selective depletion of testicular macrophages and prevention of leydig cell repopulation after treatment with ethylene dimethane sulfonate in rats. *Journal of Reproduction and Fertility* **101** 175-182.

Gerdprasert O & 'et al.' 2002 The response of testicular leukocytes to lipopolysaccharide-induced inflammation: Further evidence for heterogeneity of the testicular macrophage population. *Cell and Tissue Research* **308** 277-285.

Gomez E, Morel G, Cavalier A, Liénard MO, Haour F, Courtens JL & Jégou B 1997 Type I and type II interleukin-1 receptor expression in rat, mouse, and human testes. *Biology of Reproduction* **56** 1513-1526.

Hales DB 2002 Testicular macrophage modulation of leydig cell steroidogenesis. *Journal of Reproductive Immunology* **57** 3-18.

Hales DB 1992 Interleukin-1 inhibits leydig cell steroidogenesis primarily by decreasing 17alpha-hydroxylase/C17-20 lyase cytochrome P450 expression. *Endocrinology* **131** 2165-2172.

Hales DB, Xiong Y & Tur-Kaspa I 1992 The role of cytokines in the regulation of leydig cell P450c17 gene expression. *The Journal of Steroid Biochemistry and Molecular Biology* **43** 907-914.

Hardy MP, Zirkin BR & Ewing LL 1989 Kinetic studies on the development of the adult population of leydig cells in testes of the pubertal rat. *Endocrinology* **124** 762-770.

Hassan M & 'et.al.' 2002 A phase II trial of liposomal busulphan as an intravenous myeloablative agent prior to stem cell transplantation: 500 mg/m2 as a optimal total dose for conditioning. *Bone Marrow Transplantation* **30** 833-841.

Hedger MP 2002 Macrophages and the immune responsiveness of the testis. *Journal of Reproductive Immunology* **57** 19-34.

Henriksén K, Hakovirta H & Parvinen M 1995 Testosterone inhibits and induces apoptosis in rat seminiferous tubules in a stage-specific manner: In situ quantification in squash preparations after administration of ethane dimethane sulfonate. *Endocrinology* **136** 3285-3291.

Henriksén K, Kulmala J, Toppari J, Mehrotra K & Parvinen M 1996 Stage-specific apoptosis in the rat seminiferous epithelium: Quantification of irradiation effects. *Journal of Andrology* **17** 394-402.

Hideshima T, Raje N, Richardson PG & Anderson KC 2008 A review of lenalidomide in combination with dexamethasone for the treatment of multiple myeloma. *Therapeutics and Clinical Risk Management* **4** 129-136.

Hong CY, Park JH, Ahn RS, Im SY, Choi HS & et. al. 2004 Molecular mechanism of suppression of testicular steroidogenesis by proinflammatory cytokine tumor necrosis factor alpha. *Molecular and Cellular Biology* **24** 2593-2604.

Horstman AM, Dillon EL, Urban RJ & Sheffield-Moore M 2012 The role of androgens and estrogens on healthy aging and longevity. *The Journals of Gerontology Series A: Biological Sciences and Medical Sciences* **67** 1140-1152.

Hsueh AJ, Dufau ML & Catt KJ 1977 Gonadotropin-induced regulation of luteinizing hormone receptors and desensitization of testicular 3':5'-cyclic AMP and testosterone responses
. *Proceedings of the National Academy of Sciences of the United States of America* **74** 592-595.

Hutson JC 1993 Secretion of tumor necrosis factor alpha by testicular macrophages. *Journal of Reproductive Immunology* **23** 63-72.

Ivell R, Heng K & Anand-Ivell R 2014 Insulin-like factor 3 and the HPG axis in the male. *Frontiers in Endocrinology* **5** .

Ivell R, Wade JD & Anand-Ivell R 2013 INSL3 as a biomarker of leydig cell functionality. *Biology of Reproduction* **88** 147.

Jahnukainen K, Ehmcke J & Schlatt S 2006 Testicular xenografts: A novel approach to study cytotoxic damage in juvenile primate testis. *Cancer Research* **66** 3813-3818.

Jégou B, Le Gac F & de Kretser D 1982 Seminiferous tubule fluid and interstitial fluid production. 1. effects of age and hormonal regulation in immature rats. *Biology of Reproduction* **27** 590-595.

Kern S, Robertson SA, Mau VJ & Maddocks S 1995 Cytokine secretion by macrophages in the rat testis. *Biology of Reproduction* **53** 1407-1416.

Kerr JB, Donachie K & Rommerts FFG 1985 Selective destruction and regeneration of rat leydig cells in vivo. *Cell and Tissue Research* **242** 145-156.

Kiaei M & et al. 2006 Thalidomide and lenalidomide extend survival in a transgenic mouse model of amyotrophic lateral sclerosis. *The Journal of Neuroscience* **26** 2467-2473.

Kim J, Luo L & Zirkin BR 2000 Caspase-3 activation is required for leydig cell apoptosis induced by ethane dimethanesulfonate. *Endocrinology* **141** 1846-1853.

Kim YC, Yim HK, Jung YS, Park JH & Kim SY 2007 Hepatic injury induces contrasting response in liver and kidney to chemicals that are metabolically activated: Role of male sex hormone. *Toxicology and Applied Pharmacology* **223** 56-65.

Kotula-Balak M & et al 2012 Hydroxysteroid dehydrogenases – localization, function and regulation in the testis . In *Biochemistry, Genetics and Molecular Biology* Chapter 11RA Canuto Ed. InTech.

Lagarrigue M, Becker M, Lavigne R, Deininger S, Walch A, Aubry F, Suckau D & Pineau C 2011 Revisiting rat spermatogenesis with MALDI imaging at 20-µm resolution. *Molecular & Cellular Proteomics* **10** .

Lee J, Richburg J, Shipp E & Meistrich, ML., Boekelheide, K. 1999 The fas system, a regulator of testicular germ cell apoptosis, is differentially up-regulated in sertoli Cell*Versus* Germ cell injury of the testis. *Endocrinology* **140** 852-858.

Lee J, Richburg J, Younkin S & Boekelheide K 1997 The fas system is a key regulator of germ cell apoptosis in the testis. *Endocrinology.* **138** 2081-2088.

Li M, Xia W, Mruk D, Wang C, Yan H & et.al. 2006 Tumor necrosis factor a reversibly disrupts the blood–testis barrier and impairs sertoli–germ cell adhesion in the seminiferous epithelium of adult rat testes. *Journal of Endocrinology* **190** 313-329.

Li X, Youngblood GL, Payne AH & Hales DB 1995 Tumor necrosis factor-alpha inhibition of 17alpha-hydroxylase/c17-20 lyase gene (Cyp17) expression. *Endocrinology* **136** 3519-3526.

Lin T, Wang D & Stocco D 1998 Interleukin-1 inhibits leydig cell steroidogenesis without affecting steroidogenic acute regulatory protein messenger ribonucleic acid or protein levels. *Journal of Endocrinology* **156** 461-467.

Lin T, Wang D, Nagpal ML, Calkins JH, Chang WC & Chi R 1991 Interleukin-1 inhibits cholesterol side-chain cleavage cytochrome P450 expression in primary cultures of leydig cells. *Endocrinology* **129** 1305-1311.

Lukyanenko Y, Carpenter A, Brigham D, Stocco D & Hutson J 1998 Regulation of leydig cells through a steroidogenic acute regulatory protein-independent pathway by a lipophilic factor from macrophages. *Journal of Endocrinology* **158** 267-275.

Luo L, Chen H & Zirkin BR 2001 Leydig cell aging: Steroidogenic acute regulatory protein (StAR) and cholesterol side-chain cleavage enzyme. *Journal of Andrology* **22** 149-156.

Lysiak J 2004 The role of tumor necrosis factor-alpha and interleukin-1 in the mammalian testis and their involvement in testicular torsion and autoimmune orchitis. *Reproductive Biology and Endocrinology* **2** 9.

Lysiak JJ, Nguyen QAT, Kirby JL & Turner TT 2003 Ischemia-reperfusion of the murine testis stimulates the expression of proinflammatory cytokines and activation of c-jun N-terminal kinase in a pathway to E-selectin expression. *Biology of Reproduction* **69** 202-210.

MacEwan DJ 2002 TNF receptor subtype signalling: Differences and cellular consequences. *Cellular Signalling* **14** 477-492.

MacKenzie S, Fernàndez-Troy N & Espel E 2002 Post-transcriptional regulation of TNF-a during in vitro differentiation of human monocytes/macrophages in primary culture. *Journal of Leukocyte Biology* **71** 1026-1032.

Maini RN, Elliott MJ, Brennan FM & Feldmann M 1995 Beneficial effects of tumour necrosis factor-alpha (TNF-?) blockade in rheumatoid arthritis (RA). *Clinical & Experimental Immunology* **101** 207-212.

Manna PR & Stocco DM 2011 The role of specific mitogen-activated protein kinase signaling cascades in the regulation of steroidogenesis. *Journal of Signal Transduction* **2011** 13 pages.

Matsui H'a 2009 Direct toxic effects of ethylene-1, 2-dimethanesulfonate (eds) on the rat epididymis. *Journal of Toxicologic Pathology* **9** 65-72.

Mauduit C, Chauvin MA, Hartmann DJ, Revol A, Morera AM & Benahmed M 1992 Interleukin-1 alpha as a potent inhibitor of gonadotropin action in porcine leydig cells: Site(s) of action. *Biology of Reproduction* **46** 1119-1126.

Mauduit C, Gasnier F, Rey C, Chauvin M, Stocco DM, Louisot P & Benahmed M 1998 Tumor necrosis factor-α inhibits leydig cell steroidogenesis through a decrease in steroidogenic acute regulatory protein expression. *Endocrinology* **139** 2863-2868.

McIlwain DR, Berger T & Mak TW 2013 Caspase functions in cell death and disease. *Cold Spring Harbor Perspectives in Biology* **5** .

McLennan IS 1993 Resident macrophages (ED2- and ED3-positive) do not phagocytose degenerating rat skeletal muscle fibres. *Cell and Tissue Research* **272** 193-196.

Mijatovic T, Houzet L, Defrance P, Droogmans L, Huez G & Kruys V 2000 Tumor necrosis factor-alpha mRNA remains unstable and hypoadenylated upon stimulation of macrophages by lipopolysaccharides. *European Journal of Biochemistry* **267** 6004-6012.

Molenaar R, De Rooij DG, Rommerts FF, Reuvers PJ & Van der Molen HJ 1985 Specific destruction of leydig cells in mature rats after in vivo administration of ethane dimethyl sulfonate. *Biology of Reproduction* **33** 1213-1222.

Moore C & Hutson JC 1994 Physiological relevance of tumor necrosis factor in mediating macrophage-leydig cell interactions. *Endocrinology* **134** 63-69.

Morales V, Santana P, Díaz R, Tabraue C & Gallardo G 2003 Intratesticular delivery of tumor necrosis factor-α and ceramide directly abrogates steroidogenic acute regulatory protein expression and leydig cell steroidogenesis in adult rats. *Endocrinology* **144** 4763-4772.

Mori H & Christensen AK 1980 Morphometric analysis of leydig cells in the normal rat testis. *The Journal of Cell Biology* **84** 340-354.

Muller GW'a' 1999 Amino-substituted thalidomide analogs: Potent inhibitors of TNF-α production. *Bioorganic & Medicinal Chemistry Letters* **9** 1625-1630.

Nandi S, Banerjee PP & Zirkin BR 1999 Germ cell apoptosis in the testes of sprague dawley rats following testosterone withdrawal by ethane 1,2-dimethanesulfonate administration: Relationship to fas? *Biology of Reproduction* **61** 70-75.

Nasr IW, Wang Y, Gao G, Deng S, Diggs L, Rothstein DM, Tellides G, Lakkis FG & Dai Z 2005 Testicular immune privilege promotes transplantation tolerance by altering the balance between memory and regulatory T cells. *The Journal of Immunology* **174** 6161-6168.

Niemi M, Sharpe RM & Brown WRA 1986 Macrophages in the interstitial tissue of the rat testis. *Cell and Tissue Research* **243** 337-344.

Onofre G, Kolácková M, Jankovicová K & Krejsek J 2009 Scavenger receptor CD163 and its biological functions. *ACTA MEDICA (Hradec Králové)* **52** 57-61.

O'Reilly D & Greaves DR 2007 Cell-type-specific expression of the human CD68 gene is associated with changes in pol II phosphorylation and short-range intrachromosomal gene looping. *Genomics* **90** 407-415.

Parry GCN, Martin T, Felts KA & Cobb RR 1998 IL-1β–Induced monocyte chemoattractant protein-1 gene expression in endothelial cells is blocked by proteasome inhibitors. *Arteriosclerosis, Thrombosis, and Vascular Biology* **18** 934-940.

Payne AH & Hardy MP Eds. 2007 *The leydig cell in health and disease*Totowa, New Jersey: Humana press inc.

Pentikainen V, Erkkila K, Suomalainen L, Otala M, Pentikainen MO, Parvinen M & Dunkel L 2001 TNFalpha down-regulates the fas ligand and inhibits germ cell apoptosis in the human testis. *J Clin Endocrinol Metabol* **86** 4480-4488.

Quinn P, Dombrausky L & Chen Y&,A. 1981 Serum lipoproteins increase testosterone production in hCG-desensitized leydig cells. *Endocrinology* **109** 1790-1792.

Riccioli A, Salvati L, D'Alessio A, Starace D, Giampietri C, De Cesaris P, Filippini A & Ziparo E 2003 The fas system in the seminiferous epithelium and its possible extra-testicular role. *Andrologia* **35** 64-70.

Riccioli A, Starace D, D'Alesssio A, Starace G, Padula F, De Cesaris P, Filippini A & Ziparo E 2000 TNF-alpha and IFN-gamma regulate expression and function of the fas system in the seminiferous epithelium. *Journal of Immunology* **165** 743-749.

Richburg J & Boekelheide K 1996 Mono-(2-ethylhexyl) phthalate rapidly alters both sertoli cell vimentin filaments and germ cell apoptosis in young rat testes. *Toxicology and Applied Pharmacology* **137** 42-50.

Rommerts FF, Teerds KJ & Hoogerbrugge JW 1988 In vitro effects of ethylene-dimethane sulfonate (EDS) on leydig cells: Inhibition of steroid production and cytotoxic effects are dependent on species and age of rat. *Molecular and Cellular Endocrinology* **55** 87-94.

Saito H & et al. 2007 A tumor necrosis factor receptor loop peptide mimic inhibits bone destruction to the same extent as anti?tumor necrosis factor monoclonal antibody in murine collagen-induced arthritis. *Arthritis & Rheumatism* **56** 1164-1174.

Sharpe RM 1983 Local control of testicular function. *Quarterly Journal of Experimental Physiology* **68** 265-287.

Spahn TW, Eugster H, Fontana A, Domschke W & Kucharzik T 2005 Role of lymphotoxin in experimental models of infectious diseases: Potential benefits and risks of a therapeutic inhibition of the lymphotoxin-ß receptor pathway. *Infection and Immunity* **73** 7077-7088.

Spooner CE, Markowitz NP & Saravolatz LD 1992 The role of tumor necrosis factor in sepsis. *Clinical Immunology and Immunopathology* **62** S11-S17.

Sprando RL, Santulli R, Awoniyi CA, Ewing LL & Zirkin BR 1990 Does ethane 1,2-dimethanesulphonate (EDS) have a direct cytotoxic effect on the seminiferous epithelium of the rat testis? *Journal of Andrology* **11** 344-352.

Spratt DI, Bigos ST, Beitins I, Cox P, Longcope C & Orav J 1992 Both hyper- and hypogonadotropic hypogonadism occur transiently in acute illness: Bio- and immunoactive gonadotropins. *The Journal of Clinical Endocrinology & Metabolism* **75** 1562-1570.

Suescun MO, Rival C, Theas MS, Calandra RS & Lustig L 2003 Involvement of tumor necrosis factor-a in the pathogenesis of autoimmune orchitis in rats. *Biology of Reproduction* **68** 2114-2121.

Suominen J, Wang Y, Kaipia A & Toppari J 2004 Tumor necrosis factor-alpha (TNF-alpha) promotes cell survival during spermatogenesis, and this effect can be blocked by infliximab, a TNF-alpha antagonist. *European Journal of Endocrinology* **151** 629-640.

Taylor M, de Boer-Brouwer M, Woolveridge I, Teerds K & Morris I 1999 Leydig cell apoptosis after the administration of ethane dimethanesulfonate to the adult male rat is a fas-mediated process. *Endocrinology* **140** 3797-3804.

Teerds KJ, de Boer-Brouwer M, Dorrington JH, Balvers M & Ivell R 1999 Identification of markers for precursor and leydig cell differentiation in the adult rat testis following ethane dimethyl sulphonate administration. *Biology of Reproduction* **60** 1437-1445.

Theas MS, Rival C, Jarazo-Dietrich S, Jacobo P, Guazzone VA & Lustig L 2008 Tumour necrosis factor-α released by testicular macrophages induces apoptosis of germ cells in autoimmune orchitis. *Human Reproduction* **23** 1865-1872.

Troiano L & 'et.al.' 1994 Apoptosis and spermatogenesis: Evidence from an in vivo model of testosterone withdrawal in the adult rat. *Biochemical and Biophysical Research Communications* **202** 1315-1321.

Van der Poll T, Romijn JA, Endert E & Sauerwein HP 1993 Effects of tumor necrosis factor on the hypothalamic-pituitary-testicular axis in healthy men. *Metabolism* **42** 303-307.

Van Dullemen H'a' 1995 Treatment of Crohn's disease with anti-tumor necrosis factor chimeric monoclonal antibody (cA2). *Gastroenterology* **109** 129-135.

Vasanthi P, Nalini G & Rajasekhar G 2007 Role of tumor necrosis factor-alpha in rheumatoid arthritis: A review. *APLAR Journal of Rheumatology* **10** 270-274.

Verhoeven G, Cailleau J, Damme JV & Billiau A 1988 Interleukin-1 stimulates steroidogenesis in cultured rat leydig cells. *Molecular and Cellular Endocrinology* **57** 51-60.

Vermeulen Jea 2009 RNA pre-amplification enables large-scale RT-qPCR gene-expression studies on limiting sample amounts. *BMC Research Notes* **2** .

Virve P, Erkkilä K & Dunkel L 1999 Fas regulates germ cell apoptosis in the human testis in vitro. *American Journal of Physiology - Endocrinology and Metabolism Published 1* **276** E310-E316.

Walker WH & Cheng J 2005 FSH and testosterone signaling in sertoli cells. *Reproduction* **130** 15-28.

Wang J, Wreford NG, Lan HY, Atkins R & Hedger MP 1994 Leukocyte populations of the adult rat testis following removal of the leydig cells by treatment with ethane dimethane sulfonate and subcutaneous testosterone implants. *Biology of Reproduction* **51** 551-561.

Waring P & Müllbacher A 1999 Cell death induced by the fas/fas ligand pathway and its role in pathology. *Immunology and Cell Biology* **77** 312-317.

Windahl SH & 'et.al.' 2011 Reduced bone mass and muscle strength in male 5α-reductase type 1 inactivated mice. *PLoS One* **6** .

Winnall WR, Muir JA & Hedger MP 2011 Rat resident testicular macrophages have an alternatively activated phenotype and constitutively produce interleukin-10 in vitro. *Journal of Leukocyte Biology* **90** 133-143.

Woolveridge I, de Boer-Brouwer M, Taylor MF, Teerds KJ, Wu FCW & Morris ID 1999 Apoptosis in the rat spermatogenic epithelium following androgen withdrawal: Changes in apoptosis-related genes. *Biology of Reproduction* **60** 461-470.

Xiong Q & 'et.al.' 2009 Involvement of fas/FasL system in apoptotic signaling in testicular germ cells of male wistar rats injected i.v. with microcystins. *Toxicon* **54** 1-7.

Xiong Y & Hales DB 1993a The role of tumor necrosis factor-alpha in the regulation of mouse leydig cell steroidogenesis. *Endocrinology* **132** 2438-2444.

Xiong Y & Hales DB 1993b Expression, regulation, and production of tumor necrosis factor-alpha in mouse testicular interstitial macrophages in vitro. *Endocrinology* **133** 2568-2573.

Yang Y'a 2015 Directed mouse embryonic stem cells into leydig-like cells rescue testosterone-deficient male rats in vivo. *Stem Cells and Development* **24** 459-470.

Yee J & Hutson J 1985 Effects of testicular macrophage-conditioned medium on leydig cells in culture. *Endocrinology* **116** 2682-2684.

Zirkin BR, Santulli R, Awoniyi CA & Ewing LL 1989 Maintenance of advanced spermatogenic cells in the adult rat testis: Quantitative relationship to testosterone concentration within the testis. *Endocrinology* **124** 3043-3049.

APPENDIX A

List of Abbreviations

LIST OF ABBREVIATIONS

Abbreviation	Full Name
ΔΔC(q)	Delta Delta Quantitative Cycle Number
17β-HSD	17β-Hydroxysteroid Dehydrogenases
3β-HSD	3-β-Hydroxyl Steroid Dehydrogenase
AC	Adenylyl Cyclase
ALCs	Adult Leydig cells
ANOVA	Analysis of Variance
AP-1	Activation Protein 1
ARs	Androgen Receptors
ATP	Adenosine Triphosphate
BLAST	Basic Local Alignment Search Tool
BSA	Bovine Serum Albumin
cAMP	Cyclic Adenosine Monophosphate
CD120	Cluster of Differentiation 120
CD120a	Cluster of Differentiation 120a
CD120b	Cluster of Differentiation 120b
CD163	Cluster of Differentiation 163
CD68	Cluster of Differentiation 68
CD95L	Cluster of Differentiation 95 Ligand
cDNA	Complementary DNA
COX-2	Cyclooxygenase 2
Cq	Quantification Cycle

CRE	cAMP Response Element-binding protein
DAB	3,3’-Diaminobenzidine
DAG	Diacylglycerol
DHT	Dihydrotestosterone
DMSO	Dimethyl Sulfoxide
dNTP	Deoxy Nucleotide Triphosphate
dsDNA	Double Stranded Deoxy Ribonucleic Acid
EDS	Ethane Dimethane Sulfonate
EDTA	Ethylene Diamine Tetra Acetic acid
ELISA	Enzyme Linked Immuno Sorbent Assay
FADD	Fibroblast-Associated Death Domain
Fas	Fibroblast-Associated Death Domain Receptor
FasL	Fibroblast-Associated Cell-Surface Ligand
FSH	Follicle Stimulating Hormone
FSHR	Follicle-Stimulating Hormone Receptor
GAPDH	Glyceraldehyde 3-Phosphate Dehydrogenase
GPCR	Guanine nucleotide-binding Protein Coupled Receptor
H&E	Hematoxylin and Eosin
hCG	Human Chorionic Gonadotropin
HCl	Hydrochloric Acid
HDL	High Density Lipoprotein
HPT	Hypothalamic, Pituitary and Testicular
HRP	Horseradish Peroxidase
HSD-3β	3-β-hydroxyl Steroid Dehydrogenase

Hsd3b2	3-β-hydroxyl Steroid Dehydrogenase Type 2 gene
HSDs	Hydroxyl Steroid Dehydrogenases
I	Interstitial Tissue
IACUC	Institutional Animal Care and Use Committee
ICAMs	Intercellular Adhesion Molecules
IFN-γ	Interferon Gamma
IHC	Immunohistochemistry
IL-1	Interleukin-1
IL-1β	Interleukin-1 beta
IL-6	Interleukin-6
iNOS	Inducible Nitric Oxide Synthase
INSL3	Insulin Like peptide 3
IP3	Inositol Triphosphate
JNK	Janus Kinase
JNKs	c-Jun N-terminal Kinases
LDL	Low Density Lipoprotein
LH	Luteinizing Hormone
LHR	Luteinizing Hormone Receptor
MAPKs	Mitogen-Activated Protein Kinases
MCP-1	Monocyte Chemo Attractant Protein-1
mDF	Modified Davidson's Fluid
MEK1/2	Mitogen activated protein Kinase Kinase 1 and 2
mESCs	Mouse Embryonic Stem Cells
$MgCl_2$	Magnesium Chloride

NaCl	Sodium Chloride
NaF	Sodium Fluoride
NF-κB	Nuclear Factor Kappa-Light-Chain-Enhancer of Activated B Cells
NKC	Natural Killer Cell
NP-40	Nonidet P-40
P-StAR	Phosphorylated StAR
P450c17	17 alpha-hydroxylase/17,20 lyase
$P450_{scc}$	P450 Cholesterol Side-Chain Cleavage Enzyme
PBS	Phosphate Buffered Saline
PHS	Public Health Services
PKA	Protein Kinase A
PKC	Protein kinase C
PLC	Phospholipase C
PMSF	Phenyl Methyl Sulfonyl Floride
Protein-P	Phosphorylated Protein
Q.S.	Quantity Sufficient
qPCR	Quantitative Polymerase Chain Reaction
RAP/Ras/Raf	Small Protein Kinase
RIP1	Receptor Interacting Protein 1
RNA	Ribonucleic Acid
RT-PCR	Reverse Transcription- Polymerase Chain Reaction
RXFP2	Relaxin/Insulin-Like Family Peptide Receptor 2
SER	Smooth Endoplasmic Reticulum

SF-1	Steroidogenic factor-1
ST	Seminiferous Tubules
StAR	Steroidogenic Acute Regulator
T	Testosterone
TdT	Terminal Deoxynucleotidyl Transferase
TMB	3,3′,5,5′-Tetramethylbenzidine
TNF-α	Tumor Necrosis Factor Alpha
TNF-β	Tumor Necrosis Factor Beta
TNFR1	Tumor Necrosis Factor Receptor 1
TNFR2	Tumor Necrosis Factor Receptor 2
TNFRs	Tumor Necrosis Factor Receptors
Tnfrsf1a	Tumor Necrosis Factor Receptor 1 gene
Tnfrsf1b	Tumor Necrosis Factor Receptor 2 gene
TRADD	Tumor Necrosis Factor Receptor Type 1-Associated Death Domain
TRAF1	TNF Receptor-Associated Factor 1
TRAF2	TNF Receptor-Associated Factor 2
TRMs	Tissue Resident Macrophages
TUNEL	Terminal Deoxynucleotidyl Transferase dUTP Nick End Labeling
VCAM-1	Vascular Cell Adhesion Protein-1